

NUCLEOTIDE SEQUENCE OF THE HANTAAVIRUS S
RNA SEGMENT AND EXPRESSION OF ENCODED PROTEINS

1987

JENNINGS

Report Documentation Page				Form Approved OMB No. 0704-0188	
Public reporting burden for the collection of information is estimated to average 1 hour per response, including the time for reviewing instructions, searching existing data sources, gathering and maintaining the data needed, and completing and reviewing the collection of information. Send comments regarding this burden estimate or any other aspect of this collection of information, including suggestions for reducing this burden, to Washington Headquarters Services, Directorate for Information Operations and Reports, 1215 Jefferson Davis Highway, Suite 1204, Arlington VA 22202-4302. Respondents should be aware that notwithstanding any other provision of law, no person shall be subject to a penalty for failing to comply with a collection of information if it does not display a currently valid OMB control number.					
1. REPORT DATE AUG 1987		2. REPORT TYPE N/A		3. DATES COVERED -	
4. TITLE AND SUBTITLE Nucleotide Sequence of the Hantaan Virus S RNA Segment and Expression of Encoded Proteins				5a. CONTRACT NUMBER	
				5b. GRANT NUMBER	
				5c. PROGRAM ELEMENT NUMBER	
6. AUTHOR(S)				5d. PROJECT NUMBER	
				5e. TASK NUMBER	
				5f. WORK UNIT NUMBER	
7. PERFORMING ORGANIZATION NAME(S) AND ADDRESS(ES) Uniformed Services University Of The Health Sciences Bethesda, MD 20814				8. PERFORMING ORGANIZATION REPORT NUMBER	
9. SPONSORING/MONITORING AGENCY NAME(S) AND ADDRESS(ES)				10. SPONSOR/MONITOR'S ACRONYM(S)	
				11. SPONSOR/MONITOR'S REPORT NUMBER(S)	
12. DISTRIBUTION/AVAILABILITY STATEMENT Approved for public release, distribution unlimited					
13. SUPPLEMENTARY NOTES					
14. ABSTRACT					
15. SUBJECT TERMS					
16. SECURITY CLASSIFICATION OF:			17. LIMITATION OF ABSTRACT SAR	18. NUMBER OF PAGES 242	19a. NAME OF RESPONSIBLE PERSON
a. REPORT unclassified	b. ABSTRACT unclassified	c. THIS PAGE unclassified			



UNIFORMED SERVICES UNIVERSITY OF THE HEALTH SCIENCES
F. EDWARD HÉBERT SCHOOL OF MEDICINE
4301 JONES BRIDGE ROAD
BETHESDA, MARYLAND 20814-4799



GRADUATE AND
CONTINUING EDUCATION

APPROVAL SHEET

TEACHING HOSPITALS
WALTER REED ARMY MEDICAL CENTER
NAVAL HOSPITAL, BETHESDA
MALCOLM GROW AIR FORCE MEDICAL CENTER
WILFORD HALL AIR FORCE MEDICAL CENTER

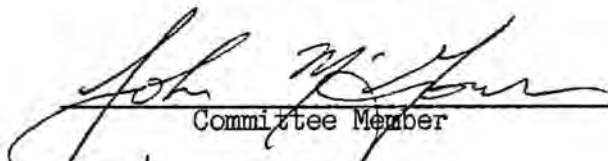
Title of Thesis: Nucleotide Sequence of the Hantaan Virus S
RNA Segment and Expression of Encoded Proteins

Name of Candidate: MAJ Gerald B. Jennings, VC, USA
Doctor of Philosophy Degree
November 3, 1987

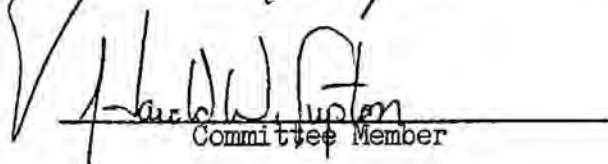
Thesis and Abstract Approved:


Committee Chairperson

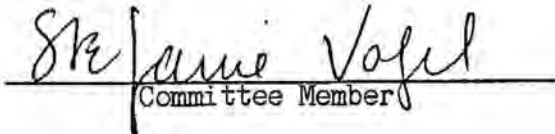
11/2/87
Date


Committee Member

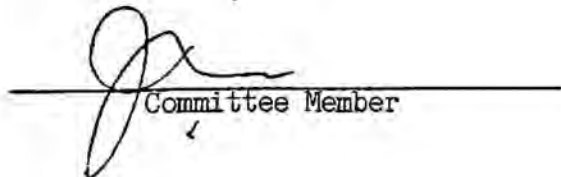
11/3/87
Date


Committee Member

11/3/87
Date


Committee Member

11/3/87
Date


Committee Member

11/3/87
Date

The author hereby certifies that the use of any copyrighted material in the dissertation manuscript entitled:

"Nucleotide Sequence of the Hantaan Virus S

RNA Segment and Expression of Encoded Proteins"

beyond brief excerpts is with the permission of the copyright owner, and will save and hold harmless the Uniformed Services University of the Health Sciences from any damage which may arise from such copyright violations.

A handwritten signature in cursive script, reading "Gerald B. Jennings".

MAJ Gerald B. Jennings, VC, USA
Department of Microbiology
Uniformed Services University
of the Health Sciences

ABSTRACT

Title of Dissertation: Nucleotide Sequence of the Hantaan Virus S RNA
Segment and Expression of Encoded Proteins

Gerald B. Jennings, Doctor of Philosophy, 1987

Dissertation directed by: John Hay, Ph.D., Professor and Vice-Chairman,
Department of Microbiology

The determination of the nucleotide sequence of the Hantaan virus (HTV) genome M RNA segment was begun to devise a strategy for expressing the encoded proteins in a eukaryotic expression system and to allow a comparison with other HTV RNA segments. Concurrently, the complete nucleotide sequence of the HTV S RNA segment was determined from three overlapping cDNA clones. The S RNA segment was 1695 nucleotides in length encoding two possible proteins in a unique coding strategy for members of the Bunyaviridae family. A large open reading frame (ORF) followed by a second smaller ORF was found in the viral complementary-sense RNA. Complementary sequences were found at the 3' and 5' termini of the RNA molecules which would allow formation of a stable stem-loop structure and the formation of the circular nucleocapsid. The M and S RNA segments contained 3' noncoding regions of similar length with 20 of the nucleotides conserved. Conserved sequences which could act as possible transcription termination signals in the 5' noncoding regions were also observed. Expression of the S segment cDNA through in vitro transcription and translation resulted in the synthesis

of a protein with the same apparent molecular weight as that predicted from the large open reading frame (48,196 daltons). Authentic HTV nucleocapsid protein, as well as the protein synthesized from the S segment cDNA, was identified by antibodies to a synthetic peptide the sequence of which was deduced from the nucleotide sequence of the large ORF. The construction and characterization of a vaccinia virus recombinant containing the S segment cDNA is described. Expression of this recombinant vaccinia virus in vivo produced the HTV nucleocapsid protein, yet the fluorescent pattern of the protein was quite distinct from HTV-infected cells. In addition, a protein, previously undetected in HTV infection, was synthesized. A possible explanation and function for this protein is discussed. Animals were vaccinated with the recombinant vaccinia viruses containing either the M segment cDNA or the S segment cDNA from HTV. Both constructs elicited antibodies to their respective encoded proteins, however only antibodies to the HTV glycoproteins neutralized the virus in vitro. The possibility of utilizing the two recombinant viruses as vaccines for Korean hemorrhagic fever is discussed.

NUCLEOTIDE SEQUENCE OF THE
HANTAAN VIRUS S RNA SEGMENT
AND EXPRESSION OF ENCODED PROTEINS

by

Gerald B. Jennings

Dissertation submitted to the Faculty of the Department of Microbiology
Graduate Program of the Uniformed Services University of the
Health Sciences in partial fulfillment of the
requirements for the degree of
Doctor of Philosophy 1987

TO JEANNINE
GREG AND JESSICA

ACKNOWLEDGEMENTS

I would like to thank the members of the Department of Microbiology for their words of wisdom over the course of my studies and especially thank my committee for their help, time, and effort during the preparation of this dissertation.

A special thanks to my collaborators: Dr. C.S. Schmaljohn, for providing the initial HTV cDNA clones; Dr. M.N. Pensiero, for collaboration in the animal studies; Dr. R. Williams, for collaboration in the preparation of the antipeptide antiserum; USAMRIID personnel, for their assistance with animals plus space to work; Mike Flora, Mark Wellman, and Ted Osgood, for their technical assistance; Jace Hougland and Paul Ling, for being fellow graduate students in the Hay lab; and Sarah Gaffen, for her charm, beauty, intelligence, and assistance.

To Dr. Paul Kinchington, for being an excellent instructor and living next door for the past three years.

To Dominic Johnson, for his assistance when I first walked into the laboratory environment.

To Dr. Iain Hay, for training, advice, and encouragement.

Last, but not least, to my family who have endured, for their love, patience, and understanding; and who now deserve my full attention.

TABLE OF CONTENTS

	<u>Page</u>
I. INTRODUCTION	1
Historical	2
Epidemiology	5
The disease	12
Morphological and molecular characterization	16
Purpose	33
II. MATERIALS AND METHODS	34
Cells	34
Viruses	34
Plasmids	35
HTV cDNA clones	39
Isolation of DNA	39
Restriction endonuclease digestion of DNA	41
Exonuclease Bal 31 digestion of DNA	42
Gel electrophoresis	43
Purification of DNA fragments from agarose gels	45
Molecular cloning of DNA fragments	45
Transformation of bacteria	46
Identification of recombinant plasmids containing HTV sequences	47

Southern blots	48
Radiolabeling of DNA for probes	48
DNA Sequencing	49
Preparation of synthetic oligonucleotides	50
<u>In vitro</u> transcription and translation	51
Formation and isolation of recombinant vaccinia virus	52
Preparation of anti-peptide antibody	53
Western blots	53
Indirect immunofluorescence	54
Animal studies	55
Virus neutralization tests	56
Immunoprecipitation	56
 III. RESULTS	 58
Nucleotide sequence determination of the HTV M segment	58
Determination and analysis of the HTV S segment nucleotide sequence	 77
<u>In vitro</u> translation of HTV S segment cDNA	119
Expression of HTV S segment cDNA in a vaccinia virus vector system	 139
Immunogenicity of HTV recombinant vaccinia viruses	168
 IV. DISCUSSION	 175
Comparison of the 3' terminal sequences of the HTV M and S genome segments	 176
Sequences flanking the AUG initiation codon of the HTV M	

and S genome segments	180
Possible transcription termination signals in the HTV M	
and S genome segments	181
Complementarity at the 5' and 3' termini of the HTV M and S	
genome segments	184
Coding strategy of the HTV S genome segment	184
Characterization of the large ORF protein in the HTV S	
genome segment	186
Characterization of the small ORF protein in the HTV S	
genome segment	187
<u>In vitro</u> and <u>in vivo</u> expression of the HTV nucleocapsid	
protein from the HTV S segment cDNA	189
<u>In vivo</u> expression of the small ORF from the HTV S segment	
cDNA	190
Expression of the 56,000 dalton protein	193
Possible function for the "read-through" protein	194
Experiments to identify the HTV 56,000 dalton protein	196
Encapsidation of RNA by the HTV nucleocapsid protein	198
Evaluation of the immune response to HTV recombinant	
vaccinia viruses	201
Immunogenic properties of the HTV nucleocapsid protein	202
V. REFERENCES	207

LIST OF TABLES

<u>Table</u>	<u>Page</u>
1. Serum neutralization titers to HTV of mice vaccinated with vMP2, v1009A, vSC8, or mock-vaccinated	171

LIST OF FIGURES

<u>Figure</u>	<u>Page</u>
1. Schematic representation of a bunyavirus	17
2. Schematic diagram of Bunyavirus transcription and translation .	20
3. Schematic representation of the coding strategy of the S segment of Aino virus (<u>Bunyavirus</u> genus)	28
4. Schematic representation of the coding strategy of the S segment of Punta Toro virus (<u>Phlebovirus</u> genus)	30
5. Schematic diagram of cloning plasmids used in this study	36
6. Pst I digests of HTV cDNA clones M-35, M-17, and S-16	60
7. Sequencing strategy of HTV M segment cDNA clone M-17	62
8. A representative M13 DNA sequencing gel	64
9. Identification of recombinant HTV-M13 phage by plaque hybridiza- tion and Southern blot	67
10. Bal 31 digest of HTV M segment cDNA clone M-17	70
11. The nucleotide sequence of the HTV M segment cDNA clone M-17 . .	73
12. Complementary termini of the HTV M segment	75
13. Hydropathic plot of the predicted gene product of the HTV M segment	78
14. Characteristics of the HTV cDNA clone S-8	82
15. Restriction endonuclease digestion of HTV cDNA clone S-8	86
16. Restriction endonuclease map of the HTV S segment cDNA	89
17. The sequencing strategy for the HTV S segment cDNA	92
18. DNA sequencing gel analysing the 5' viral-sense terminus of the	

HTV S segment cDNA clone S-8	95
19. Comparison of the molecular weights of the HTV cDNA plasmid clones S-8 and S-86	98
20. Acc I digest of HTV cDNA clone S-86	100
21. Complementary termini of the HTV S segment	103
22. The nucleotide sequence of the HTV S segment	106
23. The nucleotide sequence of the HTV S segment	108
24. The nucleotide sequence of the HTV S segment	110
25. Schematic representation of the coding strategy of the HTV S segment RNA	112
26. Structural predictions for the large ORF-derived protein from HTV S segment RNA	115
27. Structural predictions for the small ORF-derived protein from HTV S segment RNA	117
28. Partial digestion with Pst I to obtain an intact HTV cDNA (1695bp) fragment	121
29. Identification of bacterial colonies containing plasmids with HTV S segment cDNA sequences	124
30. Identification of HTV S segment cDNA subclones in pUC9 and pGEM-2126	
31. Determination of the orientation of the HTV S segment cDNA in the pGEM-2 plasmid	129
32. Characterization of RNA transcribed <u>in vitro</u> from pGEM-2 plasmids	131
33. <u>In vitro</u> translation of RNA derived from HTV S segment cDNA . .	134
34. Identification of the pGEM-2 plasmid containing the Bam HI-Pst I fragment of the HTV S segment cDNA	137
35. Partial digestion of the A-4 plasmid to obtain an intact HTV cDNA	

(1695bp) fragment	142
36. Characterization of the pSC11 plasmids containing the HTV S segment cDNA	146
37. Schematic diagram of the possible orientations of the HTV S segment cDNA in the pSC11 plasmid	148
38. Identification of recombinant vaccinia viruses containing HTV S segment cDNA	152
39. Identification by rabbit antipeptide serum of HTV nucleocapsid protein in HTV- and recombinant vaccinia virus-infected cells	155
40. Comparison of HTV nucleocapsid protein synthesis in the three recombinant vaccinia viruses	158
41. Time course of HTV nucleocapsid protein synthesis in v1009A- infected cells	161
42. Immunofluorescent studies of HTV nucleocapsid protein synthesis in v1009A-infected cells	164
43. Immunofluorescent studies of HTV nucleocapsid protein synthesis in v1009A-infected cells	166
44. Immunoprecipitation of HTV nucleocapsid protein with serum from v1009-infected mice	172
45. Comparison of the 3' sequence of the HTV M and S RNA segments .	177

INTRODUCTION

Korean Hemorrhagic Fever (KHF) is an acute, often fatal, but otherwise self-limiting, infectious disease. First recognized by the Western world during the Korean war, it continues to be a problem there today with approximately 300-900 cases hospitalized each year (Lee et al., 1980). However, the true global nature of this disease has only recently emerged through its subsequent intensive study. Similar diseases have been described, for example, in most areas of the Eurasian continent. China alone in 1982 reported 61,705 cases with a 5% fatality rate (Song et al., 1984).

Hantaan virus (HTV) is the causative agent of KHF. Although the virus was isolated from near the Hantaan River, the name has a more symbolic meaning, as the river is located in the demilitarized zone separating North and South Korea (PHLS Report 1985). HTV is the prototype virus of the new genus, Hantavirus, in the family Bunyaviridae. Evidence for the presence of members of the genus have been found on every continent except Antarctica. It remains to be seen whether all members of this genus cause human disease, but the increase in reported cases indicate unrecognized endemic areas and/or an increased awareness of the disease by physicians.

This disease and its related causative agent have been a constant challenge for investigators since the Korean War. The difficulty in isolating and growing the virus and the absence of an animal model have impeded progress in developing an effective treatment and vaccine for this disease. There remain, therefore, many questions regarding the pathogenesis, immunology, and molecular biology of HTV.

Historical

In June 1951, a disease heretofore unknown to Western medicine was described in United States forces in Korea. Symptoms included fever, lumbar pain, and headache, with signs of kidney disease and hemorrhagic disorder including erythema of the face and neck, conjunctival injection, and petechiae (Ganong *et al.*, 1953). The fatality rate reached 18 percent (McNinch, 1953). An initial diagnosis of leptospirosis had to be abandoned due to the failure of confirmative laboratory tests. No other known disease could be found with similar symptomatology. Finally, a search of Russian and Japanese literature proved instrumental in diagnosing this "new" disease.

In the mid 1930's, the Russians in southeastern Siberia and the Japanese in Manchuria began independent studies of a disease known to the Russians as endemic hemorrhagic nephroso-nephritis and to the Japanese as epidemic hemorrhagic fever (EHF). Based on clinical and pathological descriptions, Mayer (1952) concluded that these two diseases were identical and closely resembled the Korean disease.

The Russians and Japanese conducted human experiments in their study of the disease. These experiments revealed transmission of the disease when filtered or unfiltered human blood or urine was injected intravenously. However, aerosol exposure or ingestion of urine or blood did not produce the disease. This was not unexpected, since human to human spread had never been described. Due to the filterability of the agent, they concluded the causative agent must be a virus. Based on epidemiological studies, the Manchurian field mouse or the Eastern vole in Siberia was suspected as the reservoir for the virus, with transmission of the disease to humans by the bite of a mite.

Despite these discoveries, some United States personnel in Korea remained skeptical, believing they were dealing with a rickettsial disease. The Russian and Japanese literature predicted seasonal outbreaks of the disease: one in the spring (April-May) and another in late summer/early fall (peaking in September-October). The spring outbreak had occurred, and a "wait and see" policy was adopted by medical personnel to see if the second peak of activity would occur. As predicted, the fall outbreak did occur, with a much greater number of cases than reported in June; this became the decisive event in identifying the disease and eventually naming it Korean Hemorrhagic Fever (KHF). Almost all suspected cases were evacuated to the Hemorrhagic Fever Center, the 48th Surgical Hospital in Seoul, to receive the best possible treatment. However, by the end of the Korean conflict, a 6% death rate would be reported from the greater than 3000 cases. Despite extensive efforts during this period (1951-1954), a suitable animal model for isolation and study of the causative agent was not found. Therefore no effective means for development of vaccines, diagnostic procedures, or possible treatments could be investigated.

After the war, Korean farmers returned to the endemic area. Interestingly, there was apparently no acquired resistance to the disease through prior residence, since cases of the disease began to appear in the returning populace (Gajdusek, 1982). The apparently limited geographical area of disease caused Earle (1954) to state that few Western physicians would treat patients with this disease. This idea was to change, however, and the concept of an expanding endemic area was proposed by Tamura (1964). He described thirty-two cases of a febrile disease in Osaka City, Japan during the period January 1960 to July 1962. The clinical description of the severe cases (including one

death) was identical to KHF. The milder cases were very similar to a disease known in Scandinavia as nephropathia epidemica (NE). Tamura concluded that NE and KHF may belong to the same category of disease, representing subtypes of an agent with differing virulence.

Gajdusek (1962) believing the term "hemorrhagic fever" had become ambiguous, proposed a new grouping of viral hemorrhagic fevers. Endemic hemorrhagic nephroso-nephritis of Siberia, Tamura's Japanese EHF, and KHF would be classified as Hemorrhagic Fever with Renal Syndrome (HFRS). Gajdusek also included in this group, based on symptomatology and rodent association: Chinese EHF, NE of Scandinavia, and Eastern European EHF. The descriptions of these diseases are similar to KHF, except that they are milder with fewer hemorrhagic complications and a lower mortality. By now, the global nature of KHF was emerging, but data were still lacking to determine if there was a relationship between the causative agents of these diseases.

Over twenty-five years after the initial outbreak of KHF, Lee et al. (1978) reported the first convincing evidence of a causative agent. Specific immunofluorescence (IF) using convalescent serum from a patient with KHF was demonstrated in lung tissues from wild A. agrarius, the Korean striped field mouse. The authors were able to demonstrate immunofluorescence in A. agrarius infected with a lung suspension (strain 76-118) from a naturally-infected, IF positive A. agrarius, or if infected with acute phase serum from a patient with KHF. No fluorescence was detected with antiserum to other hemorrhagic fevers. However, as with attempts in the 1950's, the agent could not be established in cell lines nor in laboratory animals.

The immunofluorescent method established by Lee et al. (1978) allowed a comparison of the HFRS causative agents. Convalescent sera

from patients tested on lung tissue from A. agrarius infected with the KHF agent demonstrated an antigenic relationship with NE (Svedmyr et al., 1979 and Lee et al., 1979a), EHF in Japan (Lee et al., 1979b), HFRS in China (Lee, P.W. et al., 1980), and HFRS in the Soviet Union (Lee et al., 1978). Although an antigenic relationship existed, the results also demonstrated variations in the response, since the mean titer of IF antibodies in KHF patients was nearly ten times higher than in NE patients (Lee et al., 1979a). This difference was later confirmed after finding the NE agent in bank vole (Clethrionomys glareolus) tissue using an IF procedure similar to Lee's (Brummer-Korvenkontio et al., 1980). Comparing the reactivity of convalescent sera from KHF and NE patients with KHF or NE infected similarly tissue revealed antigenically related but not identical agents (Svedmyr et al., 1980).

Nearly thirty years after the 1951 outbreak of KHF, the causative agent was finally propagated in tissue culture (French et al., 1981). A suspension of lung tissue from KHF infected A. agrarius was used as the infectious material for several different cell cultures. One cell type, the A-549 alveolar epithelial line from human lung, developed specific fluorescence twelve days after inoculation, but never developed cytopathic effects. Based on the agent's filterability and its growth curve in tissue culture, the agent was believed to be a virus and was named Hantaan virus.

Epidemiology

Over the years, there have been numerous epidemiological reports on HTV. These studies have provided the information necessary to define new geographical areas of disease and possible new reservoirs. With this came the identification of three forms of HFRS: rural, urban and

laboratory. Many more people are threatened by the disease than was thought at the time of the Korean War.

KHF and the other HFRS were considered to be rural diseases transmitted to man by rodents or their ectoparasites. Therefore, the diseases primarily affected farmers, soldiers, and other field workers. In a study of Korean field rodents, only A. agrarius was found to be positive for KHF antigen (Lee et al., 1981a). Laboratory infection of that species established the likely period of infectivity (Lee et al., 1981b). Virus was recovered from the saliva and feces up to forty days after infection, while urine remained infectious through 360 days after infection. Viremia, however, lasted only from day seven to day twelve. The short viremia and negative results in attempting to isolate Hantaan virus from ectoparasites, suggested the lack of a need for parasites in disease transmission. Transmission was thus thought to be due to exposure to food or dust contaminated with rodent urine.

Traditionally, the rural HFRS had been known to exist in the Far East, Scandinavia, and Eastern Europe. New cases of HFRS demonstrate a widening endemic area, with reports from France (Dournon et al., 1983, and Hurault De Ligny, et al., 1984), Belgium (van der Groen et al., 1983), Scotland (Walker et al., 1984), Germany (Zeier et al., 1986), and Greece (Antoniadis et al., 1984 and LeDuc et al., 1986a). All cases have similar histories of patients not leaving their countries but all having possible contact with rodents. The clinical description of the patients is similar to cases of NE, with the exception of the outbreak in Greece (LeDuc et al., 1986a). In Greece, the severity of infection more closely resembles the Far Eastern HFRS with severe illness and death. These new areas of infection could represent a recent spread of HFRS infection. Conversely, they could result from the spread of man

into previously undisturbed rural areas or could reflect the recognition of a formerly misdiagnosed disease.

More recently, an urban form of HFRS also has become recognized. One of the puzzling aspects in the original report of the Osaka City cases of HFRS (Tamura, 1964), was their urban nature and lack of exposure to the natural reservoir, A. agrarius. Additional cases of urban HFRS were reported in Seoul, Korea in 1976 and in 1979 (Lee et al., 1982). The disease was milder than KHF, lacking the hemorrhagic manifestations, and therefore more similar to NE. These outbreaks led to a search for Hantaan virus in urban wild rats. The virus and antibodies to it were subsequently found in Rattus rattus and Rattus norvegicus from several Korean cities (Lee et al., 1982). Sera collected in areas of China from R. norvegicus were found to contain antibodies to Chinese EHF antigen (Gan et al., 1983). Experimental infection of laboratory rats with the urban isolate caused a persistent infection of the lung similar to that seen with A. agrarius (Lee et al., 1982). This suggested that the Rattus species could harbor the same type of chronic infection as A. agrarius. However, there was concern that HTV had adapted to a new host reservoir. If this were the case, dissemination of these new hosts by the shipping industry could spread HFRS world-wide. There existed, therefore, an urgent need for surveys of urban rats in other parts of the world.

Initial serosurveys of port cities (Tsai et al., 1982 and LeDuc et al., 1982) examined rat sera collected from the wharf areas of New Orleans, Houston, and Philadelphia. Samples from each location contained anti-Hantaan virus antibodies as determined by IF antibody, and examination of tissue by immunofluorescence revealed the presence of virus antigen in the lung, spleen, and kidney. Additional serosurveys

were instituted in the United States to determine how widespread the problem really was. A survey was conducted of rat sera collected from residential areas of Baltimore, distant from the harbor (Childs *et al.*, 1985). Antibodies were found to be disseminated throughout the city's rat population. Evidence of infection was also found further inland from rats sampled in Cincinnati and Columbus, Ohio (Tsai *et al.*, 1985). It seemed unlikely, therefore, that infection of rats in the United States with HTV, or a Hantaan-related virus, was a recent event.

The next serosurvey of rodents was conducted of over 1700 samples collected from twenty different sites worldwide (LeDuc *et al.*, 1986b). Sera containing IF anti-Hantaan antibodies were found on every continent except Antarctica, which was not tested. The highest prevalence rate was found in Baltimore. A new name was proposed for the HFRS - "muroid virus nephropathies" (Editorial, 1982). This was to take into account the lack of hemorrhages in the urban form of the disease and the fact that all rodent carriers belonged to the suprafamily Muroidae. However, this new title was rejected (Hsiang, 1986) due to the evidence of HFRS virus-related antigen in the lungs of Sorex araneus, an insectivore (Gavrilovakaya *et al.*, 1983), HFRS neutralizing antibody in cats (Desmyter *et al.*, 1983) and isolation of an HFRS virus from Suncus murinus, another insectivore (Tang *et al.*, 1985). Whether these new species are reservoirs for human infection has not been determined.

These global epidemiological surveys found not only new reservoirs for HFRS, but also new virus isolates. This was an important step in determining whether Hantaan virus had adapted to grow in other species or whether the surveys simply uncovered new strains of Hantaan virus. Isolates of rat viruses were made from several sites around the world. Two of the isolates were from areas where the urban form of HFRS

exists, China (strain R22) (Song et al., 1984) and Korea (strain 80-39) (Lee et al., 1982). Rat isolates from non-HFRS areas included Techoupitoulas virus, Girard Point virus and strain TR-352, isolated from New Orleans (Tsai et al., 1985), Philadelphia (LeDuc et al., 1984), and a nonendemic area of Japan (Sugiyama et al., 1984a), respectively. Prospect Hill virus was isolated from the native meadow vole (Microtus pennsylvanicus) captured in Frederick, MD (Lee, P.W. et al., 1982). All of the rodent isolates were shown to be antigenically related to Hantaan virus by immunofluorescence. However plaque-reduction neutralization tests were able to demonstrate the antigenic distinction between HTV and the new rodent isolates and the antigenic relationship among the various rat isolates (Schmaljohn et al., 1985).

The results of the plaque-reduction neutralization test provided evidence for the discovery of a previously unrecognized group of Hantaan-related viruses. However, human disease has not been associated with the new isolates other than the Chinese and Korean isolates. Human sera from Canada (Lee et al., 1984) and the United States (Gibbs et al., 1982 and Yanagihara et al., 1985) contained IF antibody against Hantaan virus, but there has been no correlation between this and infection. There has been evidence of infection in humans with Prospect Hill virus, as serum samples from mammalogists contained neutralizing antibodies to the virus (Yanagihara et al., 1984). The risk of infection, however, appears very low and again, no clinical disease has been described. The Hantaan-related viruses isolated in rodents in the United States either cause no human disease or cause an undiagnosed disease due to a mild form or a lack of suspicion by the physician. If the rat isolates from the U.S. cause no disease, the question arises as to the difference between them and the rat isolates causing disease.

Besides the rural and urban exposures, a third form of HFRS has become recognized. Two outbreaks of a disease with features resembling KHF occurred in the staff of a Japanese university (Umenai et al., 1979). Sera from the affected individuals contained IF antibodies against Hantaan virus, although no experiments with KHF were being conducted. Epidemiological studies suggested the laboratory rat as the probable source of the infection. A similar outbreak occurred in a Korean university (Lee and Johnson, 1982). Evaluation of these patients suggested aerosol exposure to chronically infected rodents as the source of infection. This resulted in the implementation of stricter containment of animals in laminar-flow, filtered cage racks. Three other incidents have since occurred: in Belgium (Desmyter et al., 1983), England (Lloyd et al., 1984) and France (Dournon et al., 1984). Rats were the source of infection in each case. A Hantaan-related virus (SR-11) was isolated from the lungs of rats involved in the Japanese outbreak (Kitamura et al., 1983). Plaque-reduction neutralization tests showed the virus to be antigenically distinct from the Hantaan virus, more closely resembling the other rat-associated, Hantaan-related viruses.

Not surprisingly, these results alarmed many laboratory workers, some of whom called for a Hantaan screening program (Lloyd et al., 1984). Australia began to require a screening of rats for Hantaan virus before importation (Desmyter et al., 1983). Due to the chronic nature of Hantaan infection in rodents, cell lines of rat origin also could have been sources of infection. ATCC cell lines of rat origin were tested and were found to be negative for Hantaan antigen (LeDuc et al., 1985). A serological survey of rat colonies in the United States similarly revealed no evidence of a Hantaan-related infection. It was

believed that this was due to the system of cesarean-originated and barrier-sustained rodent colonies commonly used in the U.S. (Tsai et al., 1985). This system reduces the opportunity for vertical and horizontal transmission of rodent pathogens. Laboratory workers following these safeguards should be at little risk of infection.

Several different tests have been employed to differentiate the various isolates of HTV. Early studies (Sugiyama et al., 1984b), testing sera from patients with Chinese EHF and Japanese HFRS in an immune adherence assay, found that the test could discriminate between antibodies to different types of HFRS isolates. HTV serotypes were defined later using enzyme-linked immunosorbent assay (ELISA) (Goldgaber et al., 1985) or radioimmunoassay (RIA) or plaque-reduction neutralization tests (PRNT) (Schmaljohn et al., 1985). The tests suggested a pattern of cross-reactivity that correlated more with the rodent host of origin than the geographical location. Four serotypic groups emerged from these studies: Type 1 (Apodemus derived strains), Type 2 (Rattus derived strains), Type 3 (Clethrionomys derived strains), and Type 4 (Microtus derived strains) (Lee, P.W. et al., 1985). The clearest distinction between isolates was seen in the plaque-reduction neutralization tests. Antisera to the original HTV (strain 76-118) isolate did not neutralize the other isolates. Conversely, antisera to the rat isolates neutralized all rat viruses including the original HTV isolate. Antisera to Prospect Hill or Puumala viruses did not neutralize any other virus. Although these studies were carried out with rodent sera, these same classifications have been made using human sera (Lee, P.W. et al., 1985) and monoclonal antibodies (Sugiyama et al., 1987). However, human sera from patients in Yugoslavia (Lee, P.W. et al., 1985) and Greece (LeDuc et al., 1986a) could not be classified into any of the

four serotypes.

It is now clear that the study of KHF and its causative agent is more than the study of a geographically-isolated disease. The importance of these epidemiological studies is even more evident when one considers a possible vaccination strategy. Populations likely to become infected must be defined, and since more than one strain of virus has been found, which strain(s) should be used in a vaccine remains to be determined.

The disease

Although the clinical and pathological descriptions of KHF originate from the Korean war, they are still accurate and form the basis of our understanding of the disease today. Symptoms of the disease can range from an inapparent or mild illness to a hemorrhagic disorder with renal failure and death. Generally, the severity of the disease is associated with specific geographic areas. The milder cases are found in Europe (Scandinavian NE type) and the more severe cases in the Far East (KHF type). However, this characterization is not always straightforward as evidenced by the severe cases in Greece (LeDuc et al., 1986a) and the 30-40% of mild cases in Korea. Nor is there a correlation between severity and rodent source of infection, as deaths have occurred from exposure to rats as well as to Apodemus agrarius.

The clinical disease is divided into five phases, as first described by Sheedy et al., 1954: febrile, hypotensive, oliguric, diuretic, and convalescence. There is considerable variation among patients with regard to these phases. In particular, the duration and severity of each phase can vary from patient to patient and not all phases will be present in each patient. The severity of the early

phases has not always correlated with the final outcome of the disease.

Patients usually report to the physician during the febrile phase. The incubation period is variable, ranging from 4-42 days. Symptoms resemble a flu-like illness: headache, backache, malaise, weakness, and anorexia. This symptomatology can result in mild cases being unreported. Physical examination reveals flushing of the head, neck, and upper thorax. The conjunctiva is often injected and occasionally petechia are found on the skin. Protein begins to appear in the urine about the fifth day.

Around day five there is an abrupt decrease in the patient's blood pressure, signalling the beginning of the hypotensive phase. Many of the signs and symptoms of the febrile phase continue into this phase. However, the patient does develop tachycardia, an increase in hematocrit, and a marked proteinuria. Blood platelets decrease and bleeding time is prolonged. This phase may last for several hours to three days.

Blood pressure returns to normal limits and urinary output falls dramatically in the oliguric phase which may last for three to seven days. Due to the renal failure, blood urea nitrogen increases and electrolyte abnormalities appear. A remarkable finding is that the number of blood platelets return to normal values while hemorrhagic manifestations become more prominent. Gross hematuria frequently appears, as can cutaneous, conjunctival, and gastrointestinal bleeding.

With the onset of the diuretic phase, patients begin to improve. Azotemia and proteinuria disappear, as urinary volume can increase to three to six liter per day. Other clinical signs and symptoms present during the course of the disease begin to regress. The most difficult problem during this phase is to maintain proper fluid intake preventing overhydration or dehydration.

Complete recovery is the rule, with the exception of those few individuals who suffer central nervous system damage due to hemorrhage. Polyuria and the inability to concentrate urine can continue for months, but few if any other symptoms or signs appear. Recovery from disease appears to provide protection from subsequent infections. Antibodies to KHF have been detected fourteen years after recovery from the disease (Lee et al., 1980).

Although the disease is known as hemorrhagic fever, the name overstates the importance of hemorrhage in the disease. In one study (Giles et al., 1954) only 11% of KHF patients had obvious hemorrhages and very few of them were severe enough to require transfusions. Only occasionally were the hemorrhagic features a direct cause of death (Hullinghorst and Steer, 1953). Yet, based on pathology reports, vascular damage constitutes the basic disease process (Lukes, 1954). Although there is no specific vascular lesion, vascular alterations are evidenced by capillary engorgement, diapedis of erythrocytes, focal hemorrhage, and altered capillary permeability (as evidenced by interstitial and retroperitoneal edema). The cause of death, therefore, in the early phases of the disease is usually shock. In the oliguric and diuretic phases, as vascular damage subsides, death is usually due to pulmonary complications or electrolyte abnormalities.

The cause of the vascular damage remains a mystery. It could be a direct effect of the virus on the vasculature. Hullinghorst and Steer (1953) proposed the idea of a toxin from the causative agent causing the altered capillary function. Others have proposed an immunologically-mediated cause for the damage based on the formation of antigen-antibody complexes in the disease (Penttinen et al., 1981) or on the activation of complement (Yan et al., 1981), but these remain unproven.

One major problem in answering questions about the disease has been the lack of an animal model system. Several species of colonized rodents infected with HTV fail to develop any clinical signs, although some developed antibody to HTV (Lee et al., 1981a). Persistent infection of HTV occurs in rats (Lee, P.W. et al., 1986) and Apodemus agrarius (Lee et al. 1981a), but neither species displays any signs of clinical illness and attempts to colonize A. agrarius (Lee et al., 1981a) have failed.

Kurata et al. (1983) were able to produce a lethal infection in suckling mice infected with a mouse-adapted strain of HTV. This animal model was recently improved by Kim and McKee (1985) who were able to produce disease with the HTV laboratory strain 76-118. In their studies, suckling mice infected before 72 hours of age showed progressive weight loss during the course of the disease. The mean time to death is 19 days with 100% mortality, and the cause of death is a central nervous system disease (McKee et al., 1985). This contrasts with the basic lesions of human HTV infection, and represents one of the problems with the model. Another problem is the small window of vulnerability for mouse infection. This makes studies of potential vaccines impossible due to the time necessary for vaccination and then challenge.

Despite these limitations the model has proved useful in attempts to study KHF infection. The suckling mouse model has been used, for example, to suggest that the antiviral drug ribavirin be used in treatment of KHF patients (Huggins et al., 1986). Results from this mouse model also appear to indicate an immune-mediated mechanism in the disease process (McKee et al., 1985). A role for T cells in resistance to fatal infection has been recently proposed (Nakamura et al., 1985).

Transfer of immune T cells to newborn mice within 48 hours of HTV infection prevented death of the mice. More recently, Asada *et al.* (1987) suggested helper and cytotoxic T cells were important for protection from HTV infection, while cytotoxic T cells were more important than helper T cells in recovery from infection. The question still remains, however, whether findings from the mouse model system are applicable to HTV infection in humans.

Morphological and molecular characterization

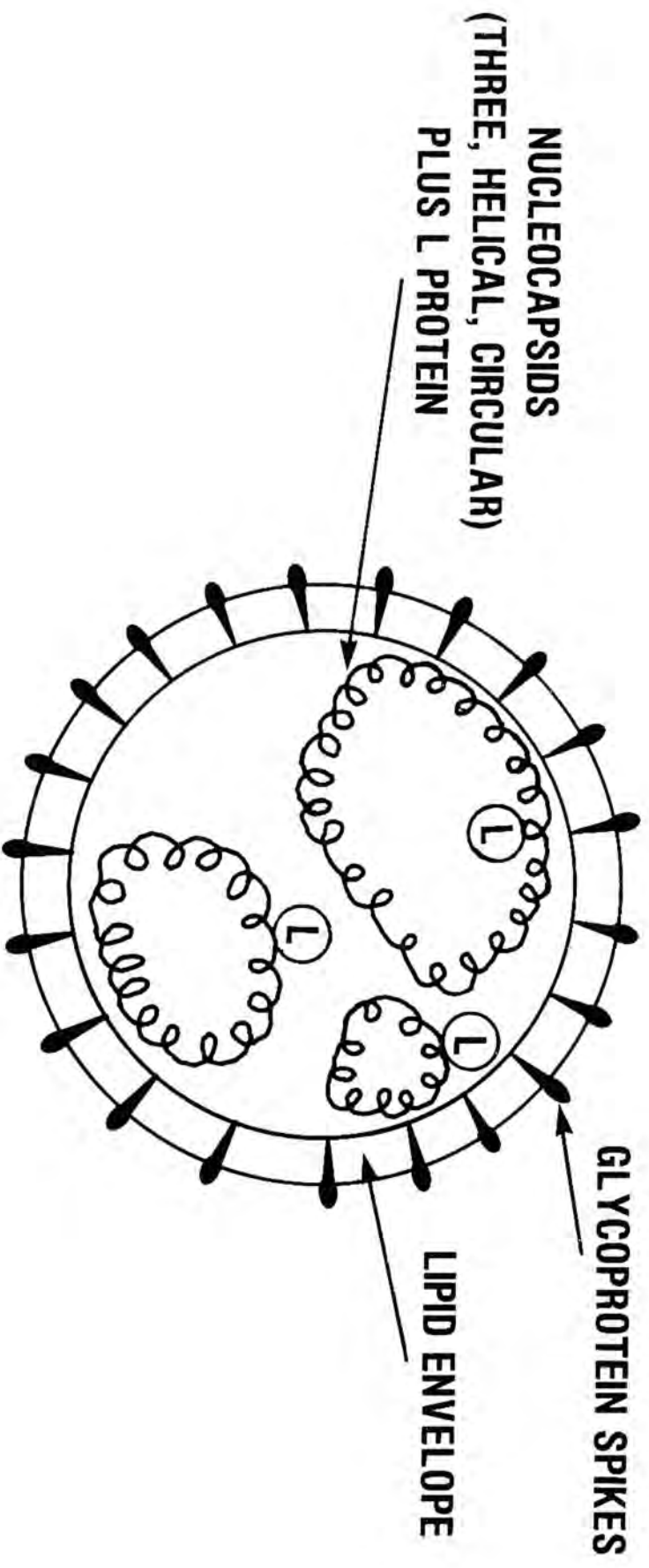
Hantaan virus has been recently classified, within the viral family Bunyaviridae, in a new genus, Hantavirus (Schmaljohn *et al.*, 1986a). Previously the Bunyaviridae had been divided into four genera: Bunyavirus, Phlebovirus, Nairovirus, and Uukuvirus (Bishop *et al.*, 1980). The classification of HTV has been based on structural, morphological, and molecular evidence gathered over the last six years. These data clearly placed HTV in the family Bunyaviridae, but with sufficient distinctive features to warrant the introduction of a separate new genus. Details of these studies are given below.

Bunyaviruses are enveloped, spherical particles approximately 90 to 100 nm in diameter (Figure 1). The lipid envelope, derived from cellular membranes during budding of the virus, contains the viral glycoproteins. It is not known whether the glycoproteins penetrate through the envelope to make contact with the nucleocapsids, but some means of glycoprotein-nucleocapsid association is presumably necessary since the virus lacks the specialized internal matrix protein found in the Orthoviridae, Paramyxoviridae, and Rhabdoviridae. The nucleocapsid protein binds to the three circular genomic RNA strands to form the nucleocapsids which are circular, helical structures (Figure 1). The

FIGURE 1

Schematic representation of a bunyavirus. The three circular RNA segments form individual helical structures with the nucleocapsid protein. These structures are associated with an RNA polymerase activity (L protein) and are surrounded by a lipid envelope. The two viral glycoproteins are within the lipid envelope, although the actual arrangement is unknown.

BUNYAVIRUS



arrangement of the three nucleocapsids within the virion is unknown and may be random. The nucleocapsids are designated large (L), medium (M), and small (S) based on the molecular weight of the RNA. (Obijeski and Murphy, 1977 and Bishop, 1985).

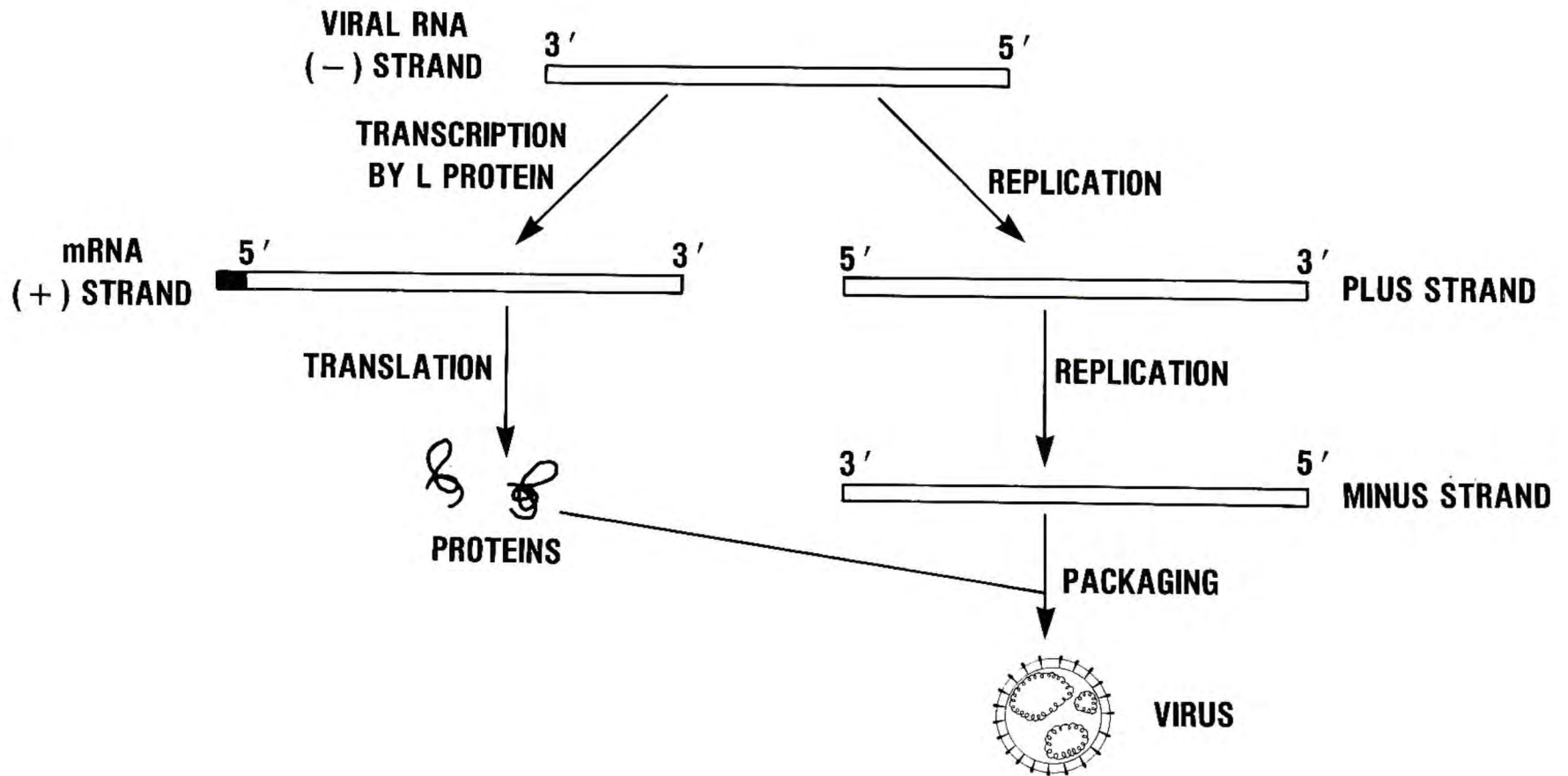
The naked RNA is non-infectious (Obijeski *et al.*, 1976) and is therefore referred to as "negative-sense". To be infectious, the virions are required to contain a RNA-dependent RNA polymerase (transcriptase or L protein) (Figure 2). Upon entry into the cell, the L protein transcribes viral RNA into message-sense RNA for translation. The 5' end of the message-sense RNA contains heterogenous, nonviral sequences which are believed to be scavenged from cytoplasmic host cell messages. In addition, these message-sense RNAs have been found to be truncated since they lack the sequences which are complementary to the 5' terminus of the viral-sense RNA (Eshita *et al.*, 1985). These messages are then translated into viral proteins on host ribosomes. A full length, positive or plus strand of RNA is formed when the negative strand is replicated. This plus strand is replicated to form the negative strand which is then packaged with the viral proteins.

HTV, following its initial propagation in A-549 cells, was shown to be sensitive to lipid solvents and to be acid-labile, which is indicative of an enveloped virus (French *et al.*, 1981). Soon after this, the morphological appearance of HTV was reported simultaneously by two groups (White *et al.*, 1982 and McCormick *et al.*, 1982). The virus appeared to be spherical to oval in shape having a unit membrane envelope with surface projections and was 80 to 115 nm in diameter. The buoyant density of the virus was between 1.15 to 1.19 gm/ml. These features and the overall appearance of the virus were comparable to viruses classified in the Bunyaviridae family, yet HTV was not recog-

FIGURE 2

Schematic diagram of Bunyavirus transcription and translation. Upon entry into the cell, the L protein (RNA polymerase) transcribes the negative(genomic)-sense RNA of the virus into positive(message)-sense RNA. These messages are capped and translated to produce the proteins needed for replication and packaging of the virus. The negative-sense RNA's are also replicated to produce full length positive strands which are copied to produce the negative-sense (genomic) RNA for packaging. The darkened area at the 5' end of the message-sense RNA represents sequences "stolen" from the 5' end of cellular mRNA.

BUNYAVIRUS TRANSCRIPTION AND REPLICATION STRATEGIES



nized by antibodies to other bunyaviruses.

Further characterization was possible only after HTV was adapted to growth in Vero E6 cells, which produced higher virus yields (Schmaljohn *et al.*, 1983a). Purified virions from these cultures, disrupted with a nonionic detergent, released three distinct nucleocapsids which were shown to be associated with a single protein species of approximately 50 kilodaltons (KDa). Each nucleocapsid contained a single RNA molecule with apparent molecular weights of 2.7, 1.2, or 0.6×10^6 and designated L, M, and S, respectively. Oligonucleotide maps revealed each of these RNA species to be unique (Schmaljohn *et al.*, 1983b). The Bunyaviridae is the only animal virus family known to contain a tripartite, single-stranded RNA genome. In common with other members of the family, the HTV virion has been found to contain an RNA-dependent RNA polymerase. Additionally, the encapsidated RNA was found to be sensitive to ribonucleases, similar to other members of the Bunyaviridae and to viruses of the Orthomyxoviridae, but unlike Rhabdoviridae members. On the basis of all of these findings, it became clear that HTV should be classified into the Bunyaviridae family. However, it must represent a separate genus, since HTV does not have serological relationships with other known bunyaviruses and was also rodent-, rather than arthropod-transmitted.

Viruses within a genus of the Bunyaviridae have glycoproteins and nucleocapsid proteins of similar size. Elliott *et al.* (1984) have investigated the virion and cell-associated proteins of Hantaan virus. The four proteins found were of apparent molecular weights 200 KDa, 72 KDa, 56 KDa, and 45 KDa. The 45 KDa protein was associated with the nucleocapsid and is slightly smaller than the value reported earlier (Schmaljohn *et al.*, 1983a). The 72 KDa and 56 KDa proteins were shown

to be glycoproteins and were termed G_2 and G_1 , respectively. The 200 KDa protein was assumed to be the L protein or RNA transcriptase. The apparent molecular weights of the HTV glycoproteins and nucleocapsid protein were unique amongst the Bunyaviridae genera. This supports the classification of HTV in a separate genus.

Viruses within a genus of the Bunyaviridae also contain a unique sequence at the 3' terminus of each strand of genomic RNA, and viruses can be assigned to a particular genus based on this sequence (Clerx-van Haaster et al., 1982). The three RNA strands of HTV were found to contain a common 3' terminal sequence: 3'-AUCAUCAUCUG (Schmaljohn et al., 1983b). This sequence was distinct from the 3' sequences reported for other genera of the Bunyaviridae. Predictably, this identical sequence was found on the 3' terminus of all other Hantaan-related viruses (Schmaljohn et al., 1985). Thus, the existence of a new genus was defined based on the lack of serological relationships, the different mode of transmission, the molecular weights of the RNAs and proteins, and the unique 3' terminal sequences of the genomic RNAs.

The morphogenesis of bunyaviruses occurs on internal cellular membranes, in or adjacent to the Golgi structures (Smith and Pifat, 1982). Prior to morphogenesis, the viral glycoproteins are synthesized in the endoplasmic reticulum and transported to the Golgi for glycosylation. In addition, the synthesized nucleocapsid protein encapsidates the replicated, genomic RNA. Smith and Pifat (1982) believe the initial event in morphogenesis occurs when the cytoplasmic nucleocapsid structures recognize a transmembranal sequence of the glycoproteins. What follows then is the envelopment of the three nucleocapsid structures and the internal protein(s) of the virus. The details of how the proteins and the correct number and type of RNA segments are packaged is

unknown (Obejeski and Murphy, 1977).

Kuismanen *et al.*, 1982 showed that the glycoproteins and the nucleocapsid protein accumulated in the Golgi. In tunicamycin-treated cells, the glycoproteins accumulated in the endoplasmic reticulum and the nucleocapsid protein associated with them (Kuismanen *et al.*, 1984). Thus the site of viral maturation appeared to be determined by the location of the glycoproteins. In the final stage of maturation, viruses are transported to the cell surface in vesicles derived from the Golgi. These vesicles fuse with the plasma membrane and infectious virus is released.

The specific features of the morphogenesis of HTV have been difficult to describe experimentally, since viral maturation is not easily visualized even in cells that display viral antigen by fluorescent antibody staining (Schmaljohn *et al.*, 1986a). Studies using Hantaan-related viruses isolated in China have been more successful and have provided some information on viral morphogenesis (Hung *et al.*, 1983a, b; 1985). As with other bunyaviruses, there was no evidence of plasma membrane budding; however, the Golgi seemed to be less involved than with the other bunyaviruses. Rather, virions appeared to bud from vesicles of the endoplasmic reticulum, although a viral antigen layer was also found on the cell surface. Hung *et al.* (1985) also found a greater variation in particle size than previously reported and many aberrant particles were observed including tailed particles and rod-like structures.

The most unusual feature of the electron microscopy studies is the recent finding of inclusion bodies in infected cells (Hung *et al.*, 1987). Previously, inclusion bodies have been described for only one other bunyavirus, Rift Valley Fever virus (*Phlebovirus* genus). Three

types of HTV inclusions are described based on appearance: granular, granulofilamentous, and filamentous. The inclusions are found only in the cytoplasm, often in close association with the rough endoplasmic reticulum and Golgi. The authors suggest that the inclusion bodies represent either aggregates of virions or accumulations of virus-related precursors. The meaning of these findings is unclear, but Hung *et al.* (1987) believe that their findings more closely resemble observation from arenavirus-infected, rather than bunyavirus-infected, cell cultures. This is a surprising assertion and may indicate that members of the Hantavirus genus may have a more complex pathway of morphogenesis than other members of the Bunyaviridae.

Electron microscopy studies of the Bunyaviridae have shown that the isolated nucleocapsid structures are circular, and the RNA in the intact nucleocapsid structure to be sensitive to RNases (Obijeski *et al.*, 1976). When the RNAs are isolated from the nucleocapsid structures, the RNAs themselves are circular (Hewlett *et al.*, 1977). The circular RNA remains RNase-sensitive and is not associated with DNA or protein, since digestion with DNases or proteinase K had no effect on the circular structure. The circles appear to be stabilized by hydrogen bonding, as opposed to being covalently linked, for treatment with formamide or glyoxal destroys the circles.

Viruses of the Bunyaviridae family possess a 5' terminal sequence complementary to the sequence conserved at the 3' terminus. The extent of the complementary sequence varies from virus to virus: for example, snowshoe hare virus (Bunyavirus genus) S segment has 24 of 26 terminal nucleotides complementary (Obijeski *et al.*, 1980), Punta Toro virus (Phlebovirus genus) S segment has 16 of 24 (Ihara *et al.*, 1984), and Bunyamwera virus (Bunyavirus genus) M segment has 17 of 18 (Lees *et*

al., 1986). These complementary sequences are probably responsible for the circular nature of the RNA (Bishop et al., 1982). The importance of these structures, however, is not known, although a role in genomic replication has been postulated (Hewlett et al., 1977), as well as a role in encapsidation of the RNA (Bishop and Shope, 1979).

The three segments of Bunyaviridae RNA have been shown to contain unique genetic information; in other words, the smaller segments were not duplications of sequences in the largest segment (Pettersson et al., 1977). Since there were three segments and four known structural proteins (L, G₁, G₂, and N), it was postulated that at least one segment must code for more than one protein. The assignment of a viral encoded protein to a particular RNA segment was accomplished using recombinant viruses (Gentsch et al., 1978 and 1979). The segmented genome of the bunyaviruses allows some reassortment to occur in mixed infections. By isolating and characterizing recombinant viruses, Gentsch et al. (1978, 1979) were able to assign the coding of the nucleocapsid protein to the S segment and the coding of the glycoproteins to the M segment. It followed, therefore, that the L segment must code for the L protein, the RNA-dependent RNA polymerase, although there was no evidence to prove it directly.

Recently obtained sequencing data has supported the coding assignments derived from this genetic work. Sequences of the M segment from four bunyaviruses (Eshita and Bishop, 1984; Collett et al., 1985; Ihara et al., 1985; and Lees et al., 1986) have shown that it contains one large opening frame (ORF). This ORF encodes a single polyprotein which may be subsequently proteolytically cleaved, resulting in the formation of the two glycoproteins (G₁ and G₂) and, in some cases, a third protein which is nonstructural.

The function of the M segment nonstructural protein is unknown, while the glycoproteins have been shown to have important roles. For example, the efficient transmission of virus from mosquito to vertebrate appears related to products of the M segment (Beaty *et al.*, 1981). The products of the M segment have also been shown to be major determinants of virulence *in vivo* (Shope *et al.*, 1981 and Janssen *et al.*, 1986). The immunological response of the host to the M segment proteins is clearly critical. Neutralizing antibodies directed against bunyaviruses are elicited by the products of the M segment (Gentsch *et al.*, 1980) or to one of the glycoproteins specifically (Gonzalez-Scarano *et al.*, 1982).

The sequencing data of Bunyaviridae S segments has revealed novel coding strategies producing two proteins: the nucleocapsid protein and a nonstructural protein. The S segment of three of the members of the Bunyavirus genus has been sequenced. All three viruses use similar means to encode more than one protein from the S segment. The coding strategy of the Bunyavirus genus is exemplified in the open reading frames (ORF) of Aino virus (Figure 3). The RNA encodes two proteins on (viral complementary) mRNA (Akashi *et al.*, 1984). One protein begins at an initiation codon at nucleotide 35 and the second protein (in a different reading frame) begins at nucleotide 61. The proteins are thus read from overlapping reading frames. It has yet to be determined whether the proteins are translated from separate mRNAs or from the same mRNA using the two different initiation codons (Akashi *et al.*, 1984).

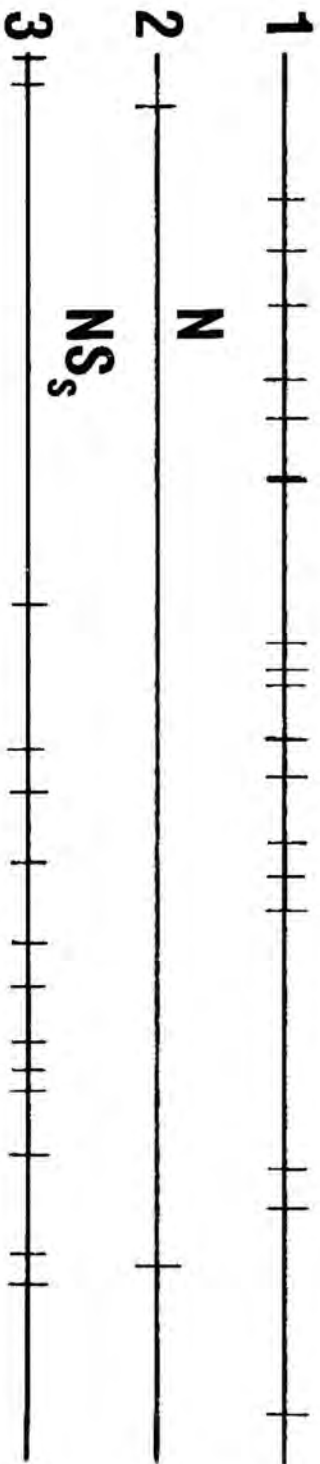
In contrast to this coding strategy is the strategy employed by Punta Toro virus, a member of the Phlebovirus genus. Sequence analysis has shown the S segment of this virus to encode two proteins in a unique manner (Ihara *et al.*, 1984). The reading frame (Figure 4) for the

FIGURE 3

Schematic representation of the coding strategy of the S segment of Aino virus (Bunyavirus genus). Each horizontal line represents one of the possible reading frames (1-3) of the S segment of Aino virus in the viral-sense RNA (vRNA) or the message-sense RNA (vcRNA). The vertical bars represent the position of translation termination codons. N refers to the open reading frame (ORF) of the nucleocapsid protein, while NS_s refers to the ORF of a nonstructural protein of unknown function. From Akashi et al. (1984).

OPEN READING FRAMES

AINO-vRNA



AINO vCRNA

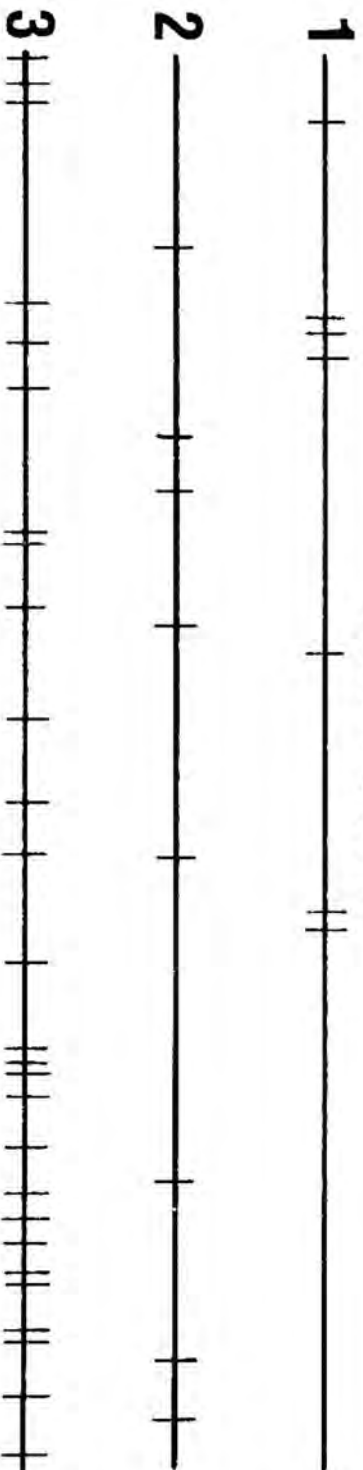
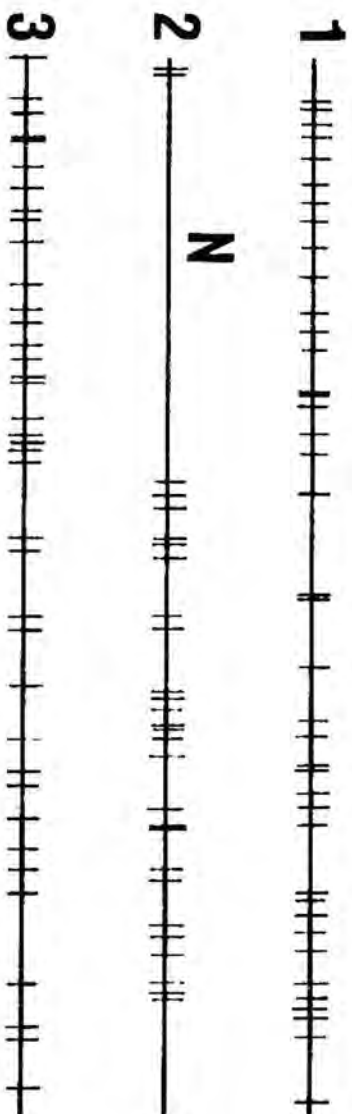


FIGURE 4

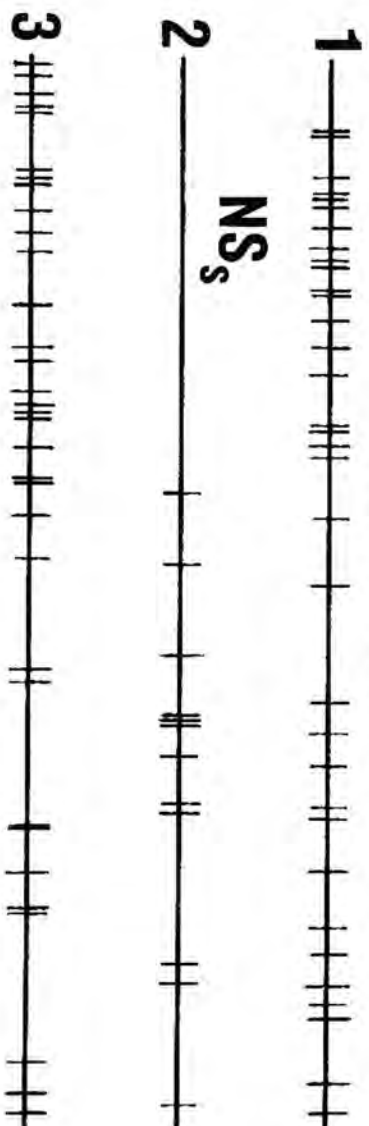
Schematic representation of the coding strategy of the S segment of Punta Toro virus (Phlebovirus genus). See Figure 3 for explanation of figure. N is the nucleocapsid protein, while NS_s is a nonstructural protein of unknown function. From Ihara et al. (1984).

OPEN READING FRAMES

PT S vcrRNA



PT S vRNA



nucleocapsid protein is found on a viral-complementary mRNA, while the reading frame for the nonstructural protein is contained in viral-sense mRNA. The term "ambisense" has been coined to describe this RNA, since both senses of the RNA encode proteins. The S segment of other Bunyaviridae genera have not been sequenced to determine the number of proteins encoded, or whether these or other unique strategies are used to encode more than one protein from the RNA segment.

A role for the nonstructural protein of the S segment has not been found, despite its being encoded in all sequenced S segments of the Bunyaviridae. Similarities in hydropathy plots and location of charged amino acids have been described for the S segment nonstructural proteins of three members of the Bunyavirus genus, suggesting some similarity in function (Akashi et al., 1984). The S segment nonstructural protein of Punta Toro virus has been identified in cells, in virions, and in the nucleocapsid structure (Overton et al., 1987). Although only small quantities of the protein are found in each location, the relative proportion of it and of the nucleocapsid protein are similar and suggest a specific association of the protein with the nucleocapsid structure.

The nucleocapsid protein has been much more closely studied. The association of this protein with the genomic RNA is known, but the exact mechanisms of encapsidation have not been elicited. The immunological importance of the products of the S segment seems less critical, as compared to the M segment products. Antibodies to the nucleocapsid protein do not neutralize the virus (Gonzalez-Scarano et al., 1982). Recently, however, the nucleocapsid protein of other RNA viruses (vesicular stomatitis virus and influenza virus) has been shown to be important in generating cytotoxic T cells in response to viral infection (Townsend et al., 1984). Whether this role for the nucleo-

capsid protein is significant in bunyavirus infections has not yet been determined, but certainly bears investigation.

Purpose

The general purpose of this work was an analysis of the coding strategy of the M and S RNA segments of the HTV genome. This analysis initially involved sequence determination of the cDNA clones from the M and S RNA segments of HTV, to determine the identity of the proteins encoded and the genetic organization of the genome. The ability of the cDNA clones to produce experimentally the encoded proteins was then studied using in vitro and in vivo expression systems. Finally, the expression of HTV proteins from their isolated genes allowed the study of their individual functions. Based on this, a potential HTV vaccine was constructed and preliminary testing was initiated.

MATERIALS AND METHODS

Cells

Four eukaryotic cell lines were used. The E-6 clone of Vero cells (ATCC #C1008) was used to produce cell lysates of Hantaan virus-(HTV) infected cells. A CV-1 clone, developed by S. Hastings, U.S. Army Medical Research Institute for Infectious Disease (USAMRIID), was used in the plaque-reduction neutralization test (PRNT) of HTV. Recombinant vaccinia viruses were grown and selected in human 143 TK⁻ cells (Rhim et al., 1973) and CV-1 cells (ATCC #CCL 70). Eagle's minimal essential media (EMEM, Flow Laboratories Inc., McLean, VA) supplemented with 5% (v/v) fetal bovine serum (Gibco Laboratories, Grand Island, NY) and penicillin/streptomycin (100,000 units/liter penicillin and 100,000 µg/liter streptomycin) was used to maintain cell lines at 37°C in 5% CO₂. Human TK⁻ 143 cells were occasionally grown in the presence of 25 µg/ml of 5-bromo-2'-deoxyuridine (BUDR, Sigma, St. Louis, MO). Cells were grown in plasticware from Becton Dickenson Labware, Oxnard, CA or Costar, Cambridge MA.

Viruses

HTV, strain 76-118, isolated by Dr. H.W. Lee, was provided by Dr. J.M. Dalrymple, USAMRIID, and used at a P-3 level of containment. Vaccinia virus, strain WR, and the recombinant vaccinia virus containing the beta-galactosidase gene, vSC 8, were provided by Dr. B. Moss, NIH. Recombinant vaccinia virus, vMP2, containing the HTV M segment cDNA and expressing both HTV glycoproteins, was supplied by Dr. M. Pensiero, USUHS. All vaccinia virus recombinants were harvested two days after

infection. Cells were scraped, pelleted at 150g for 5 minutes in the IEC HN-SII centrifuge, and resuspended in maintenance medium. Following three cycles of "freeze-thawings" (-70°C to 37°C), the cells were sonicated and vaccinia virus titers determined by plaque assay on CV-1 cells (Mackett et al., 1985a). Gradient-purified virus was prepared as described by Mackett et al. (1985a).

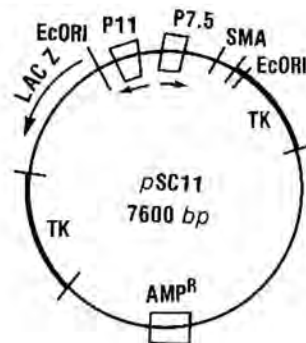
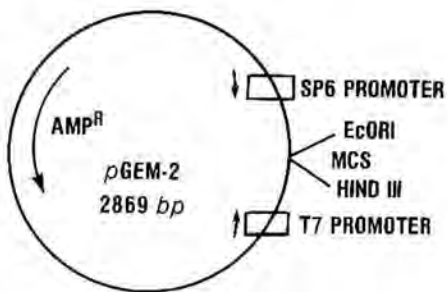
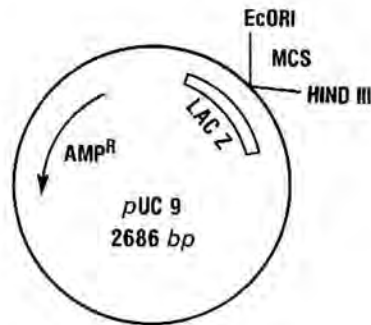
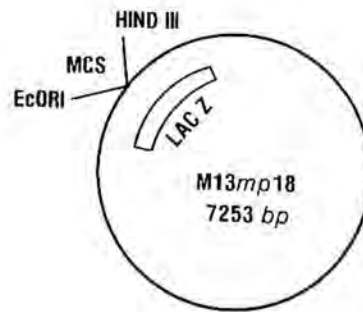
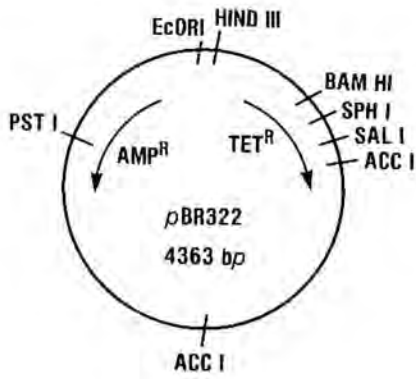
Plasmids

Several plasmids were used during the course of these experiments (Figure 5). The original HTV cDNA clones were inserted into pBR322 plasmid (Bolivar et al., 1977) as described below. Initial subcloning of the HTV cDNA was carried out in the pUC9 plasmid (Vieira and Messing, 1982). This plasmid has a "multiple cloning site" (see Figure 5) within a beta-galactosidase gene (Lac). Insertion into this site results in the inability of the bacterial colony to generate a blue color reaction with 5-bromo-4-chloro-3-indolyl-beta-D-galactoside (XGal, Bethesda Research Laboratories (BRL), Gaithersburg, MD). White transformed bacteria were selected on agar plates containing ampicillin, Xgal, and the Lac inducer, isopropylthio-beta-D-lagactoside (IPTG, BRL). The Gemini plasmid, pGEM-2, (Promega Biotec, Madison, WI) was used for in vitro transcription. In pGEM-2, a multiple cloning site is flanked on either side by the promoters for SP6 or T7 RNA polymerase. E. coli transformed by this plasmid were selected in the presence of ampicillin.

The replicative or double-stranded form of the DNA from the M13 bacteriophage has been modified to be used as a cloning plasmid vector for "dideoxy" DNA sequencing (Yanisch-Perron et al., 1985). As with the pUC9 plasmid, M13mpl8 and mpl9 have a multiple cloning site within the Lac gene. Clear recombinant plaques were therefore selected in the

FIGURE 5

Schematic diagram of cloning plasmids used in this study. The five plasmids (pBR322, M13mpl8, pUC9, pGEM-2, and pSC11) are shown with pertinent restriction endonuclease cleavage sites. Also illustrated is the relationship of cloning sites to genes for antibiotic resistance (Tet^R, Amp^R) or Lac expression. Plasmids are not drawn to scale, but sizes are given in base pairs (bp). The multiple cloning site (MCS) of M13mpl8 is arranged as follows: EcoR I, Sst I, Kpn I, Sma I, Bam HI, Sal I, Pst I, Sph I, and Hind III. For the M13mpl9 vector the orientation is reversed. The MCS for pUC9 and pGEM-2 is as follows: Hind III, Pst I, Sal I, Bam HI, Sma I, and EcoR I. TK refers to the vaccinia virus thymidine kinase gene, while P11 and P7.5 are vaccinia virus promoter sequences for an 11,000 dalton and 7,500 dalton protein, respectively. Amp is ampicillin, Tet is tetracycline, and LacZ is the gene for beta-galactosidase.



presence of XGal and IPTG. The initial cloning vector used for vaccinia virus recombinant production is the plasmid pSC 11 (Chakrabarti *et al.*, 1985). This ampicillin-resistant plasmid contains a unique cloning site (Sma I) adjacent to the P 7.5 vaccinia promoter. Under the control of a separate promoter (P11) is the entire coding sequence for the Lac gene. The site for insertion of foreign genes and the Lac gene are flanked by the two halves of the vaccinia virus thymidine kinase (TK) gene. Upon transfection of vaccinia virus-infected cells with the pSC11 plasmid, homologous recombination occurs between the TK sequences within the plasmid and the TK gene of wild type vaccinia virus. Recombinant viruses are therefore TK⁻, and produce beta-galactosidase under the control of the vaccinia P11 promoter. These viruses grow in the presence of BUdR and produce blue plaques in the presence of XGal. A diagram of pSC11 is shown in Figure 5.

Prokaryotic cells used in these experiments for plasmid propagation were the *E. coli* K-12 strains JM103, HB101, and DH5alpha. The strain JM103 (Δ lacpro, thi, strA, sbcB15, F' traD36, proAB, hsdR⁻, supE, endA, lacI^q Δ lacM15; Messing *et al.*, 1981) was used in all M13 and pUC9 cloning. The DH5alpha strain [hsdR17(r⁻, m⁺), supE44, thi-1, λ recA1, gyrA96, endA1, relA1, F⁻, lacI^q Δ lacM15; BRL], used in the pSC11 cloning, was made competent by the procedure of Hanahan *et al.* (1983) and obtained from BRL. The strain HB101 [hsdS20(r⁻, m⁻), hsdM⁻, lacZ4, leuB6, supE4, proA2, str^R, thi⁻¹ recA, Gal⁻; Boyer and Roulland-Dussoix, 1969] was used in the initial cDNA cloning involving the pBR322 plasmid (see below) and in the pGEM-2 plasmid cloning. All *E. coli* strains were grown in Luria-Bertani (LB) medium or M9 medium, made as described by Maniatis *et al.* (1982). LB medium could also be used to make agar plates by the addition of 12 gm/l Bacto-Agar (Difco Labora-

tories, Detroit, MI). Ampicillin (Sigma) was added to the LB media at a concentration of 200 µg/ml. SOC media used for the DH5alpha strain was made as per BRL's specifications.

HTV cDNA clones

The cDNA clones, M-17, S-16, S-8, and S-86, were constructed by Dr. C. Schmaljohn (Schmaljohn *et al.*, 1986b, 1987a). Briefly, synthesis of the first strand of the cDNA was primed by an oligonucleotide complementary to seventeen bases at the 3' end of the HTV RNA. The primer for the S RNA was 5'-TAGTAGTAGACTCCCTA-3', while the primer for the M RNA was 5'-TAGTAGTAGACTCCGCAA-3'. After incubation in the appropriate reaction mixture, the RNA template was degraded in NaOH, single-stranded cDNA was recovered and converted to double-stranded DNA. The cDNA was S1 nuclease-treated and tailed with oligo-dCMP before cloning into PstI-cleaved, oligo-dGMP-tailed pBR 322. Bacteria transformed by pBR322 were screened on the basis of tetracycline resistance. Colonies containing inserts were identified by probing with the above mentioned oligonucleotides or with cDNA probes prepared from gel-purified HTV RNA with random DNA primers.

Isolation of DNA

Three methods of isolating DNA were used depending on the source and subsequent use of the DNA. Large quantities of plasmid DNA for restriction enzyme digests, transcriptions, transfections, and subclonings were obtained by cesium chloride-ethidium bromide density gradient centrifugation in a modified method of Maniatis *et al.* (1982). Bacteria containing pBR322 plasmids were inoculated into 20 ml M-9 medium with 20 µg/ml tetracycline and grown overnight at 37°C with

shaking. This overnight culture was used to inoculate one liter of M-9 medium. The bacterial culture was grown to an A_{600} of 0.4-0.5, at which time 150 mg of chloramphenicol was added. The liter culture was then incubated overnight. All bacterial transformants containing other plasmids were simply inoculated directly into one liter of LB broth and grown overnight. The bacteria were pelleted at 5858g in the Sorvall GSA rotor for ten minutes. The pellet was washed in 10mM Tris-HCl pH 7.5, 0.1M ethylenediaminetetraacetic acid (EDTA) and repelleted. The cells were resuspended in 5 ml cold 50mM Tris-HCl pH 8.0, 25% (w/v) sucrose and 50 mg lysozyme (Sigma) was added. After a 15 minute incubation on ice, 8 ml of TET (0.4% (v/v) Triton-100, 0.06% (w/v) EDTA, and 0.1M Tris-HCl pH 8.0) was added. This mixture was incubated on ice for 15 minutes, then at 50°C for 5 minutes. The lysate was centrifuged at 43,140g in the Sorvall SS-34 rotor for 45 minutes. To the supernatant was added 0.97 gm CsCl (BRL) and 0.043 ml ethidium bromide (10 mg/ml) each, per ml of supernatant. This was centrifuged in the TI-50 rotor at 107,000g for 40 hours. The DNA was visualized with ultraviolet light and the lower plasmid band collected through the top of the tube using a capillary tube and peristaltic pump. The collected band was diluted in 2.5 volumes of water and precipitated with 95% (v/v) ethanol at -70°C. The DNA was pelleted at 11,950g in the Sorvall SS-34 rotor for 10 minutes and resuspended in TE (10mM Tris-HCl pH 7.5, 1mM EDTA). The DNA was treated with an equal volume of redistilled phenol, phenol-chloroform (50/50 v/v), and chloroform and ethanol-precipitated. DNA was resuspended in TE and stored at -20°C.

M13 single-stranded DNA was purified for sequencing from recombinant extracellular phage. A 1/100 dilution of an overnight culture of JM103 was grown in LB broth until growth became visible to

the naked eye (approximately 1 hour). Two ml of this culture were added to an M13 phage preparation, either an isolated plaque picked from an agar plate or a previously prepared, infected cell supernatant. The culture was then incubated with shaking at 37°C for 5 hours. Bacteria were removed by centrifugation at 2250g in the IEC centrifuge for 10 minutes. A portion of the supernatant was saved at 4°C for future isolations, while 1200 µl were added to 350 µl of 20% (w/v) polyethylene glycol containing 2.5M NaCl. After room temperature incubation for 30 minutes, phage was pelleted at 11,500g for 10 minutes. The phage was resuspended in TE and treated with an equal volume of phenol, phenol-chloroform, and chloroform. The DNA was precipitated with 95% (v/v) ethanol, washed with 95% (v/v) ethanol, and resuspended in 25 µl of TE.

DNA was isolated from eukaryotic cells as follows. Uninfected and vaccinia virus-infected cells in 60 mm dishes were washed with phosphate-buffered saline (10x PBS; 1.7M NaCl, 0.03M KCl, 0.2M NaHPO₄, 0.02M KH₂PO₄ pH 7.4), scraped, and centrifuged at 150g for 5 minutes in the IEC HN-SII centrifuge. The pellet was resuspended in 500 µl TE with 1% (w/v) sodium dodecyl sulfate (SDS) and 50 µl of proteinase K (1 mg/ml). This was incubated at 37°C for 1 hour and then treated with phenol, phenol/chloroform, and chloroform. Following ethanol precipitation, the DNA was resuspended in 50 µl of TE.

Restriction endonuclease digestion of DNA

DNA was digested with various restriction endonucleases (BRL; Boehringer Mannheim Biochemical, Indianapolis, IN; New England Biolabs, Beverly, MA; Pharmacia, Piscataway, NJ). The buffer used for digestion was that recommended by each company for its specific enzyme preparation. Digestions were carried out at 37°C except for the Sma I enzyme,

which was incubated at 25°C. With the exception of partial digestions, reactions were incubated for 1 hour and stop buffer (10x: 20% (w/v) Ficoll 400, 100mM EDTA, 40 µg/ml bromophenol blue, 40 µg/ml xylene cyanol) added before gel electrophoresis. For partial digestions, portions of the reaction mixture were removed at the indicated times, stop buffer added, and incubated on ice until electrophoresis. When two enzymes were required to digest the DNA, the enzymes were added simultaneously if they required the same buffer. If the required buffers were incompatible, the enzyme with the lower NaCl requirement was first used, corrections made in the buffer, the second enzyme added, and the reaction incubated for an additional hour. If Sma I was the first enzyme in a double digest, it was inactivated following digestion with phenol treatment. The DNA was then ethanol-precipitated, resuspended in TE, and digested with the second enzyme.

Exonuclease Bal 31 digestion of DNA

Plasmid DNA (M-17) was digested with the exonuclease Bal 31 to generate a series of overlapping, variable-length inserts for subcloning into M13mp18 or mp19 (Poncz et al., 1982). Following digestion with Bgl I, the DNA was treated with 5.0 units of Bal 31 at 30°C in a Bal 31 buffer (20mM Tris-HCl pH 7.2, 0.6M NaCl, 12.5mM MgCl₂, 12.5mM CaCl₂, and 1mM EDTA). Aliquots were removed at the appropriate times and the reaction stopped by adding an equal volume of 40mM ethyleneglycol-bis-(beta-amino-ethyl ether)N,N'-tetraacetic acid (EGTA). The DNA in each aliquot was precipitated with 95% (v/v) ethanol, resuspended in TE, and digested with Pst I. The fragments were separated by agarose gel electrophoresis, the desired fragment excised from the gel, and the DNA extracted as described below.

Gel electrophoresis

Following restriction endonuclease digestions, DNA fragments were separated by electrophoresis on horizontal, 1% (w/v) agarose gels (20 x 25 cm). Gels were electrophoresed at 40 volts overnight on a BRL model H1 or H4 apparatus using a Tris-borate-EDTA buffer (TBE; 0.089M Tris, 0.089M boric acid, 2mM EDTA, pH 8.0). The DNA was visualized by staining the gel with an ethidium bromide solution (1 µg/ml) for approximately 15 minutes and viewing it in ultraviolet light. Gels were photographed with a Polaroid MP-4 camera using a 254 nm ultraviolet light source and Polaroid type 55 positive-negative film. The molecular weights of fragments were determined by comparison with fragments of known molecular weight. DNA standards used were lambda DNA digested with Hind III, phage ϕ X174 DNA digested with Hae III, and a 1 kilobase (KB) ladder (BRL).

Polyacrylamide gels were used to separate oligonucleotide fragments following M13 "dideoxy" sequencing (Sanger and Coulson, 1978). An 8% (w/v) polyacrylamide concentration was used, cross-linked with a 1:20 ratio of bis (N,N' methylene-bis-acrylamide) to polyacrylamide in sequencing TBE buffer (STBE; 0.05M Tris, 0.04M boric acid, 1mM EDTA pH 8.3). To denature the DNA, urea was added to a final concentration of 8M and the solution filtered through a 0.45 µm filter. Polymerization was initiated by the addition of 50 mg of ammonium persulfate and 50 µl of tetramethylethylenediamine (TEMED, Bio Rad Laboratories, Richmond, CA) both per 75 mls of acrylamide. The gels were 33 x 42 cm and 0.4 mm thick and wells were formed with a "sharkstooth" comb (BRL). Gels were allowed to set overnight and then pre-electrophoresed at 1000 volts for 1-2 hours in STBE buffer on a BRL Model S0 Sequencing Gel Apparatus. After loading the samples, the gels were electrophoresed at 2000 volts

until the bromophenol blue marker dye had migrated three-quarters of the gel length. Occasionally the samples were reloaded and electrophoresis continued to obtain further sequences on one gel. After stopping the electrophoresis, the glass plates were separated and the gel transferred to cardboard, after soaking in a solution of 5% (v/v) acetic acid and 5% (v/v) methanol for 20 minutes. The gel was dried overnight with vacuum and heat using a slab gel dryer (Model SE 1150, Hoefer Scientific Instruments, San Francisco, CA) and then exposed to Kodak (Rochester, NY) X-Omat RP radiograph film (35 x 43 cm).

Polyacrylamide gel electrophoresis (PAGE) of proteins was based on a procedure developed by Laemmli (1970). A stock acrylamide solution (29.2% (w/v) acrylamide, 0.8% (w/v) bis) was diluted in water and buffer to give a final mixture concentration of 10 or 16% (w/v) acrylamide, 0.1% (w/v) SDS, 0.38M Tris-HCl pH 8.8, 0.033% (w/v) APS, and 0.05% (v/v) TEMED. Following polymerization, the gel was covered with buffer and allowed to set overnight. The buffer was washed away with distilled water and the gel layered with a "stacking gel" (4.5% (w/v) acrylamide, 0.1% (w/v) SDS, 0.125M Tris-HCl pH 6.8, 0.03% (w/v) APS, 0.3% (v/v) TEMED). The gel, 16 x 20 cm and 1.0 mm thick, was electrophoresed on a Protean II system (Bio-Rad Laboratories, Richmond, CA) in a buffer of 0.025M Tris-glycine, pH 8.5, 0.1% (w/v) SDS. Samples containing 1x disruption buffer (5x: 0.25M Tris-HCl pH 7.0, 1.43M beta-mercaptoethanol (BioRad), 10% (w/v) SDS, 15% (w/v) sucrose, 40 µg/ml bromophenol blue) were electrophoresed at 20 mAmps through the stacker and at 30 mAmps thereafter until the dye front had reached the bottom of the plates. The apparent molecular weight of the protein was approximated by comparison to protein molecular weight standards (BRL; low or high range; 3-200 KDa).

RNA was electrophoresed in 1.5% (w/v) agarose gels containing 6% (v/v) formaldehyde in MOPS buffer (20mM 3-(N-Morpholino)propanesulfonic acid (MOPS), 5mM sodium acetate, 1mM EDTA, pH 7.0) (Ostrove *et al.*, 1985). The gel, 14 x 16 cm and 3 mm in width, was electrophoresed on a vertical slab gel unit (Model SE 600, Hoeffer Scientific Instruments, San Francisco, CA). RNA was heated at 60°C for 10 minutes in MOPS buffer with 50% (v/v) formamide and 6% (v/v) formaldehyde. Xylene cyanol (1 mg/ml) was added and the RNA then electrophoresed at 30 mAmps until the dye marker was at the bottom of the gel. The radiolabeled RNA was visualized after exposed to radiographic film (Kodak).

Purification of DNA fragments from agarose gels

DNA was extracted from agarose gels using an analytical electroeluter (Model UEA, International Biotechnologies, Inc., New Haven, CT) and following the manufacturer's protocol. The DNA in the gel was visualized using ethidium bromide and the agarose containing the required band was excised. The electroeluter was filled with TBE buffer and the V-shaped wells filled with 7.5M ammonium acetate containing bromophenol blue. The gel slice was placed in the gel receptacle and electrophoresed at 100 volts for 60 minutes. Using a tuberculin syringe, the ammonium acetate solution was removed and DNA precipitated with 2-2.5 volumes of 95% (v/v) ethanol at -20°C overnight. The DNA was pelleted at 11,500g for 10 minutes, washed with 95% (v/v) ethanol, dried and resuspended in TE. A sample was electrophoresed to determine the percent recovery and to check the purity of the DNA fragment.

Molecular cloning of DNA fragments

Plasmid DNA was cut with a restriction enzyme to give ends

compatible with the isolated DNA fragment. If necessary, a fragment with a 5' overhang was changed to a blunt-ended fragment by incubation with 5 units of the large fragment of DNA Polymerase I (Klenow fragment, BRL) in 7mM Tris-HCl pH 7.5, 7mM MgCl₂, 1mM dithiothreitol (DTT), 2mM each dNTP in a total reaction volume of 25 μ l. After the mixture was incubated for 30 minutes at room temperature, the enzyme was inactivated at 70°C for 5 minutes. The fragment was mixed with the plasmid at different ratios to obtain optimal concentrations for ligation. To this mixture was added 2 units of T4 DNA ligase (BRL), ligase buffer (BRL, 25mM Tris-HCl pH 7.6, 5mM MgCl₂, 5% (w/v) polyethylene glycol, 1mM ATP, 1mM DTT) in a final volume of 20 μ l. The ligation was incubated at room temperature overnight. A portion of the ligation mix was then added to competent bacteria for transformation.

Transformation of bacteria

Bacteria were supplied as competent (DH5alpha, BRL) or made competent to take up foreign DNA by a modified method of Maniatis *et al.* (1982). Bacteria were grown to an A₆₀₀ of 0.4-0.5. The cells were pelleted at 2250g for 10 minutes in an IEC centrifuge and resuspended in a volume of 50mM CaCl₂ equal to one-half the original culture volume. The bacteria were incubated on ice for 2 hours, pelleted as above, and resuspended in a volume of 50mM CaCl₂ equal to one-twentieth the original culture volume. To each ligation sample, 0.3 ml of these competent bacteria or 20 μ l of DH5alpha were added and incubated for 30 minutes on ice. The bacteria were heat-pulsed for 45 seconds at 42°C. At this point, except for transformations with the M13 vector, 3.7 ml of LB broth with 0.2% (w/v) glucose was added to each sample (80 μ l of S.O.C. media for DH5alpha). The tubes were incubated at 37°C with

shaking for 60-90 minutes. Transformed bacteria were plated out in duplicate on LB-agar plates, containing the appropriate antibiotic, and incubated overnight at 37°C. For M13 transformations, to heat-pulsed bacteria was added 3.5 mls of 0.6% (w/v) agar in LB containing 50 µl of XGal (2% w/v), 10 µl of IPTG (25 mg/ml) and 200 µl of an overnight culture of JM103. This mixture was poured on to LB-agar plates and incubated overnight at 37°C.

Identification of recombinant plasmids containing HTV sequences

Bacterial transformants or M13 phage recombinants were screened for the presence of fragments from the original HTV M or S segment cDNA by a colony hybridization method of Grunstein and Hogness (1975). Bacteria were transferred from the original transformant plates onto Biodyne membrane, 1.2 µm, (Pall Ultrafine Filtration Corp., Glen Cove, NY) placed on LB agar plates and incubated overnight before treatment. M13 phage plaques were screened by placing Biodyne membrane directly on the original transformant plate for 5 minutes and then treating. Treatment for both types of recombinants then consisted of first placing the Biodyne membrane in a solution of 0.5M NaOH and 1.5M NaCl for 10 minutes. The Biodyne membrane was then transferred through two 1 minute and one 10 minute washes in 1M Tris-HCl pH 7.5 and 1.5M NaCl. The Biodyne membrane was rinsed in 2x SSC (1x: 0.15M NaCl, 0.01M Na citrate pH 7.0) and baked for 2 hours at 80°C in a vacuum oven. These filters were prehybridized at 50°C for 2 hours in 30% (w/v) formamide, 6x SSC, 1x Denhardt's (1966) solution (0.02% w/v Ficoll type 400, 0.02% (w/v) polyvinylpyrrolidone, 0.02% (w/v) bovine serum albumin), 0.1% (w/v) SDS, and 50 µg/ml of salmon sperm DNA. Filters were hybridized at 50°C for 2 hours in fresh prehybridization solution containing a specific, ³²P.

labeled DNA probe. The filters were then washed four times in 2x SSC at 50°C and placed in cassettes for autoradiography on XAR-5 film.

Southern blots

The blotting procedure for DNA agarose gels was a modification of the method of Southern (1975). After the gel had been stained and photographed, it was treated for 1 hour in a solution of 0.5M NaOH and 0.2M NaCl. The NaOH was neutralized by treatment of the gel for 1 hour in a solution of 1.0M Tris-HCl pH 7.5 and 0.5M NaCl. The DNA was transferred to a Biodyne membrane overnight in 6x SSC. The blot was then baked, prehybridized, hybridized, and placed to film as described above.

Radiolabeling of DNA for probes

Isolated fragments of DNA were radiolabeled with alpha-³²P-deoxycytidine triphosphate using one of two methods, as detailed by the manufacturer. In the first method, DNA was labeled by nick-translation (Rigby *et al.*, 1977) using a BRL Nick Translation Reagent Kit. Briefly, 100-500 ng of DNA was incubated with the labeled dCTP and the supplied DNA polymerase I/DNase I mix (5 µl) and the dNTP minus the dCTP mix (5 µl) in a final volume of 50 µl. The reaction was incubated at 15°C for 60 minutes. The second method, a random primer method (Feinberg and Vogelstein, 1983), uses the Multiprime DNA Labelling System (Amersham, Arlington Heights, IL). Briefly, 100-500 ng of DNA was denatured by heating to 95-100°C for two minutes and then chilled on ice. The DNA was then incubated with the labeled dCTP and the supplied buffer (15 µl) and DNA polymerase I solution (2 µl) in a total reaction volume of 50 µl. The reaction was incubated at 25°C for 3-5 hours. For both methods, radioactive ³²P-dCTP was supplied by NEN Research Products,

Boston, MA at a specific activity of >3000 Ci/mmol and 1 to 5 μ l were used per reaction. Unincorporated label was removed by precipitation of the DNA with 95% (v/v) ethanol or by spin dialysis chromatography on a Sephadex G-50 (Pharmacia) column (Maniatis *et al.*, 1982). The labeled DNA was heat denatured and used as a probe in identifying recombinant clones.

DNA Sequencing

The nucleotide sequence of the cDNA from the HTV S segment and a portion of the M segment was determined using the dideoxynucleotide chain termination method (Sanger *et al.*, 1980). Early experiments used ^{32}P -labeled nucleotides, while later experiments used ^{35}S -labeled nucleotides. The M13 universal primer, 2 ng, was annealed to 10 μ l of single-stranded recombinant DNA by incubation for 30 minutes at 70°C in 7mM Tris-HCl pH 7.5, 7mM MgCl_2 . A reaction mixture was made for each of the four nucleotides (A, C, G, and T), the concentrations varying dependent upon the labeled nucleotide used. Dideoxynucleotides (ddNTP, Pharmacia) and deoxynucleotides (dNTP, Pharmacia) were diluted in a buffer of 10 mM Hepes, 2mM DTT. Reaction mixtures for ^{32}P sequencing were as follows: A mix (150 μ M ddATP, 4.2 μ M dATP, 40 μ M dGTP, 40 μ M TTP), C mix (60 μ M ddCTP, 30 μ M dCTP, 30 μ M dGTP, 30 μ M dTTP), G mix (150 μ M ddGTP, 40 μ M dATP, 4.2 μ M dGTP, 40 μ M dTTP), and T mix (150 μ M ddTTP, 40 μ M dATP, 40 μ M dGTP, 1.7 μ M dTTP). Reaction mixtures for ^{35}S sequencing were as follows: A mix (20 μ M ddATP, 37.5 μ M dCTP, 37.5 μ M dGTP, 37.5 μ M dTTP), C mix (300 μ M ddCTP, 5.4 μ M dCTP, 54 μ M dGTP, 54 μ M dTTP), G mix (300 μ M ddGTP, 54 μ M dCTP, 5.4 μ M dGTP, 54 μ M dTTP), and T mix (600 μ M ddTTP, 54 μ M dCTP, 54 μ M dGTP, 5.4 μ M dTTP). To the primer reaction was added 1 unit of Klenow DNA polymerase, 1 μ l 0.1M DTT, and either 1 μ l of alpha- ^{32}P -

dCTP, (NEN Research Products, specific activity 400 Ci/mmol) or 1 μ l of alpha-³⁵S-dATP (NEN Research Products, specific activity 500 Ci/mmol). This was divided equally into the four reaction mixes and incubated for 15 minutes at 37°C. Then 1 μ l of a deoxynucleotide mix (250 μ M of each) was added and incubation continued for another 15 minutes. The reaction was stopped by adding 10 μ l of formamide loading buffer (deionized formamide containing 10mM EDTA, 0.3% (w/v) xylene cyanol/bromophenol blue). The samples were boiled for 5 minutes and loaded on to the gel. Sequences were analyzed on the IBM PC computer using the Sequence Analysis System (International Biotechnologies, Inc., New Haven, CT) and the Protolyze Structure Predictor (Scientific and Educational Software, Silver Spring, MD).

Preparation of synthetic oligonucleotides

Oligonucleotides corresponding to nucleotides 593-610 and complementary to nucleotides 337-357 of the HTV S segment cDNA sequence (Figures 22 and 23) were synthesized on the Applied Biosystems Model 380A DNA Synthesizer and provided by Dr. J. McGowan (USUHS). Synthetic oligonucleotides were end-labeled by incubation with 10 units of T4 polynucleotide kinase, buffer (50mM Tris-HCl pH 7.5, 10mM MgCl₂, 5mM DTT, 0.1mM spermidine, and 0.1mM EDTA), and 200 μ Ci of gamma-³²P-adenosine triphosphate (NEN Research Products) in a total volume of 25 μ l for 1 hour at 37°C. Then 40 μ l of 2M NH₄ acetate and 4 μ l (4 μ g) calf thymus DNA was added and precipitated with 160 μ l 95% (v/v) ethanol. The pellet was resuspended in 200 μ l 2M NH₄ acetate and 600 μ l 95% (v/v) ethanol and reprecipitated. The pellet was washed with 95% (v/v) ethanol and resuspend in 8 μ l TE. The labeled oligonucleotide was then purified by electrophoresis in a 20% polyacrylamide gel in STBE buffer.

Bands were visualized by autoradiography, the correct band identified using standard oligonucleotides, and the band was then excised from the gel. The DNA was extracted from the gel slice using the electroelution method described previously. The purified oligonucleotides were then used in sequencing reactions in place of the universal primer.

In vitro transcription and translation

RNA was synthesized in vitro using the Gemini System (Promega Biotec, Madison, WI) following protocols provided by the manufacturer. Briefly, linearized plasmid DNA (0.5-1.0 μ g) was incubated in a 20 μ l reaction volume containing the prescribed buffer plus 20mM DTT, 1 unit of RNasin, 0.5mM of each rNTP except rUTP, 50 μ Ci alpha- 32 P-uridine triphosphate (Amersham, specific activity 3000 Ci/mmol), and 10 units of RNA polymerase. Following a 60 minute incubation at 37°C, the RNA was electrophoresed in a formaldehyde-agarose gel to determine the approximate size of the synthesized RNA. Larger amounts of RNA were synthesized for translation reactions by increasing the reaction volume to 100 μ l while maintaining the same concentration of reagents and using unlabeled uridine triphosphate. Plasmid 403-2 was linearized with the restriction enzyme Xmn I, while plasmid 5-6-43 was linearized with Hind III. Both plasmids were transcribed with SP6 RNA polymerase to make message sense RNA. Negative sense RNA was made by linearizing plasmid 403-2 with Sal I and transcribing with T7 RNA polymerase.

The synthesized RNA was translated using a rabbit reticulocyte lysate (Promega Biotec) following the procedure outlined by the manufacturer. Briefly, 17.5 μ l of reticulocyte lysate was incubated for 60 minutes at 37°C in a final reaction volume of 25 μ l containing 1-3 μ g of RNA, 1mM amino acid mixture (minus methionine), and 50 μ Ci of 35 S.

methionine (NEN Research Products, specific activity 1200 Ci/mmol). Protein translation products were analyzed by polyacrylamide gel electrophoresis (described earlier) by loading one-half of the reaction mix following addition of 1x disruption buffer.

Formation and isolation of recombinant vaccinia virus

Monolayers of CV-1 cells in 60 mm dishes were infected with wild type vaccinia virus (strain WR) at a multiplicity of infection (MOI) of 0.05 plaque-forming units (pfu)/cell in a volume of 0.5 ml. After a virus adsorption period of 45 minutes, medium was added and the cells incubated at 37°C for 2 hours. Plasmid DNA, containing sequences to be recombined into vaccinia virus, was prepared for transfection by the calcium phosphate protocol of Graham and van der Eb (1973) and modified by Weir *et al.* (1982): 1 µg plasmid DNA and 19 µg calf thymus DNA were mixed in HEPES-buffered saline (0.14M NaCl, 5mM KCl, 1mM Na₂HPO₄·2H₂O, 0.1% (w/v) dextrose, 20mM HEPES; pH solution to 7.05 with 0.5M NaOH), and CaCl₂ added to a final concentration of 125mM in a total volume of 1 ml. This mixture was incubated at room temperature for 30 minutes. The vaccinia-infected cells were washed with serum-free medium and 0.5 ml of the DNA-CaPO₄ suspension added to the cells. After a 30 minute incubation, growth medium was added to the cells. The medium was changed 3.5 hours later and the cells were incubated for a further 48 hours. The cells were then scraped into the medium, "freeze-thawed" three times, sonicated, and titrated in TK⁻ cell monolayers. The plaque assay overlay consisted of 1% (w/v) low gelling temperature agar (SeaPlaque, FMC BioProducts, Rockland, MA) in medium with 0.025 mg/ml BUdR. After 48 hours, a second overlay consisting of 1% (w/v) agar noble (Difco) in medium with 300 µg/ml XGal was applied. Under these conditions, TK⁻

Lac⁺ (vaccinia) virus yields blue plaques. Following an overnight incubation, blue plaques could be visualized, were picked with a sterile Pasteur pipette, and then placed in 1 ml of medium. Each recombinant virus was plaque-purified three times using this technique and then grown to a high titer in CV-1 cells.

Preparation of anti-peptide antibody

An antiserum was prepared to a synthetic peptide based on the procedure of Richardson *et al.* (1985). The sequence of the peptide was deduced from the nucleotide sequence of the HTV S segment cDNA and was selected by the criteria of Palfreyman *et al.* (1984). The peptide was purchased from the laboratory of Dr. Alice Huang, Harvard University, and coupled to a protein carrier protein, keyhole limpet hemocyanin (KLH) prior to rabbit injection. The peptide (5 mg), KLH (5 mg), and 1-ethyl-3-(3-dimethylaminopropyl)carbodiimide (EDAC) were dissolved in PBS at 4°C. The reaction was incubated overnight at 4°C and then dialyzed against PBS. The rabbits were injected and serum supplied by Duncroft, Inc., Lovettsville, VA. The initial serum samples were screened by enzyme-linked immunosorbent assay, and then all subsequent serum samples were tested directly in the Western blot procedure outlined below.

Western blots

Proteins separated in polyacrylamide gels were transferred to nitrocellulose for Western blot analysis based on a method developed by Towbin *et al.* (1979). Samples to be tested were taken from 60 mm dishes of confluent, uninfected or infected cells. Cells were infected with an MOI of 0.5-1.0 pfu/cell. HTV-infected cells were harvested seven days after infection while recombinant vaccinia virus-infected cells were

harvested at 48 hours, unless otherwise noted. Cells were washed three times in PBS and lysed with 0.5 ml of 1x disruption buffer. After the lysates were fractionated by polyacrylamide gel electrophoresis, the gel was soaked for 20 minutes in the transfer electrophoresis buffer (0.012M Tris-glycine, pH 8.5 with 20% (v/v) methanol). The gel was placed in contact with nitrocellulose, 0.45 μ m, (Schleicher & Schuell, Keene, NH), sandwiched between two pieces of Whatman chromatography paper (17 mm; Ace Scientific, East Brunswick, NJ), and placed in an electrophoretic transfer apparatus (Model TE 52, Hoefer Scientific Instruments). The proteins were transferred overnight at 0.5 Amps in transfer electrophoresis buffer. Following transfer, the blots were immersed for 2 hours at room temperature in 10% (w/v) Carnation Instant non-fat dried milk in a buffer containing 0.15M NaCl, 50mM Tris-HCl, 0.05% (v/v) Tween 20, 10mM EDTA, 0.02% (w/v) Na azide, pH 7.6. All subsequent incubations and washes were carried out in this buffer. The blots were washed and then incubated with a 1:100 dilution of an appropriate antiserum in this buffer plus 1% (w/v) milk for 2 hours at room temperature. The antibody used for Western blots was rabbit antiserum prepared following injection of a synthetic peptide (see above). Excess antiserum was washed from the blots with buffer and bound antibodies detected with a 1:1000 dilution of 125 I-labeled Staphylococcus protein A (NEN Research Products, specific activity 120 μ Ci/ml) in buffer for 2 hours at room temperature. The blots were washed, dried, and placed to film (XAR 5) for autoradiography.

Indirect immunofluorescence

Cells were prepared in the following manner for examination of internal immunofluorescence. CV-1 cells were grown on sterile cover-

slips in 60 mm dishes until 50-75% confluent and then infected with an MOI of 0.5-1.0 pfu/cell of recombinant vaccinia virus. At appropriate times, cells were washed with PBS and fixed in acetone at -20°C for 10 minutes. Coverslips were stored dry at -20°C until needed. Prior to staining, cells were rehydrated in PBS for 15 minutes. Coverslips were inverted onto drops of diluted antiserum and incubated at 37°C for 30 minutes. The antiserum, provided by Dr. C. Schmaljohn (USAMRIID) was a polyclonal preparation from rabbits infected with HTV. This antiserum had been absorbed on CV-1 cells infected with the vSC8 recombinant vaccinia virus and was diluted 1:50 for these studies. Excess antiserum was removed by two 15 minute washes in PBS. The coverslips were then inverted onto drops of a 1:40 dilution of goat anti-rabbit IgG-rhodamine conjugate (Boehringer Mannheim Biochemicals) and incubated for 30 minutes at 37°C in the dark. Coverslips were washed as above and mounted on glass slides with 40% (v/v) glycerol. Cells were viewed and photographed with Kodak Ektachrome film on a Zeiss microscope equipped with a planapo objective lens (63x).

Animal studies

Animals were housed at USAMRIID under P-3 containment. Care of the animals was as described in the National Research Council's Guide for the Care and Use of Laboratory Animals. Female, 5 week old Balb/cByJ mice were divided into four groups of 10 mice each. The five groups were defined as receiving: no virus, vSC8 recombinant vaccinia virus, recombinant vaccinia virus with the HTV M segment, and recombinant vaccinia virus with the HTV S segment. The mice were inoculated on day 0 with 1×10^8 pfu of virus (or sterile saline for the uninfected control) by tail scarification using a bifurcated needle (as used for

human vaccinia vaccination). A second dose of virus was given in the same manner on day 28. Mice were bled on day 0, 14, 28, and 42 following initial vaccination. Approximately 0.5 ml of blood was taken from the retro-orbital plexus using a capillary tube. Blood samples were centrifuged at 11,500g for 10 minutes and the serum withdrawn and stored at -70°C until required.

Virus neutralization tests

Serum samples were tested for the ability to neutralize HTV and prevent plaque formation on cell monolayers. Specific mouse sera, serially diluted two-fold, were incubated at 4°C overnight with 40-50 pfu of HTV strain 76-118. All dilutions were made in medium containing 2% (v/v) fresh monkey serum. Cells were then inoculated with the mixture and incubated for 1 hour at 37°C. An overlay of 0.6% (w/v) agarose (SeaKem, FMC) in medium was applied. After a seven day incubation, plaques were stained with crystal violet. Titers were reported as the reciprocal of the highest dilution of sera resulting in greater than 80% reduction of plaques.

Immunoprecipitation

Immunoprecipitations were accomplished using a method modified by Pensiero and Lucas-Lenard (1985). Vero E-6 cells were infected with HTV at an MOI of 0.5-1.0 pfu/cell. Intracellular viral proteins were labeled with 100 µCi/ml ³⁵S-methionine (NEN Research Products) at 24 hours post infection. Prior to labeling, cells were maintained in medium without methionine for 1 hour, then pulsed for 4 hours. Cells were then washed three times in ice cold PBS and lysed in 1 ml of mRSB buffer containing 20mM HEPES-KOH pH 7.4, 1.5mM MgCl₂, 20mM KCl, 1% (v/v)

NP-40, 1% (w/v) aprotinin (Sigma), and 10 μ g/ml alpha-2-macroglobulin (Boehringer Mannheim Biochemical). Cell nuclei were removed by centrifugation at 12,000g for 5 minutes at 4°C. Cell lysates were diluted with 1 ml of mRSB and 10 μ l of pooled mouse antisera from recombinant virus-infected mice (see above). The control antiserum was that described in the IF studies. Following overnight incubation at 4°C, 100 μ l 33% (v/v) Protein A-Sepharose (Sigma) in mRSB was added and incubated for 1 hour at 4°C with end-over-end agitation. Precipitates were prepared by centrifugation at 250g for 5 minutes and washed three times in 1 ml mRSB. The pellet was resuspended in a final volume of 150 μ l l_x disruption buffer for polyacrylamide gel electrophoresis. The gel was dried with vacuum and heat using the slab gel dryer and then exposed to radiograph film.

RESULTS

Nucleotide sequence determination of the HTV M segment

The M segment of bunyaviruses codes for the glycoproteins of the virus and, in some instances, a nonstructural protein. As a major part of the proposed work for this dissertation was identification of immunogenic HTV polypeptides, our analysis of this segment was deemed critical since glycoproteins of other bunyaviruses had been shown to be important in eliciting anti-viral neutralizing antibodies. First, we believed that sequence determination of HTV M segment cDNA would provide an essential basis for further studies. Then the extent of the 3' viral-sense conserved sequences and the complementarity at the 3' and 5' termini would be determined, allowing a comparison with other bunyaviruses. From these data, the coding regions of the glycoproteins as well as their gene order, which varies amongst the bunyaviruses, would be ascertained and used in designing strategies for subsequent expression experiments.

Following cDNA synthesis of the HTV M segment RNA and its cloning into the pBR322 plasmid, our first task was to characterize the HTV cDNA inserts. Bacterial colonies containing plasmids with HTV cDNA inserts were identified by Dr. C. Schmaljohn. Colony blots were probed with synthetic oligonucleotides used for priming cDNA synthesis or with cDNA probes made from gel-purified M RNA using random DNA primers. Two of the HTV cDNA clones, M-17 and M-35, were identified as originating from the M segment. Our initial aim was to size the cDNA inserts and determine a restriction map of the M segment cDNA. This would enable us to outline a strategy for determining the sequence of the cDNA.

DNA from clones M-17 and M-35 were digested with Pst I and fragment sizes determined by comparison with marker fragments of known size electrophoresed in the same agarose gel (Figure 6). On the same gel is shown S-16, an HTV cDNA construct from the S segment (see later). The size of the Pst I inserts of HTV cDNA appeared to be approximately 870 nucleotides for M-17 and 330 nucleotides for M-35 (Figure 6, lanes b and c, respectively). M-17 was selected for further analysis as it was longer than M-35 and thus would yield more sequence data. Subsequent restriction endonuclease analysis of the clone showed an Sph I site at approximately nucleotide 500 in the M-17 insert, but no other restriction endonuclease site which might be useful in cloning into the M13 vector was found (Figure 7).

The approach used for obtaining cDNA fragments amenable to sequencing was similar throughout this study, and is illustrated here. The initial problem, due to the size limitations of the sequencing system, was determining which cDNA fragments to subclone for sequencing. The resolution of the polyacrylamide gel allowed determination of only 150-200 nucleotides of the inserted fragment, even though the sequencing reaction can synthesize an entire second strand (Figure 8). Therefore, fragments larger than 400 nucleotides (200 nucleotides in each orientation) had to be reduced in size before sequencing. This could be achieved using convenient restriction endonuclease sites but in their absence (the usual situation), exonuclease digestion with the enzyme Bal 31 was used to trim larger fragments down to approximately 400 nucleotides.

Once selected, the isolated cDNA fragments were then ligated into the M13 vector for sequencing. An estimate of the success of the ligation was based on the number of clear plaques versus the number of

FIGURE 6

Pst I digests of HTV cDNA clones M-35, M-17, and S-16. Recombinant plasmid DNA from M-35, M-17, and S-16 were digested with Pst I and the fragments separated by electrophoresis in a 1.0% (w/v) agarose gel at 40 volts for 18 hours. The depicted gel was stained with ethidium bromide and photographed with ultraviolet light. Lane a contains S-16 DNA; lane b contains M-17 DNA; lane c contains M-35 DNA; lane d contains lambda DNA digested with Hind III; and lane e contains ϕ X174 DNA digested with Hae III. Lanes d and e contain markers and their sizes in base pairs are given on the right of the figure.

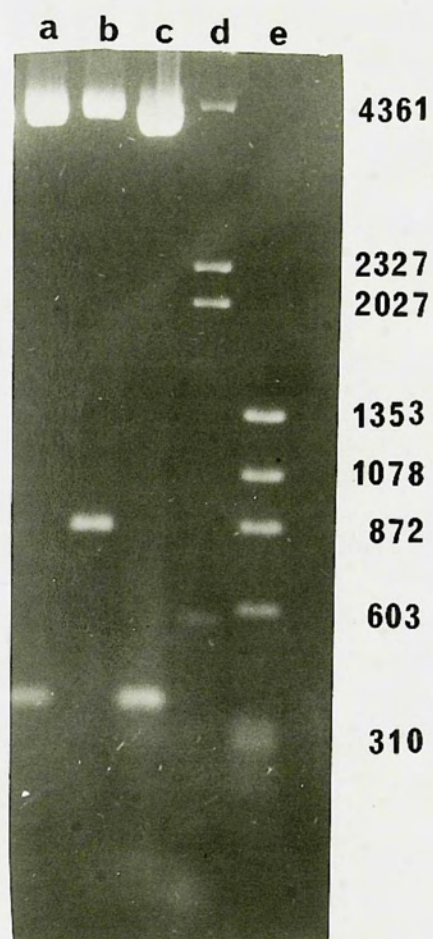


FIGURE 7

Sequencing strategy of HTV M segment cDNA clone M-17. The horizontal line depicts the length of the Pst I insert of M-17 in the viral complementary-sense RNA 5'-3'. Thus, the 5' end of the figure is complementary to the 3' end of the viral-sense RNA. Location of the single Sph I site in the cDNA is shown. The arrows correspond to regions of the cDNA that were sequenced in individual M13 clones generated by Bal 31 digestion and indicate the direction of sequencing.

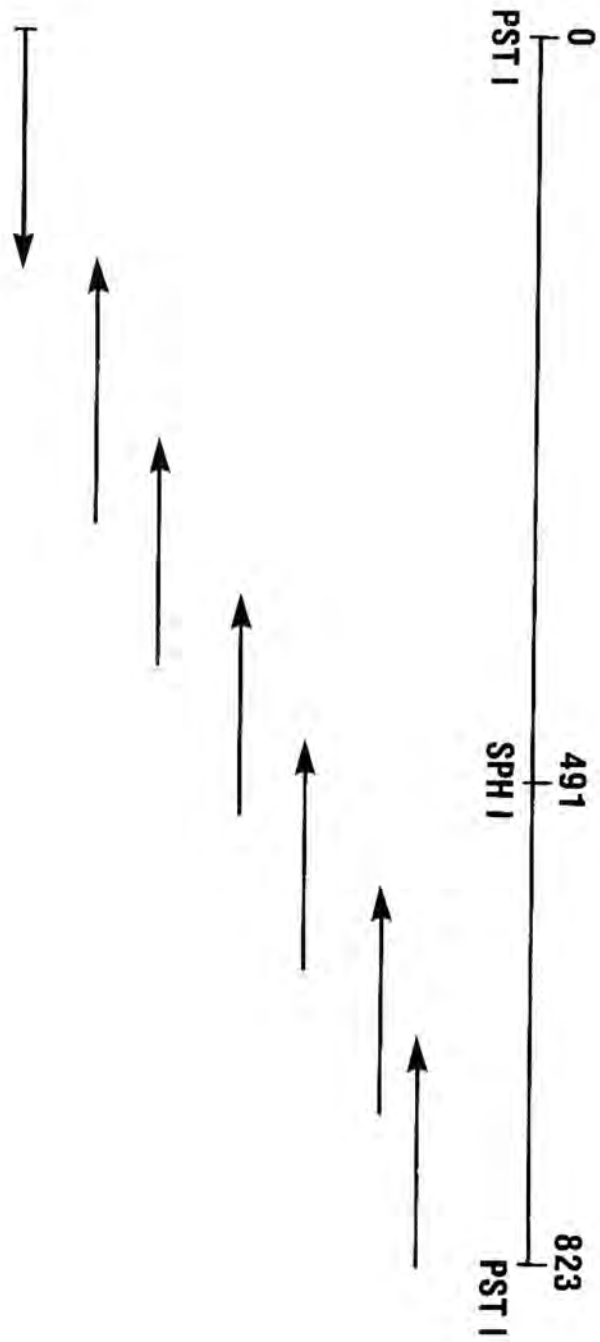
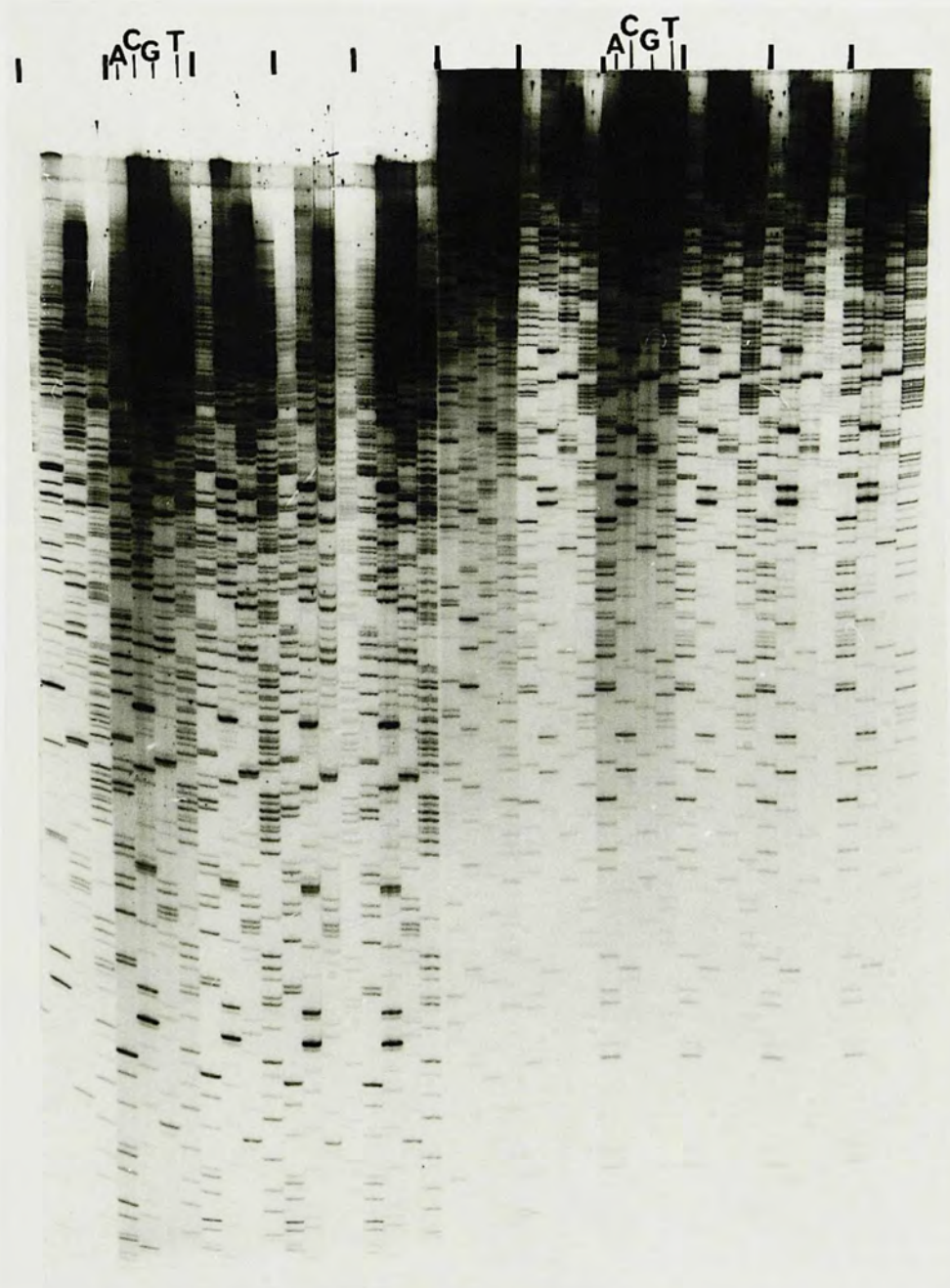


FIGURE 8

A representative M13 DNA sequencing gel. The complementary strand of DNA from recombinant M13 phage was synthesized in four separate sequencing reactions (one for each base) as described in Materials and Methods. The labeled DNA from each reaction was electrophoresed on a 8% polyacrylamide gel until the dye front reached the bottom of the gel, at which time a second sample of the same DNA was loaded onto the gel and electrophoresis continued until the dye front again reached the bottom of the gel. The gel was dried and placed to film. A sample autoradiogram of a DNA sequencing gel is shown. Eleven sets of the four sequencing reactions could be loaded on the gel. Six samples were electrophoresed once (right half of the gel), while five samples were electrophoresed twice (left half of the gel). The presence of bands in the lanes labeled A, C, G, and T indicate the location in the sequence of that specific base. The sequence is read in a step-ladder fashion upward from the bottom of the gel. The lanes labeled on the left half of the gel are a continuation of the sequences from the labeled lanes of the right half of the gel.



blue plaques, but this selection procedure had its limitations. Although only recombinant plaques should be clear, we found clear plaques which, after sequencing, were determined to be single base deletions in the MCS of the M13 vector. Therefore, recombinant phage had to be specifically identified by transfer of phage to Biodyne membrane and subsequent probing of the membrane with a radiolabeled HTV cDNA fragment. Following isolation of phage DNA, the presence of HTV inserts was again confirmed by Southern blot analysis, once more probing with the HTV cDNA fragment. An example of the membrane transfer and Southern blot procedures, used throughout this study, are shown in Figure 9.

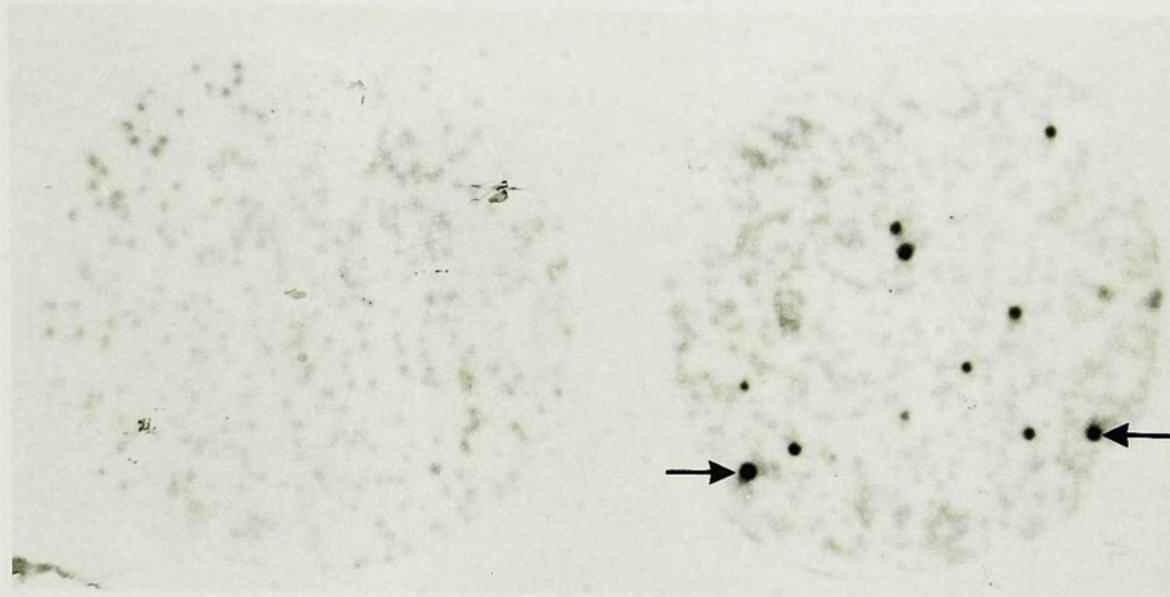
Positive clones were then sequenced both to confirm the presence and determine the orientation of the insert in the vector. Occasionally, HTV-positive clones were found to be contaminated with non-recombinant M13 phage. Resolution of this problem required diluting the phage supernatant to obtain individual plaques, and screening those phages by membrane transfer and Southern blot as described above. Each clone was then sequenced twice and sequences compared to insure no mistakes occurred in the sequencing reaction. The DNAs from at least two different phage recombinants for each subcloned fragment were also sequenced to protect against errors in the subcloning process. Having worked out this approach to sequencing and its pitfalls, we were ready to analyze the HTV M segment cDNA clones.

The M-17 Pst I insert was excised from an agarose gel, purified, and ligated into the M13 vector at the Pst I site. Following identification of recombinant phage, sequence determination identified M13 clones in which the M-17 insert had been subcloned in either orientation. This also allowed sequence determination of the 150 nucleotides at the

FIGURE 9

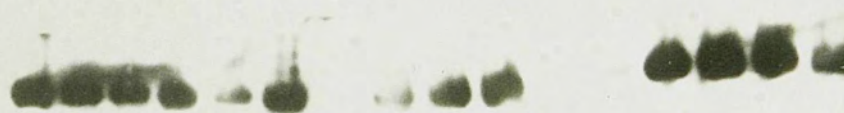
Identification of recombinant HTV-M13 phage by plaque hybridization and Southern blot. M13 phage plaques on LB agar plates were transferred to Biodyne membrane and the membranes hybridized with a specific labeled HTV probe. Panel A depicts a sample autoradiogram of a phage hybridization. Positive plaques, containing the desired insert, appear as dark spots (arrows), while negative plaques are faint. DNAs from these positive phage were prepared and electrophoresed in an agarose gel. The single-stranded DNA of the phage migrates as a single band in the gel. The DNA is transferred to Biodyne membrane and hybridized with a specific labeled HTV probe. Panel B is a sample autoradiogram of a Southern blot used to determine the presence of inserts in the M13 phage DNA. Positive samples appear as dark bands (for example, lane a), while negative samples are blank lanes or appear as faint bands (for example, lane 1).

A



B

a b c d e f g h i j k l m n o p



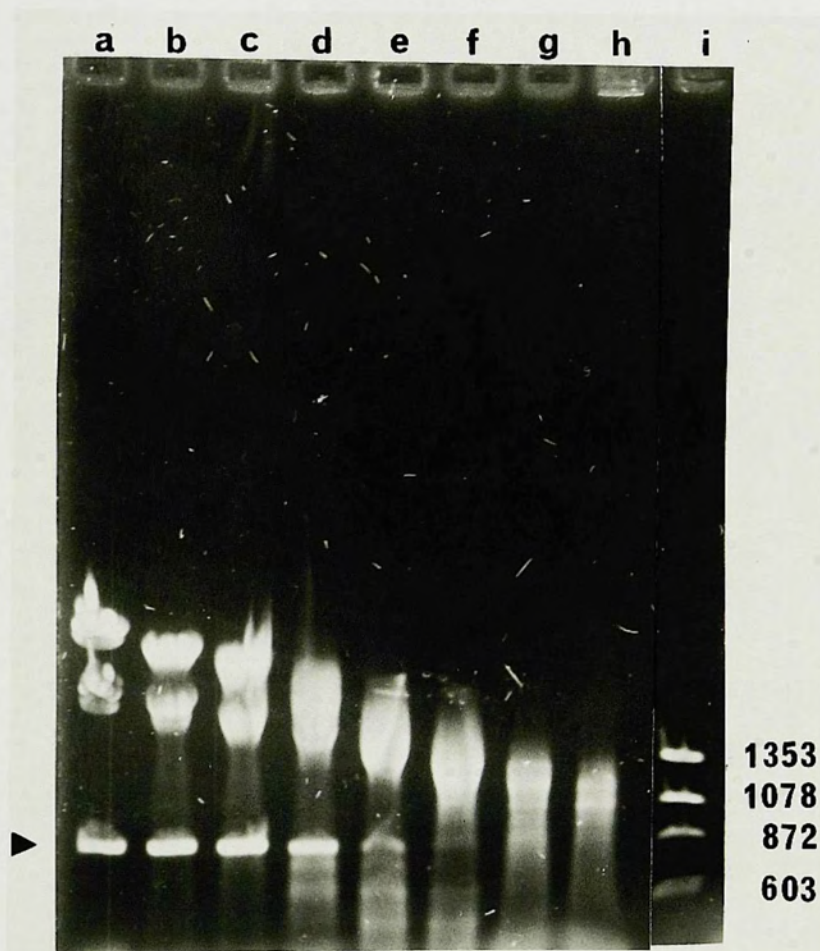
5' and 3' ends of the HTV insert. A comparison of our sequence with the direct RNA sequencing of the 3' viral-sense terminal 25 nucleotides by Schmaljohn *et al.* (1985) confirmed the sequences as originating from the M segment and corresponded to the 3' terminus of the viral-sense M segment RNA.

As fragments of less than 400 nucleotides could not be generated using the single restriction endonuclease site (Sph I; Figure 7), an alternative approach had to be devised to complete the sequence of the M-17 HTV cDNA. A Bal 31 digest of the insert was carried out to generate a series of smaller fragments for sequencing. The M-17 plasmid was digested with the enzyme Bgl I, which cleaves the pBR322 plasmid three times. The 3' viral-sense end of the M17 cDNA was 1685 base pairs from one Bgl I site, while the 5' end was only 125 base pairs from a second Bgl I site. Thus, the Bgl I digestion results in three fragments, two composed of pBR322 sequences alone, and one containing the HTV cDNA insert with pBR322 terminal sequences. The three fragments were then incubated with the exonuclease Bal 31 which digests the ends of the DNA strands in both directions resulting in a shortened and blunt-ended fragment. The longer the incubation with Bal 31, the shorter the DNA becomes.

The Bal 31-treated fragments were subsequently digested with Pst I to allow separation by electrophoresis of the shortened HTV cDNA from pBR322 DNA. The result of these digestions is shown in Figure 10. With increasing time of Bal 31 digestion, the band representing the HTV 823bp Pst I insert (arrow) became less visible with time (lanes d-h) and was replaced with a smear of bands beneath it. The 5' viral-sense end of the cDNA was more rapidly digested since it was closest (125bp) to the end of the Bgl I fragment. The agarose containing these smaller

FIGURE 10

Bal 31 digest of HTV M segment cDNA clone M-17. Recombinant plasmid DNA from M-17 was digested with Bgl I and then subjected to Bal 31 digestion for the times indicated below. The DNA was then digested with Pst I and the fragments separated by electrophoresis in a 1.0% (w/v) agarose gel (11 x 14 cm) at 100 volts for 2.5 hours. The gel was stained with ethidium bromide and photographed with ultraviolet light. The DNA was digested by Bal 31 for the indicated times: lane a, 0 minutes; lane b, 0.5 minutes; lane c, 1 minute; lane d, 2 minutes; lane e, 3 minutes; lane f, 4 minutes; lane g, 5 minutes; and lane h, 6 minutes. Lane i is ϕ X174 DNA digested with Hae III. Numbers to the right of the gel are marker DNA fragment sizes in base pairs. The arrow indicates the intact 823bp HTV cDNA insert fragment of M-17.



fragments was excised and the DNA isolated. The isolated fragments were ligated into the M13 vector digested with Pst I and Sma I, to have ends compatible with the fragments. The recombinant phage were then identified by blotting in the manner described above.

Many clones had to be analyzed before it was possible to use their overlapping nature to piece together the sequence from end to end. The sequencing strategy shown in Figure 7, therefore, illustrates only one series of clones used to sequence the entire M-17 cDNA insert. The length of the HTV M segment cDNA in M-17 was found to be 823 nucleotides (Figure 11). The nucleotide sequence was analyzed using the IBI sequencing program for the IBM PC. A noncoding region was found which was 39 nucleotides in length, with the translation start site (ATG) at nucleotide positions 40-42. One open reading frame was found which began at nucleotide 40 and continued through the end of the sequence. A second possible in-frame ATG initiation codon was found at nucleotide positions 64-66. It is not clear which of these is utilized by the virus.

While this work was in progress, Dr. M. Pensiero in our laboratory sequenced the HTV M segment cDNA corresponding to the 5' terminus of the viral-sense RNA. We were then able to confirm the complementarity of the 3' and 5' sequences, as found in other bunyavirus segments, although the 5' terminal AUG appears to be missing as compared to the 3' terminal sequence (Figure 12).

At this point in our analysis, however, the remainder of the sequence of the M segment was obtained commercially and was published subsequently by Schmaljohn *et al.* (1987a). The sequences presented here (Figure 11) are in agreement with the published sequence, with the exception of nucleotides 12, 495, 812, and 818 which differ from

FIGURE 11

The nucleotide sequence of the HTV M segment cDNA clone M-17. The sequence is presented as the viral complementary DNA strand, 5'-3'. Thus, the 5' end of the sequence is complementary to the 3' end of the viral-sense RNA. Nucleotides 1 through 823 are shown with the corresponding amino acid below the codon. The initiation codon for the predicted glycoproteins is shown beginning at nucleotide 41, although a second possible start is at nucleotide 65.

	10		20		30		40		50		60								
	*		*		*		*		*		*								
TGT	AGT	AGA	CTC	CCT	AAA	AGA	AAG	CAG	TCA	ATC	AGC	AAC	ATG	GGG	ATA	TGG	AAG	TGG	CTA
													Met	Gly	Ile	Trp	Lys	Trp	Leu
	70		80		90		100		110		120								
	*		*		*		*		*		*								
GTG	ATG	GCC	AGT	TTA	GTA	TGG	CCT	GTT	TTG	ACA	CTG	AGA	AAT	GTC	TAT	GAC	ATG	AAA	ATT
Val	Met	Ala	Ser	Leu	Val	Trp	Pro	Val	Leu	Thr	Leu	Arg	Asn	Val	Tyr	Asp	Met	Lys	Ile
	130		140		150		160		170		180								
	*		*		*		*		*		*								
GAG	TGC	CCC	CAT	ACA	GTA	AGT	TTT	GGG	GAA	AAC	AGT	GTG	ATA	GGT	TAT	GTA	GAA	TTA	CCC
Glu	Cys	Pro	His	Thr	Val	Ser	Phe	Gly	Glu	Asn	Ser	Val	Ile	Gly	Tyr	Val	Glu	Leu	Pro
	190		200		210		220		230		240								
	*		*		*		*		*		*								
CCC	GTG	CCA	TTG	GCC	GAC	ACA	GCA	CAG	ATG	GTG	CCT	GAG	AGT	TCT	TGT	AAC	ATG	GAT	AAT
Pro	Val	Pro	Leu	Ala	Asp	Thr	Ala	Gln	Met	Val	Pro	Glu	Ser	Ser	Cys	Asn	Met	Asp	Asn
	250		260		270		280		290		300								
	*		*		*		*		*		*								
CAC	CAA	TCG	TTG	AAT	ACA	ATA	ACA	AAA	TAT	ACC	CAA	GTA	AGT	TGG	AGA	GGA	AAG	GCT	GAT
His	Gln	Ser	Leu	Asn	Thr	Ile	Thr	Lys	Tyr	Thr	Gln	Val	Ser	Trp	Arg	Gly	Lys	Ala	Asp
	310		320		330		340		350		360								
	*		*		*		*		*		*								
CAG	TCA	CAG	TCT	AGT	CAA	AAT	TCA	TTT	GAG	ACA	GTG	TCC	ACT	GAA	GTT	GAC	TTG	AAA	GGA
Gln	Ser	Glu	Ser	Ser	Gln	Asn	Ser	Phe	Glu	Thr	Val	Ser	Thr	Glu	Val	Asp	Leu	Lys	Gly
	370		380		390		400		410		420								
	*		*		*		*		*		*								
ACA	TGT	GTT	CTA	AAA	CAC	AAA	ATG	GTG	GAA	GAA	TCA	TAC	CGT	AGT	AGG	AAA	TCA	GTA	ACC
Thr	Cys	Val	Leu	Lys	His	Lys	Met	Val	Glu	Glu	Ser	Tyr	Arg	Ser	Arg	Lys	Ser	Val	Thr
	430		440		450		460		470		480								
	*		*		*		*		*		*								
TGT	TAC	GAC	CTG	TCT	TGC	AAT	AGC	ACT	TAC	TGC	AAG	CCA	ACA	CTA	TAC	ATG	ATT	GTA	CCA
Cys	Tyr	Asp	Leu	Ser	Cys	Asn	Ser	Thr	Tyr	Cys	Lys	Pro	Thr	Leu	Tyr	Met	Ile	Val	Pro
	490		500		510		520		530		540								
	*		*		*		*		*		*								
ATT	CAT	GCA	TGC	AAG	ATG	ATG	AAA	AGC	TGT	TTG	ATT	GCA	TTG	GGA	CCA	TAC	AGA	GTA	CAG
Ile	His	Ala	Cys	Lys	Met	Met	Lys	Ser	Cys	Leu	Ile	Ala	Leu	Gly	Pro	Tyr	Arg	Val	Gln
	550		560		570		580		590		600								
	*		*		*		*		*		*								
GTG	GTT	TAT	GAG	AGA	AGT	TAC	TGT	ATG	ACA	GGA	GTC	CTG	ATT	GAA	GGG	AAA	TGC	TTT	GTC
Val	Val	Tyr	Glu	Arg	Ser	Tyr	Cys	Met	Thr	Gly	Val	Leu	Ile	Glu	Gly	Lys	Cys	Phe	Val
	610		620		630		640		650		660								
	*		*		*		*		*		*								
CCA	GAT	CAA	AGT	GTG	GTC	AGT	ATT	ATC	AAG	CAT	GGG	ATC	TTT	GAT	ATT	GCA	AGT	GTT	CAT
Pro	Asp	Gln	Ser	Val	Val	Ser	Ile	Ile	Lys	His	Gly	Ile	Phe	Asp	Ile	Ala	Ser	Val	His
	670		680		690		700		710		720								
	*		*		*		*		*		*								
ATT	GTA	TGT	TTC	TTT	GTT	GCA	GTT	AAA	GGG	AAT	ACT	TAT	AAA	ATT	TTT	GAA	CAG	GTT	AAG
Ile	Val	Cys	Phe	Phe	Val	Ala	Val	Lys	Gly	Asn	Thr	Tyr	Lys	Ile	Phe	Glu	Gln	Val	Lys
	730		740		750		760		770		780								
	*		*		*		*		*		*								
AAA	TCC	TTT	GAA	TCA	ACA	TGC	AAT	GAT	ACA	GAG	AAT	AAA	GTG	CAA	GGA	TAT	TAT	ATT	TGT
Lys	Ser	Phe	Glu	Ser	Thr	Cys	Asn	Asp	Thr	Glu	Asn	Lys	Val	Gln	Gly	Tyr	Tyr	Ile	Cys
	790		800		810		820												
	*		*		*		*												
ATT	GTA	GGG	GGA	AAC	TCT	GCA	CCA	ATA	TAT	GGT	CCA	AAA	CTT	G					
Ile	Val	Gly	Gly	Asn	Ser	Ala	Pro	Ile	Tyr	Gly	Pro	Lys	Leu						

FIGURE 12

Complementary termini of the HTV M segment. Sequences shown are the 3' and 5' terminal 27 nucleotides (derived from our sequences) arranged to form a loop of the HTV M segment RNA. Horizontal bars indicate spacing to allow best alignment of the sequences. Vertical lines indicate possible base pairing between the complementary ends of the RNA.



Schmaljohn *et al.* (1987a) and nucleotides 15 and 16 which differ from Schmaljohn *et al.* (1985,1987a). These differences could be attributed to clonal differences or to copying mistakes during cDNA synthesis, and will be discussed later.

The entire HTV M segment cDNA sequence was analyzed using the IBI program, and one ORF was found. The hydropathy plot of the M segment polypeptide product (Figure 13) shows this large open reading frame. The derived protein is probably cleaved to form the two glycoproteins (G₁, G₂) of HTV. The gene order is G₁-G₂ with respect to the viral complementary-sense RNA, and the hydrophobic regions at the amino and carboxy termini of the ORF are characteristic of membrane-bound proteins, with N-linked glycosylation sites. This is discussed in detail in subsequent sections.

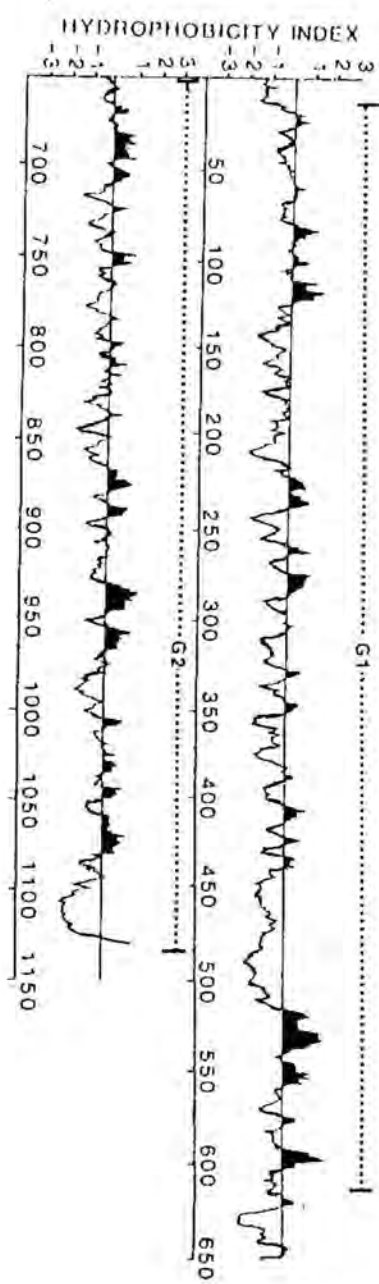
We concluded from these studies that features found in the HTV M segment sequence were similar to other bunyaviruses. The important information for our further studies was that the HTV M segment appears to code for the viral glycoproteins, and that we had obtained the sequence data necessary to carry out further expression studies.

Determination and analysis of the HTV S segment nucleotide sequence

Our next task in quest of characterizing the immunogenic HTV proteins was the analysis of the viral genomic S segment RNA. The S segment of the bunyaviruses encodes the nucleocapsid protein and a nonstructural protein, often by way of novel coding strategies (see earlier). We believed that sequence determination of the HTV S segment would provide basic molecular information about the virus and be essential in planning necessary expression experiments. An examination of the nucleotide sequence of the S segment would reveal the proteins

FIGURE 13

Hydropathic plot of the predicted gene product of the HTV M segment. A hydropathic plot is shown of the gene product predicted from the cDNA sequence of viral complementary-sense HTV M segment RNA. Data points represent a running average taken over seven amino acid residues. Sequences with a net hydrophobicity appear below the line, while sequences with a net hydrophilicity appear above the line and are shaded. The coding regions of G₁ and G₂ are overscored with a dashed line. From Schmaljohn et al. (1987a).



encoded, and also the coding strategy employed by HTV, which differs markedly amongst bunyaviruses. In addition, synthetic peptides could be made based on the acquired nucleotide sequence and antibodies to them used in further studies analysing the S segment proteins. A comparison of the sequences of the S and M segments would determine the extent of the conserved 3' terminal nucleotides and similarities in the degree of complementarity of the 3' and 5' terminal sequences. The 3' and 5' noncoding regions could also be examined for similar sequences surrounding the translation initiation site, or to reveal a common transcription termination signal.

Following cDNA synthesis of the HTV S segment RNA, recombinant pBR322 plasmids had to be characterized. Bacterial colonies were screened for the presence of HTV S segment cDNA by Dr. C. Schmaljohn in the same manner as described for the M segment. A total of three such HTV cDNA clones of the S segment were utilized in this study. As before, our initial aim was to size the cDNA insert and determine a restriction enzyme map of the fragment. Once this was accomplished, a strategy could be designed to sequence the cDNA of the HTV S segment.

Of the initial HTV cDNA clones received, one (S-16) had been identified by hybridization as containing S segment sequences. DNA was prepared from the S-16 clone, digested with Pst I, and electrophoresed in a agarose gel with DNA fragments of known size (Figure 6). The Pst I insert of the clone was determined to be approximately 350 nucleotides in length (Figure 6, lane a), far short of the expected size of a full length clone of the HTV S segment (approximately 1700 nucleotides). Further restriction endonuclease analyses revealed a useful Bam HI restriction endonuclease site within the insert (Figure 16, nucleotide position 140). However, by subcloning the Pst I insert into M13 in both

orientations the entire sequence, theoretically, should be obtained, since the fragment was less than 400 nucleotides in length. If necessary, the fragment could be reduced in size for sequencing, using the Bam HI restriction enzyme site.

The entire Pst I fragment was ligated into the M13 vector and recombinant phage selected and extensively checked, in the manner described for the M segment recombinants. DNA from recombinant phage was then obtained and both orientations sequenced. Using this approach, the entire 330 nucleotide sequence of the Pst I cDNA insert was obtained (Figure 22) and the Bam HI site was located at nucleotide position 140. A comparison of our sequence with the direct RNA sequencing of the 3' viral-sense 25 nucleotides by Schmaljohn *et al.* (1985) confirmed the sequences as originating from the S segment and corresponded to the 3' terminus of viral-sense S segment RNA.

The second HTV S segment clone which was analysed was designated S-8. As with the S-16 clone, the DNA first was digested with Pst I and fragment sizes determined by agarose gel electrophoresis. The Pst I insert of the S-8 cDNA clone was found to contain an internal Pst I site, and therefore two cDNA fragments were generated with apparent sizes of 1000 and 650 base pairs (Figure 14A, lane e). The combined size of these two fragments was close to the expected size of a full length S segment cDNA clone (approximately 1700 nucleotides). We concluded that the S-8 clone may represent a full length clone, although sequence data showing the 3' and 5' terminal complementarity was needed to confirm this.

The next step in analyzing the S-8 clone was to determine which of the two fragments corresponded to the 3' terminus of the viral-sense RNA. The DNAs from S-16 and S-8 were electrophoresed in an agarose gel

FIGURE 14

Characteristics of the HTV cDNA clone S-8. Plasmid DNA was digested with Pst I and the fragments separated by electrophoresis in a 1.0% (w/v) agarose gel at 40 volts for 18 hours. The gel in panel A was stained with ethidium bromide and photographed with ultraviolet light. Lane a contains lambda DNA digested with Hind III; lane b contains ϕ X174 DNA digested with Hae III; lane c and d contain S-16 digested with Pst I; and lane e contains S-8 digested with Pst I. To the right of the photograph is given the size of marker fragments in base pairs. The DNA in the gel was transferred by Southern blot to Biodyne membrane and hybridized with ^{32}P -labeled S-16 Pst I fragment. The autoradiogram is shown in panel B. The lanes in panel B correspond to the lanes in panel A. The arrow indicates the location of the 1000bp fragment in lane e'.

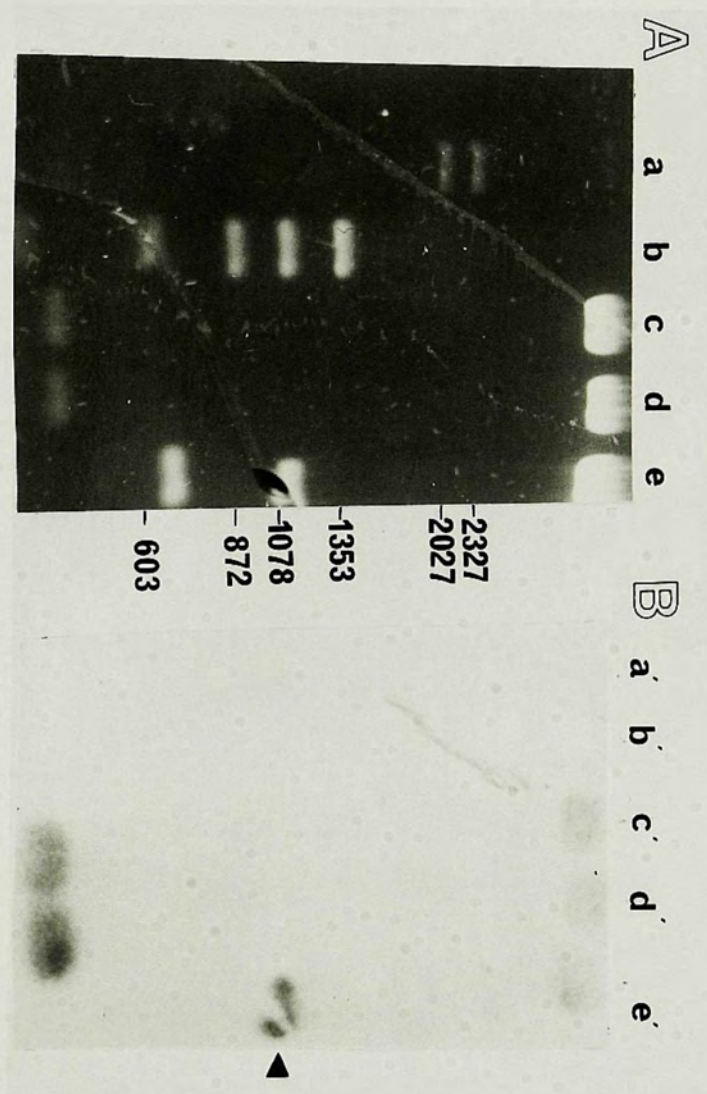


(Figure 14A) and transferred to Biodyne membrane for Southern blot analysis (Figure 14B). The isolated S-16 cDNA insert which we had already determined to be the genomic 3' 330 nucleotides was used to probe the blot. The specificity of the probe was seen (Figure 14B) by the lack of binding to the lambda and λ X174 DNA (lanes a' and b') and to the plasmid pBR322 (lanes c', d', and e'). The S-16 probe hybridized to itself (lanes c' and d') and to the larger (arrow), but not the smaller, Pst I fragment (lane e'). Thus the larger Pst I fragment (1000 base pairs) was determined to contain the 3' terminus of the HTV S segment.

A detailed restriction endonuclease map of the S-8 clone was next derived, for several reasons. The size of either of the Pst I fragments precluded obtaining the entire sequence directly from these fragments. However, the identification of restriction endonuclease sites within the cDNA would allow smaller fragments to be generated. If the fragments were approximately 400 nucleotides in length or less, the entire sequence of that fragment could be determined by sequencing in both orientations. Further, if the ends of these fragments were generated by restriction endonucleases contained in the multiple cloning site of the M13 vector, they could be easily cloned into the M13 plasmid for sequencing. Finally, if it is known that particular endonuclease sites exist, they can act as important landmarks when determining the sequence.

Generating a restriction endonuclease map involves arranging in order the restriction sites of the insert in a method similar to fitting a puzzle together. The restriction sites for the plasmid pBR 322 are known (Figure 5) and can therefore be used to orient the sites within the inserted HTV S segment cDNA. If the insert contains a particular endonuclease site, there will be an increase in the number of fragments

generated when compared to the number of fragments generated by digesting pBR 322 without the insert. For example, by digesting S-8 with Pst I and a second enzyme which creates additional fragments, one can determine where in the insert the second enzyme site lies.

Figures 15A and B depict the gel analyses used to determine the restriction endonuclease map of S-8. The S-8 plasmid was digested with Pst I in the presence or absence of a second restriction endonuclease and the fragments separated by agarose gel electrophoresis. The endonucleases selected for testing were primarily chosen due to their presence in the multiple cloning site of the M13 vector. In Figure 15A the results of the digestion are shown and the following restriction endonucleases digested the Pst I insert: Bam HI (twice), Hind III, Pvu II, and Sph I.

The thought processes used in analyzing the Bam HI digests will illustrate how all digests had to be constructed. As stated above, the larger Pst I fragment of S-8 corresponds to the 3' viral terminus of HTV S segment RNA (Figure 14). Additionally, the larger fragment must also contain a Bam HI site as one existed in the S-16 clone (nucleotide 140). When S-8 was digested with Bam HI alone, three fragments (approximately 3700, 1250, and 1100 base pairs) (Figure 15A, lane m) were generated indicating the presence of two Bam HI sites within the Pst I insert in addition to the one Bam HI site in the pBR322 plasmid (Figure 5). The distances from the Bam HI site of pBR322 to the Pst I insert site are 3231 and 1128 base pairs, respectively (Figure 5). Since the 3'-Bam HI site was 140 base pairs downstream from the Pst I insert site, the 1100bp fragment must correspond to a fragment completely derived from S-8, while the 1250bp fragment is formed by the 140bp (HTV cDNA) + 1128bp (pBR322) fragments. Thus, the orientation of the HTV cDNA insert in

FIGURE 15

Restriction endonuclease digestion of HTV cDNA clone S-8. Plasmid DNA was digested with restriction endonucleases and the fragments separated in a 1.0% (w/v) agarose gel by electrophoresis at 40 volts for 18 hours. The gels were stained with ethidium bromide and photographed with ultraviolet light. Panel A: Lane a contains lambda DNA digested with Hind III; lane b contains ϕ X174 DNA digested with Hae III; lane c and d contain S-16 DNA digested with Pst I; lanes e-n contain S-8 DNA digested as follows: lanes e and f, Pst I alone; lane g, with Pst I and Pvu II; lane h, with Pst I and Sph I; lane i, with Pst I and Bam HI; lane j, with Pst I and Hind III; lane k, with Pvu II; lane l, with Sph I; lane m, with Bam HI; and lane n, with Hind III. A separate gel is shown in Panel B. Lanes a-k contain S-8 DNA digested as follows: lane a, with Pst I; lane b, with Acc I; lane c, with Pst I and Acc I; lane d, with EcoR I; lane e, with Pst I and Sal I; lane f, with Sal I; lane g, with Pst I and Sma I; lane h, with Kpn I; lane i, with Pst I and Kpn I; lane j, with Sst I; and lane k, with Pst I and Sst I; lane l, contains lambda DNA digested with Hind III; and lane m contains ϕ X174 DNA digested with Hae III. To the right of each photograph is given the size of marker fragments in base pairs.



pBR322 could be deduced, since the 3' viral-sense S-8 HTV insert terminus must be 1128 nucleotides from the pBR322 Bam HI site.

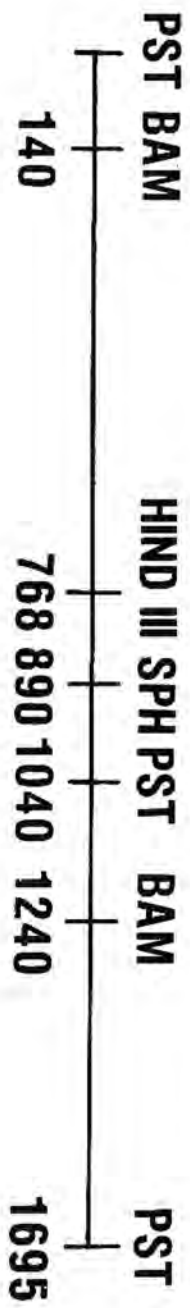
There must also be a second Bam HI site in the HTV S segment cDNA approximately 450 nucleotides from the 5' viral-sense terminus (the 3700bp S-8 fragment minus the 3231bp Bam HI-Pst I fragment of pBR322). When S-8 was double-digested with Pst I and Bam HI, the sizes of both HTV Pst I fragments decreased (Figure 15A, lanes f and i). The larger fragment (1000bp, Figure 15A, lane e) was smaller by the expected 140 nucleotides (Figure 15A, lane i). As would also be predicted from the above calculations, the smaller Pst I fragment (650bp, Figure 15A, lane e) decreased in size to approximately 450 nucleotides (Figure 15A, lane i). The faint band near the bottom of lane i in Figure 11A is likely to be a doublet, as a single band of that size should not stain so brightly. It probably consists of the 140bp Pst I-Bam HI fragment plus the 200 nucleotides cut from the smaller Pst I fragment. These Bam HI fragments can now be arranged as illustrated in Figure 16. This type of calculation was performed for each restriction endonuclease which cleaved the S-8 cDNA insert, and the analysis produced the completed restriction endonuclease map shown in Figure 16, although only those enzymes used in subsequent M13 subcloning are shown.

The following enzymes were tested but did not have cleavage sites within the Pst I insert: Sal I, Kpn I, Sst I, Sma I, and EcoR I (Figure 15B). The EcoR I digest (Figure 15B, lane d) is confusing due to the presence of multiple bands and requires an explanation. The primary EcoR I band is located at the same position (approximately 6000bp) as the single band from the Sal I digestion (Figure 15B, lane f) which cuts the pBR322 plasmid once. The smaller, fainter bands (Figure 15B, lane d; six bands from 4000 to 700bp) are most probably due to the

FIGURE 16

Restriction endonuclease map of the HTV S segment cDNA. The horizontal line represents the viral complementary-sense of the RNA 5'-3'. Thus, the 5' end of the figure is complementary to the 3' end of the viral-sense RNA. Vertical bars indicate the restriction endonuclease sites; numbers correspond to the nucleotide position of the sites as located in the final sequence (Figures 22, 23, and 24). Abbreviations for the restriction endonucleases are as follows: Pst is Pst I, Bam is Bam HI and Sph is Sph I.

HANTAAN VIRUS S SEGMENT CDNA



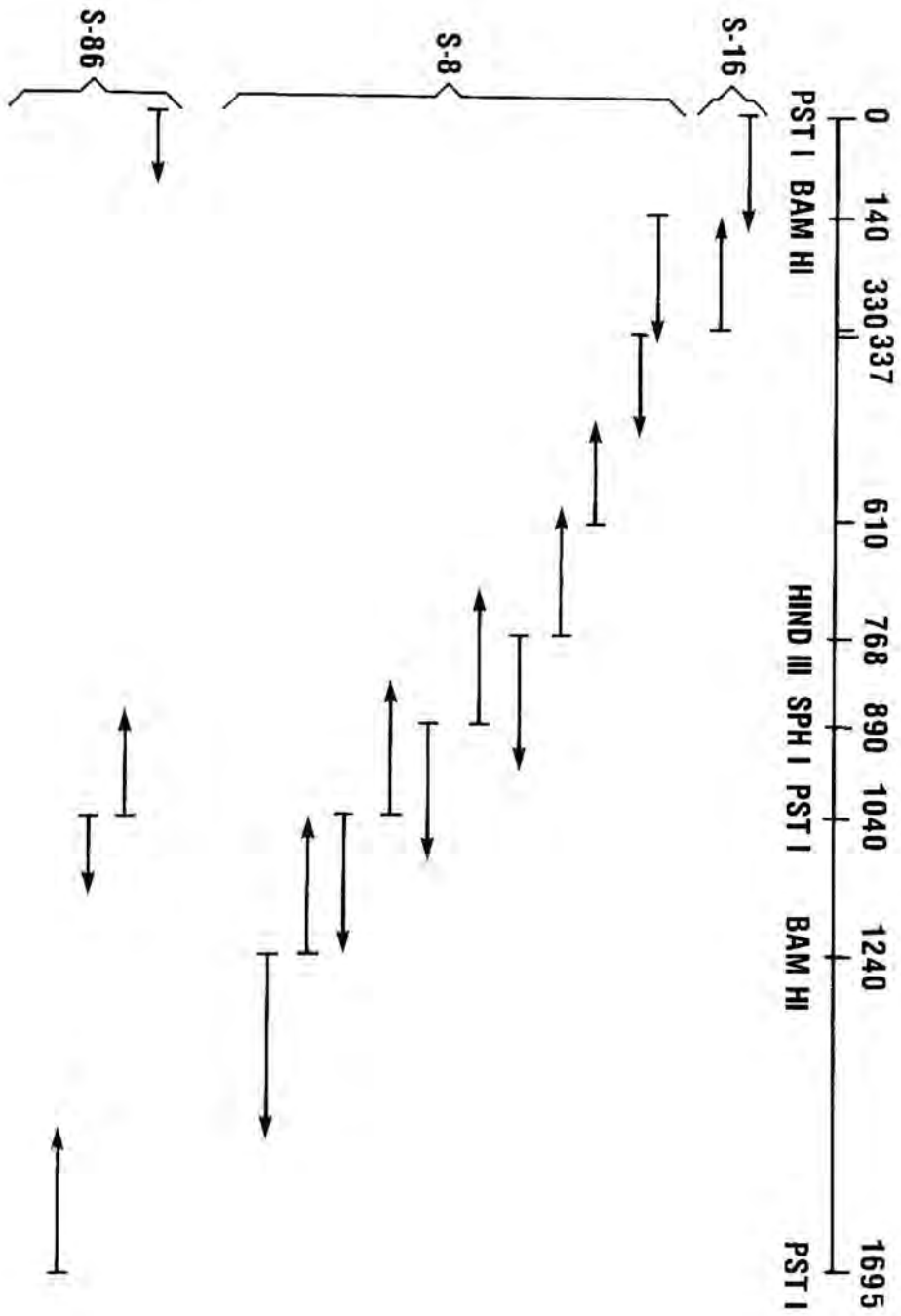
"star" activity of EcoR I, which begins to occur if the salt concentration in the reaction mixture is high. These bands were not seen on later EcoR I digests. Faint bands which appear in double digests involving Pst I (Figure 15B, lanes g and i) are probably partial digest products.

A sequencing strategy was then devised (Figure 17) based on the restriction endonuclease map. The numerous restriction endonuclease sites identified permitted the S-8 cDNA to be digested to form several smaller fragments convenient for sequencing. Each of the following fragments (with fragment size) were individually extracted from an agarose gel: Bam HI-Pst I (900bp), Pst I-Hind III (768bp), Hind III-PstI (270bp), Pst I-Sph I (890bp), Sph I-Pst I (150bp), Pst I-Pst I (1000bp), Pst I-Pst I (640bp), Pst I-Bam HI (250bp), and Bam HI-Pst I (450).

Each isolated fragment was ligated into either M13mpl8 or M13mpl9 digested with the appropriate restriction endonuclease to give ends compatible with the fragment. The recombinant phage were screened by hybridization for the presence of HTV S segment cDNA in the manner detailed for the M segment clones. Sequencing reactions were then set up as outlined earlier. Second strand synthesis (the sequencing reaction) starts at the same site and proceeds in the same direction in either M13mpl8 or M13mpl9. The advantage of using the two vectors lies in the reverse orientation of their multiple cloning site (Figure 5). One vector allows sequence determination of an insert in one orientation; using the second vector, the insert is inverted and sequences are obtained from the other orientation. Thus, each S-8 fragment could be sequenced in both orientations (Figure 17). In the regions where the restriction endonuclease sites were close (for example, from the Hind

FIGURE 17

The sequencing strategy for the HTV S segment cDNA. The horizontal line depicts the viral complementary-sense RNA 5'-3'. Thus, the 5' end of the figure is complementary to the 3' end of the viral-sense RNA. The locations of the restriction endonuclease sites are indicated by vertical lines. Numbers above the line give the nucleotide position of each site based on the final sequence. Arrows correspond to regions of the cDNA sequenced in individual M13 clones and indicate the direction of sequencing. Vertical bars at the end of the arrow indicate the nucleotide position from which sequencing began. The original cDNA clone from which each M13 clone was derived is shown on the left. Sequences originating from nucleotide positions 337 and 610 were determined using synthetic oligonucleotides as primers.



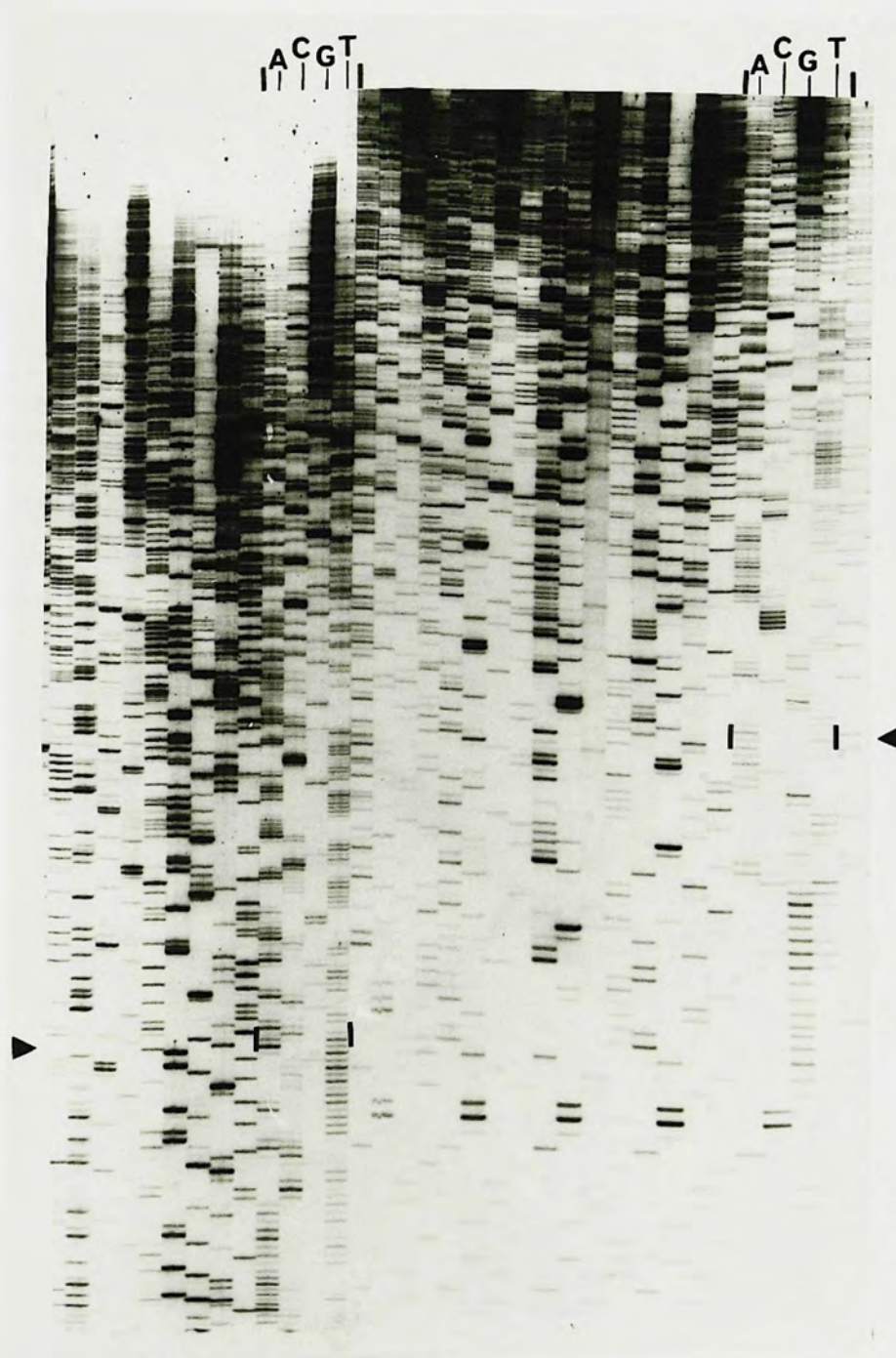
III site to the Bam HI site at nucleotide 1240) both strands of the cDNA could be sequenced (Figure 17). This provided an excellent means of verifying sequencing data as complementarity between the two strands should be (and was) exact.

Much of the sequence was resolved by this strategy, however two areas of the S-8 cDNA presented special problems. First, the sequences at the 3' and 5' termini of the S-8 clone could not be ascertained. Identification of the 3' viral-sense terminus from S-8 was not critical since the S-16 clone had already provided those sequences. However, the sequences of the 5' terminus were required to determine the degree of complementarity with the 3' terminus and whether the S-8 clone was truly full length. We determined that the inability to read terminal S-8 sequences was due to a "stuttering" of the sequencing DNA polymerase at the poly G tails used in cDNA cloning (Figure 18). Attempts to read past the poly G tails by incubating the DNA polymerase reaction at a higher temperature (45°C) or replacing the polymerase enzyme with reverse transcriptase (Karanthanas, 1982) were unsuccessful.

Previous sequencing of other M and S segment cDNA clones (for example, S-16, see above) had demonstrated that the poly G tails did not always create sequencing problems. This is probably due to the varying length of these tails. Shorter tails are likely to present less of a problem than longer tails. Therefore, other separately-derived HTV S segment cDNA clones were screened in the hope of finding another full length S segment cDNA clone. Through this search, the third S segment cDNA clone, S-86, was selected for further analysis, since in preliminary experiments it had appeared to be larger than S-8. DNA from the S-86 clone was digested with Pst I and fragment sizes compared to the S-8 clone by electrophoresis in an agarose gel (Figure 19). A size dif-

FIGURE 18

DNA sequencing gel analysing the 5' viral-sense terminus of the HTV S segment cDNA clone S-8. DNA was prepared and electrophoresed as described in Figure 8. Lanes labeled A, C, G, and T indicate the sequencing reactions for each base involving a clone of the 5' viral-sense end of S-8, with the sequences on the left side of the gel corresponding to the samples electrophoresed twice. It is impossible to read this sequence in a step-ladder fashion, since bands in several lanes are encountered for a particular base position (especially evident in marked sections). Compare this Figure with that of a normal gel in Figure 8.



ference was detected between the two clones in the smaller Pst I fragment (650bp, Figure 14A, lane e). In Figure 19, the smaller Pst I fragment of S-86 (lane a) migrated slightly slower than the S-8 fragment (lane b). The size difference was confirmed by a comparison of the Pst I-Bam HI double digests of the two clones. The Pst I-Bam HI fragments of S-8 (Figure 19, lane f) were as previously shown in lane i, Figure 15A. However, the Bam HI-Pst I 450bp fragment of S-8 migrated faster than the equivalent fragment in S-86 (Figure 19, lane e). As shown in the restriction endonuclease map (Figure 16), the two fragments demonstrating the size differences correspond to the 5' viral-sense terminal sequences. We concluded the S-86 HTV cDNA insert was larger than that in S-8 probably due to an additional 25-50 nucleotides in the terminal 450 nucleotide fragment corresponding to the 5' viral-sense sequences.

From additional analyses, the restriction endonuclease map of S-86 was determined to be the same as S-8 with one exception. The existence of an Acc I site in the S-8 clone was demonstrated by the presence of three specific fragments (Figure 15B, lane b). This site appeared to be very near the 3' viral-sense terminus, since in the double digest (Figure 15B, lane c), there was no change in the smaller Pst I fragment and the larger Pst I fragment was only slightly smaller, with no extra bands detected. Figure 20, however, demonstrated the lack of an Acc I site in the S-86 cDNA. When S-86 cDNA was digested with Acc I only two fragments were generated (Figure 20, lane c). In addition there was no change in size of the larger Pst I fragment of S-86 when digested with Pst I and Acc I (Figure 20, lane b).

We then subjected the S-86 clone to our sequencing regimen. The two Pst I fragments of S-86 were isolated and ligated into the M13 vector. Recombinant phage containing the two fragments were identified

FIGURE 19

Comparison of the molecular weights of the HTV cDNA plasmid clones S-8 and S-86. Plasmid DNAs were digested with restriction endonucleases and the fragments separated in a 1.0% (w/v) agarose gel by electrophoresis at 40 volts for 18 hours. The gel was stained with ethidium bromide and photographed with ultraviolet light. Lane a contains S-86 DNA digested with Pst I; lane b contains S-8 DNA digested with Pst I; lane c contains ϕ X174 DNA digested with Hae III; and lane d contains lambda DNA digested with Hind III. On a separate gel, lane e contains S-86 DNA digested with Pst I and Bam HI and lane f contains S-8 DNA digested with Pst I and Bam HI. Arrows indicate fragments that show a size difference between the two clones. Numbers to the right of lane d are the size of the marker fragments in base pairs. No markers are shown for lanes e and f as the size of the fragments in lane f had been determined in Figure 15A, lane i.

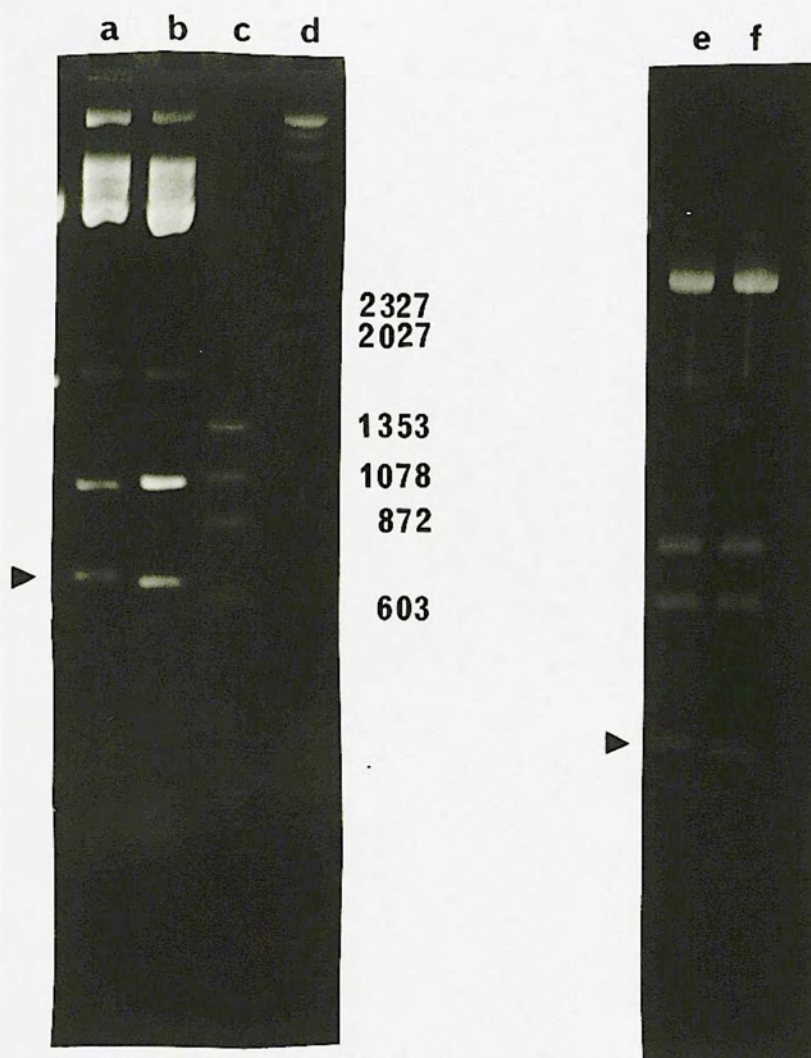
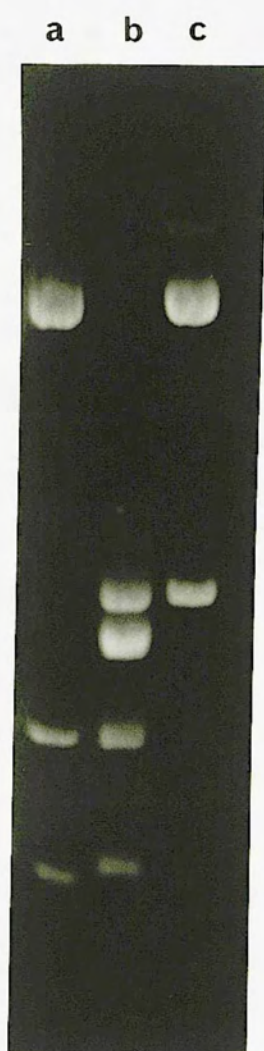


FIGURE 20

Acc I digest of HTV cDNA clone S-86. Plasmid DNA was digested with restriction endonucleases and the fragments separated by electrophoresis in a 1.0% (w/v) agarose gel at 40 volts for 18 hours. The gel was stained with ethidium bromide and photographed with ultraviolet light. Lane a contains S-8 DNA digested with Pst I; lane b contains S-86 DNA digested with Pst I and Acc I; and lane c contains S-86 DNA digested with Acc I. Marker fragments are not shown as the sizes of fragments in lane a had been determined in Figure 15A, lane e.

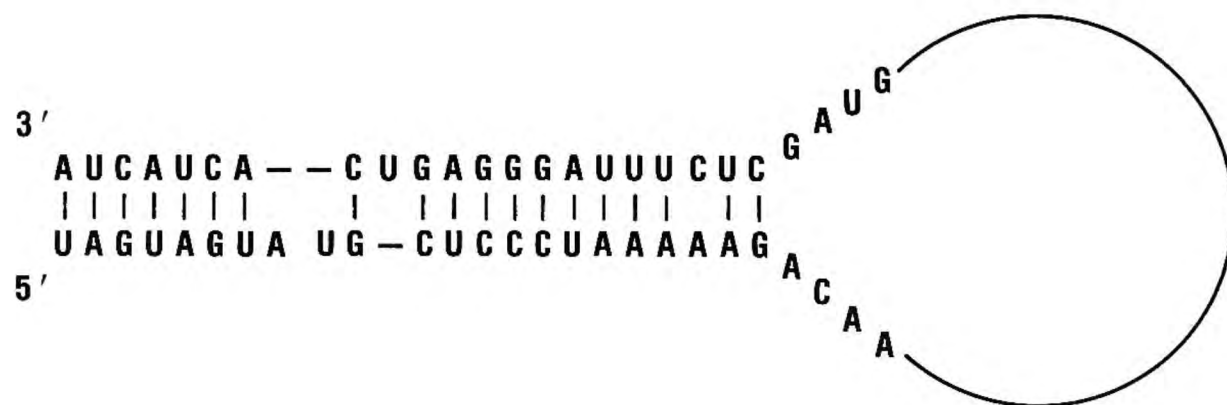


as previously outlined, and the nucleotide sequence determined for each end of both S-86 Pst I fragments (Figure 17). We were successful in determining the terminal sequences of this clone, probably due to shorter poly G tails of S-86. The S-86 sequences were identical to those already obtained from the S-16 or S-8 cDNA. In addition, the sequence representing the 5' viral-sense terminus was found to be complementary to the 3' terminus (Figure 21). This complementarity spanned 19 out of the terminal 23 nucleotides and indicated S-86 to be a full length cDNA clone of the HTV S segment. This level of complementarity should provide enough stability through hydrogen bonding to allow the RNA to circularize in its genomic form.

A second problem needed to be resolved before the sequence could be completed. The 3'-Bam HI-Hind III region of the cDNA (Figure 16) was the particular obstacle, since no useful restriction endonuclease site existed within this 630bp fragment. Approximately 200 nucleotides of each end of the fragment had been sequenced, but the middle of the fragment could not be resolved despite attempts using longer times of electrophoresis of samples or with Maxam-Gilbert sequencing (Maxam and Gilbert, 1977). We decided as an alternative approach to synthesize two oligonucleotides which were complementary to nucleotides previously sequenced within the fragment (one was from position 593 to 610, and the other complementary to position 337 to 357; Figure 17). These oligonucleotides would act to prime second strand synthesis beginning inside the HTV cDNA fragment, rather than outside the insert as occurs with the M13 universal primer. This would allow 200 nucleotides to be sequenced from the start of the oligonucleotide primer rather than 200 nucleotides from the start of the inserted cDNA. Sequencing inward from both directions in this manner successfully permitted the sequence deter-

FIGURE 21

Complementary termini of the HTV S segment. Sequences shown are the 3' and 5' terminal 27 nucleotides arranged to form a loop of the HTV S segment RNA. Horizontal bars indicate spacing to allow best alignment of the sequences. Vertical lines indicate possible base pairing between the complementary ends of the RNA.



mination of the remainder of this fragment.

Thus, using the three cDNA clones (S-16, S-8, and S-86), the numerous M13 subclones and synthetic oligonucleotides, the entire S segment cDNA sequence was determined. The HTV S segment RNA nucleotide sequence is presented in Figures 22, 23, and 24 as the viral complementary DNA strand. The entire sequence is 1695 base pairs in length. We feel confident that it represents the complete sequence since the 5' and 3' terminal sequences are complementary (Figure 20).

A computer-assisted search (IBI Sequencing program for the IBM PC) of the nucleotide sequence for possible open reading frames (ORF) is depicted in Figure 25. All three possible reading frames in both the viral and viral-complementary sense were analysed. One large and one small ORF were detected in the same reading frame of the viral-complementary RNA (i.e. mRNA sense in the HTV-infected cell). In the viral(genomic)-sense RNA, two small ORFs were found in the middle of two different reading frames. However, several translational stop codons preceded these ORFs, making them unlikely candidates for producing a protein. All other ORFs seen in Figure 25 either lack an initiating ATG or were less than 50 amino acids in length.

The large ORF had two possible initiating codons beginning at nucleotides 36 or 45 (Figure 22). This ORF encodes a protein (beginning at nucleotide 36) of 429 amino acids (Figures 22 and 23) with a molecular weight of 48,196 daltons. This is in good agreement with the reported molecular weight of the HTV nucleocapsid protein found on PAGE (Elliot *et al.*, 1984). An interesting feature of the sequence is that the stop codon for this ORF is followed immediately by a leucine codon and then a methionine codon which could initiate a second small ORF. This ORF encodes a possible viral protein of 48 amino acids (Figure 24)

FIGURE 22

The nucleotide sequence of the HTV S segment. The sequence is presented as the viral complementary DNA strand 5'-3'. Thus, the 5' end of the sequence is complementary to the 3' end of the viral-sense RNA. Nucleotides 1 through 662 are shown with the corresponding amino acid below the codon. The initiation codon for the large open reading frame is shown beginning at nucleotide 36, although a second possible start is at nucleotide 45.

10	20	30	40	50	60
*	*	*	*	*	*
TA GTA GTG ACT CCC TAA AGA GCT ACT AGA ACA ACG ATG GCA ACT ATG GAG GAA TTA CAG AGG					
			Met	Ala Thr	Met Glu Leu Gln Arg
70	80	90	100	110	120
*	*	*	*	*	*
GAA ATC AAT GCC CAT GAG GGT CAA TTA GTG ATA GCC AGG CAG AAG GTG AGG GAT GCA GAA					
Glu Ile Asn Ala His Glu Gly Gln Leu Val Ile Ala Arg Gln Lys Val Arg Asp Ala Glu					
130	140	150	160	170	180
*	*	*	*	*	*
AAA CAG TAT GAA AAG GAT CCA GAT GAG TTG AAC AAG AGA ACA TTA ACT GAC CGA GAG GGC					
Lys Gln Tyr Glu Lys Asp Pro Asp Glu Leu Asn Lys Arg Thr Leu Thr Asp Arg Glu Gly					
190	200	210	220	230	240
*	*	*	*	*	*
GTT GCA GTA TCT ATC CAG GCA AAA ATT GAT GAG TTA AAA AGG CAA CTG GCA GAT AGG ATT					
Val Ala Val Ser Ile Gln Ala Lys Ile Asp Glu Leu Lys Arg Gln Leu Ala Asp Arg Ile					
250	260	270	280	290	300
*	*	*	*	*	*
GCA ACT GGG AAA AAC CTT GGG AAG GAA CAA GAT CCA ACA GGG GTG GAG CCT GGA GAC CAT					
Ala Thr Gly Lys Asn Leu Gly Lys Glu Gln Asp Pro Thr Gly Val Glu Pro Gly Asp His					
310	320	330	340	350	360
*	*	*	*	*	*
CTG AAA GAG AGG TCA ATG CTC AGT TAT GGT AAT GTG CTG GAT TTA AAC CAT TTG GAT ATT					
Leu Lys Glu Arg Ser Met Leu Ser Tyr Gly Asn Val Leu Asp Leu Asn His Leu Asp Ile					
370	380	390	400	410	420
*	*	*	*	*	*
GAT GAA CCT ACA GGA CAG ACA GCA GAC TGG CTG AGC ATC ATC GTC TAT CTT ACA TCC TTT					
Asp Glu Pro Thr Gly Gln Thr Ala Asp Trp Leu Ser Ile Ile Val Tyr Leu Thr Ser Phe					
430	440	450	460	470	480
*	*	*	*	*	*
GTC GTC CCG ATA CTT CTG AAA GCT CTG TAT ATG TTG ACA ACA AGG GGG AGG CAA ACT ACC					
Val Val Pro Ile Leu Leu Lys Ala Leu Tyr Met Leu Thr Thr Arg Gly Arg Gln Thr Thr					
490	500	510	520	530	540
*	*	*	*	*	*
AAG GAT AAT AAA GGG ACC CGG ATT CGA TTT AAG GAT GAT AGC TCG TTC GAG GAT GTT AAC					
Lys Asp Asn Lys Gly Thr Arg Ile Arg Phe Lys Asp Asp Ser Ser Phe Glu Asp Val Asn					
550	560	570	580	590	600
*	*	*	*	*	*
GGT ATC CGG AAA CCA AAA CAT CTT TAC GTG TCC TTG CCA AAT GCA CAG TCA AGC ATG AAG					
Gly Ile Arg Lys Pro Lys His Leu Tyr Val Ser Leu Pro Asn Ala Gln Ser Ser Met Lys					
610	620	630	640	650	660
*	*	*	*	*	*
GCA GAA GAG ATT ACA CCT GGT AGA TAT AGA ACA GCA GTC TGT GGG CTC TAC CCT GCA CAG					
Ala Glu Glu Ile Thr Pro Gly Arg Tyr Arg Thr Ala Val Cys Gly Leu Tyr Pro Ala Gln					

FIGURE 23

The nucleotide sequence of the HTV S segment. This represents the continuation of the sequence in Figure 22. Nucleotides 663 through 1382 are shown with the corresponding amino acid below the codon. The termination codon (---) for the large open reading frame is shown at nucleotide 1323.

```

      670      680      690      700      710      720
      *      *      *      *      *      *
ATT AAG GCA CGG CAG ATG ATC AAT CCA GTT ATG AGT GTA ATT GGT TTT CTA GCA TTA GCA
Ile Lys Ala Arg Gln Met Ile Ser Pro Val Met Ser Val Ile Gly Phe Leu Ala Leu Ala

      730      740      750      760      770      780
      *      *      *      *      *      *
AAG GAC TGG AGT GAT CGT ATC GAA CAA TGG TTA ATT GAA CCT TGC AAG CTT CTT CCT GAT
Lys Asp Trp Ser Asp Arg Ile Glu Gln Trp Leu Ile Glu Pro Cys Lys Leu Leu Pro Asp

      790      800      810      820      830      840
      *      *      *      *      *      *
ACA GCA GCA GTT AGC CTC CTT GGT GGT CCT GCA ACA AAC AGG GAC TAC TTA CGG CAG CGG
Thr Ala Ala Val Ser Leu Leu Gly Gly Pro Ala Thr Asn Arg Asp Tyr Leu Arg Gln Arg

      850      860      870      880      890      900
      *      *      *      *      *      *
CAA GTG GCA TTA GGC AAT ATG GAG ACA AAG GAG TCA AAG GCT ATA CGC CAG CAT GCA GAA
Gln Val Ala Leu Gly Asn Met Glu Thr Lys Glu Ser Lys Ala Ile Arg Gln His Ala Glu

      910      920      930      940      950      960
      *      *      *      *      *      *
GCA GCT GGC TGT AGC ATG ATT GAA GAT ATT GAG TCA CCA TCA TCA ATA TGG GTT TTT GCT
Ala Ala Gly Cys Ser Met Ile Glu Asp Ile Glu Ser Pro Ser Ser Ile Trp Val Phe Ala

      970      980      990      1000      1010      1020
      *      *      *      *      *      *
GGA GCA CCA GAC CGT TGT CCA CCA ACA TGT TTG TTT ATA GCA GGT ATT GCT GAG CTT GGG
Gly Ala Pro Asp Arg Cys Pro Pro Thr Cys Leu Phe Ile Ala Gly Ile Ala Glu Leu Gly

      1030      1040      1050      1060      1070      1080
      *      *      *      *      *      *
GCA TTT TTT TCC ATC CTG CAG GAC ATG CGA AAT ACA ATC ATG GCA TCT AAG ACA GTT GGA
Ala Phe Phe Ser Ile Leu Gln Asp Met Arg Asn Thr Ile Met Ala Ser Lys Thr Val Gly

      1090      1100      1110      1120      1130      1140
      *      *      *      *      *      *
ACA TCT GAG GAG AAG CTA CGG AAG AAA TCA TCA TTT TAT CAG TCC TAC CTC AGA AGG ACA
Thr Ser Glu Glu Lys Leu Arg Lys Lys Ser Ser Phe Tyr Gln Ser Tyr Leu Arg Arg Thr

      1150      1160      1170      1180      1190      1200
      *      *      *      *      *      *
CAA TCA ATG GGG ATA CAA CTA GAC CAG AGA ATT ATT GTG CTC TTC ATG GTT GCC TGG GGA
Gln Ser Met Gly Ile Gln Leu Asp Gln Arg Ile Ile Val Leu Phe Met Val Ala Trp Gly

      1210      1220      1230      1240      1250      1260
      *      *      *      *      *      *
AAG GAG GCT GTG GAC AAC TTC CAC TTA GGG GAT GAT ATG GAT CCT GAG CTA AGG ACA CTG
Lys Glu Ala Val Asp Asn Phe His Leu Gly Asp Asp Met Asp Pro Glu Leu Arg Thr Leu

      1270      1280      1290      1300      1310      1320
      *      *      *      *      *      *
GCA CAG AGC TTG ATT GAT GTC AAA GTG AAG GAA ATC TCC AAC CAA GAG CCT TTG AAA CTC
Ala Gln Ser Leu Ile Asp Val Lys Val Lys Glu Ile Ser Asn Gln Glu Pro Leu Lys Leu

      1330      1340      1350      1360      1370      1380
      *      *      *      *      *      *
TAA TTA ATG AAT GTA TTA ATC CTT TTA TGT GAT TAT CAT ATA CTA CTG AAT CAT TAT CAA

```

FIGURE 24

The nucleotide sequence of the HTV S segment. This represents the continuation of the sequence in Figure 23. Nucleotides 1323 through the end of the sequence at nucleotide 1695 are shown with the corresponding amino acid below the codon. The termination codon for the large open reading frame is at nucleotide 1323. This is followed by an in-frame leucine codon and then a methionine codon. This methionine (nucleotide position 1329) may act as an initiating codon for the small open reading frame which would terminate at position 1473.

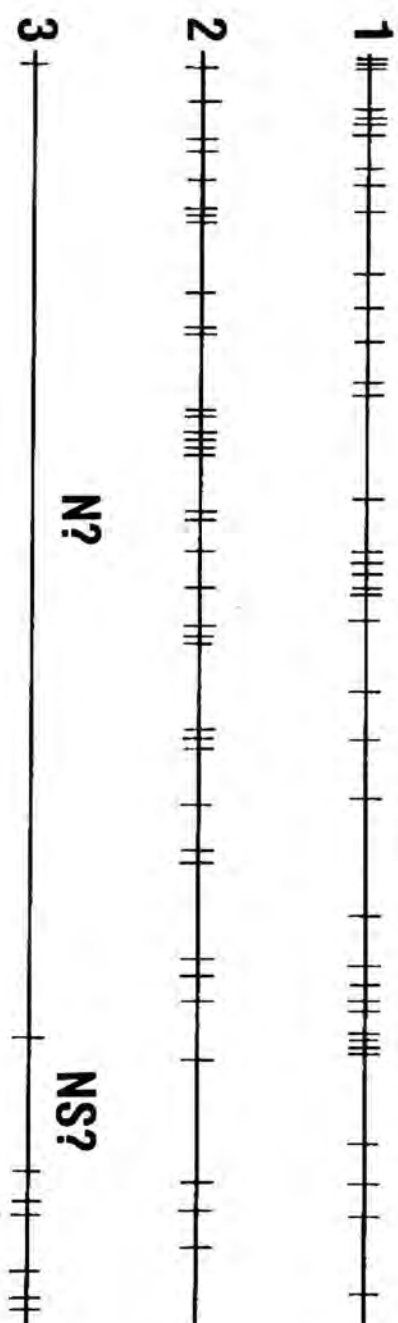
1330 *	1340 *	1350 *	1360 *	1370 *	1380 *
TAA TTA ATG AAT GTA	TTA ATC CTT	TTA TGT GAT	TAT CAT ATA CTA	CTG AAT CAT	TAT CAA
Met Asn Val	Leu Ile Leu	Leu Cys Asp	Tyr His Ile Leu	Leu Asn His	Tyr Gln
1390 *	1400 *	1410 *	1420 *	1430 *	1440 *
TCA TAT TTG CAC TAT	TAT TAT CAG	GGG AAT CAG	TAT ATC AGG	GCA TGG GAA CAT	TTA TGG
Ser Tyr Leu His Tyr	Tyr Tyr Gln	Gly Asn Gln	Tyr Ile Arg Ala	Trp Glu His	Leu Trp
1450 *	1460 *	1470 *	1480 *	1490 *	1500 *
GTG GGA ATC ATT ACT	CAG GGG TGG	GTC AGT TAA	TCC GTT GTG	GGT GGG TTT AGC	TCC AGG
Val Gly Ile Ile Thr	Gln Gly Trp Val	Ser ---			
1510 *	1520 *	1530 *	1540 *	1550 *	1560 *
CTA CCT TAA GTA GCC	TTT TTT TGT	ATA TAT GGA	TGT AGA TTT	CAT TTG ATC	CTT AAC TAA
1570 *	1580 *	1590 *	1600 *	1610 *	1620 *
TCT TGT TTT CTT TCC	CTT TCT TTC	TGC TTT CTC	TGC TTA CTA ACA	ACA ACA TTC	TAC CTC
1630 *	1640 *	1650 *	1660 *	1670 *	1680 *
AAC ACA AAA CTA CCT	CAA CTT AAC	TAC CTC ATT	TGA TTG CTC	CTT GAT TGT	CTT TTT AGG
1690 *					
GAG CAT ACT ACT A					

FIGURE 25

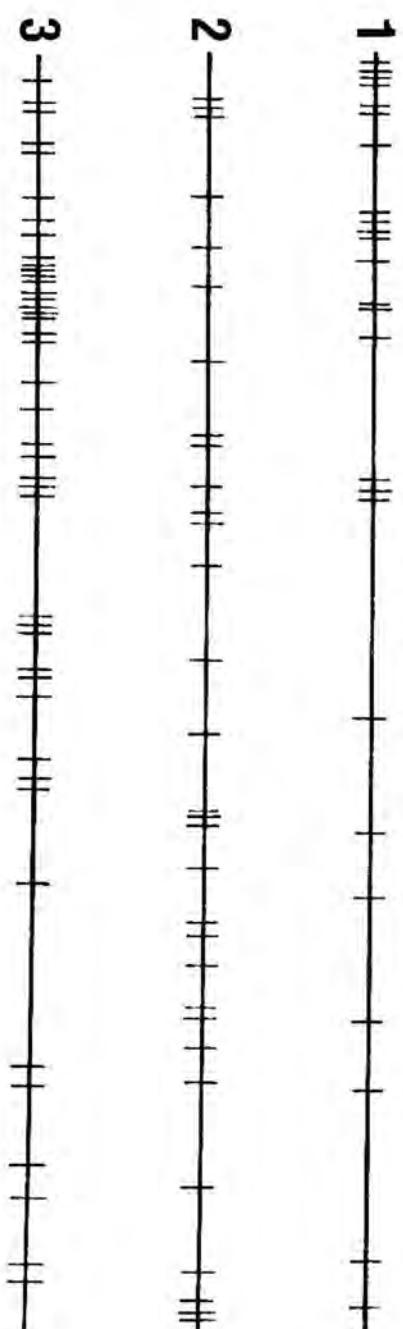
Schematic representation of the coding strategy of the HTV S segment RNA. Each horizontal line represents one of the possible reading frames in the viral-sense RNA (vRNA) or the viral complementary (message-sense) RNA (vcRNA). The vertical bars represent the position of translation termination codons. N? refers to the ORF of the predicted nucleocapsid protein, while NS_s? refers to the ORF of the predicted nonstructural protein.

OPEN READING FRAMES

HTV S vcrRNA



HTV S vrRNA



with a molecular weight of 5929 daltons. A protein of this size has not been found in association with HTV particles, therefore if it exists, it would probably be classified as nonstructural.

A computer program (Protolyze Structure Predictor for the IBM PC) was used to determine the hydropathic plot and to assign secondary structure to the predicted gene products of the HTV S segment RNA (Figures 26 and 27). The hydropathic plot for the large ORF-derived protein did not reveal any significant region of hydrophobic amino acids characteristic of a membrane-associated or a secreted protein, nor are there any sites for N-linked glycosylation. The overall net charge of the protein was +2 assuming lysine and arginine are each +1, histidine +0.5, and aspartic and glutamic acids are -1 each (Ihara *et al.*, 1984). Two hydrophilic areas of the predicted protein, however, contain clustering of charged amino acids. The two hydrophilic areas corresponding to amino acid numbers 145-175 and 338-368 (Figure 22, nucleotide positions 471-561 and Figure 23, nucleotide positions 1050-1140) had net charges of +4 and +6, respectively. The protein had a predicted structure of 43% alpha helix and 37% beta sheet, but no particular unique structure could be determined from the analyses performed.

The structure of the proposed nonstructural protein can also be predicted (Figure 27). The protein is hydrophobic at the amino and carboxy termini while the core of the protein is hydrophilic. The structure is 100% beta sheet with four beta turns predicted; two of these turns correspond to hydrophilic sequences. Such a polypeptide might possess interesting, membrane-association properties, yet may also interact with hydrophilic compounds.

We concluded, therefore, that features of the HTV S segment cDNA sequence had many similarities with other bunyaviruses, in that large

FIGURE 26

Structural predictions for the large ORF-derived protein from HTV S segment RNA. Each line graph is the result of plotting the likelihood of forming a particular polypeptide structure. Each point is taken from the average of four adjacent amino acid residues. Values above the horizontal axis represent regions which are likely to form a particular structure, while values below the line do not favor the structure. Vertical bars above the lines indicate the position of a predicted structure. In the hydropathic plot, values above the line are hydrophobic while areas below the line are hydrophilic. Each point, in that case, is the average of the values for five adjacent amino acid residues. Computer analysis using the Protolyze program was performed as described in Materials and Methods. Numbers correspond to amino acid residues arranged from the amino to the carboxy terminus.

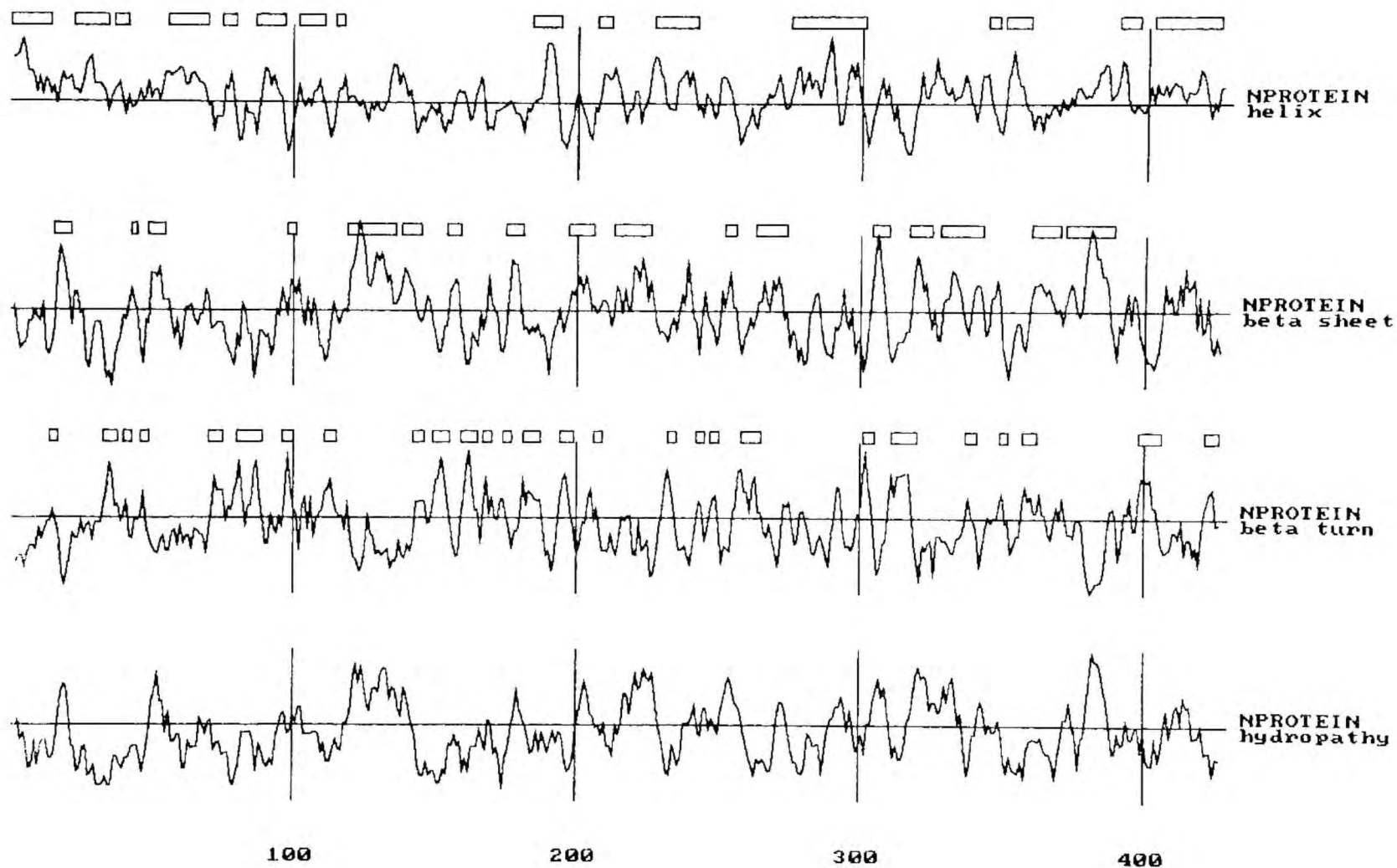
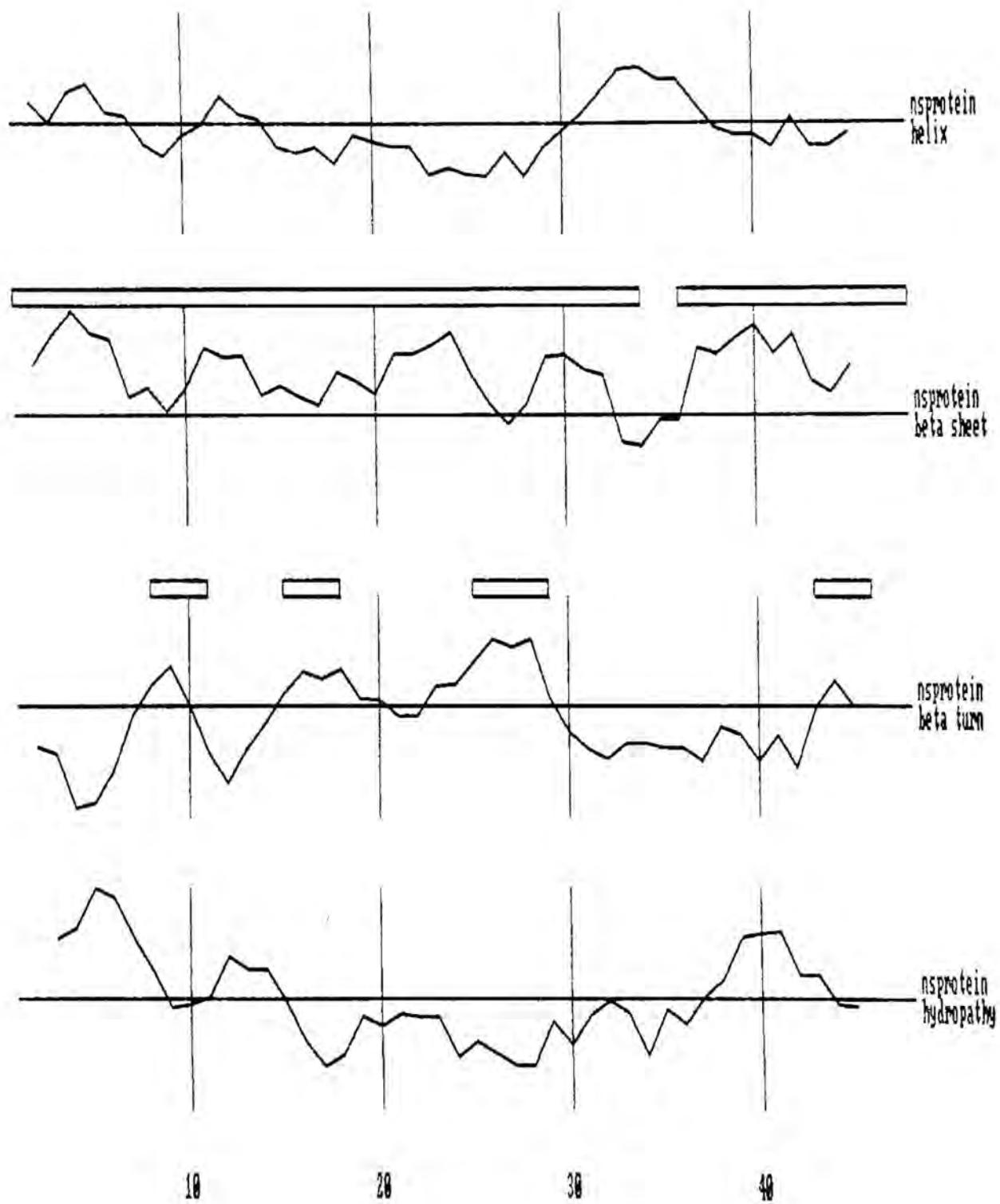


FIGURE 27

Structural predictions for the small ORF-derived protein from HTV S segment RNA. See Figure 26 for explanation of this figure.



(possible nucleocapsid protein) and small (possible nonstructural) proteins were encoded. However, the coding strategy of HTV appeared unique amongst the bunyaviruses, as the two proteins were encoded in the same reading frame.

In vitro translation of HTV S segment cDNA

Based on the limited information available regarding the characteristics of the HTV nucleocapsid protein and on our sequencing data, it seemed likely that the large ORF of the S segment RNA coded for this protein. To discern if proteins could be produced of the size predicted from the large and the small ORFs, we decided to translate in vitro RNA derived from the HTV S segment cDNA. To accomplish this, the Gemini expression system was utilized. The pGEM-2 plasmid (Figure 5) is designed with a multiple cloning site flanked by two different bacteriophage transcription promoters (T7 and SP6). This design allows RNA transcription from either strand of DNA depending on which RNA polymerase is used in the transcription reaction. The isolated RNA can subsequently be used in an in vitro translation reaction to produce encoded proteins.

Although the numerous restriction endonuclease sites in S-86 were an advantage in sequencing, they were a distinct disadvantage in this subcloning. The internal Pst I site of the S segment cDNA (Figure 16) prevented the easy removal of the Pst I insert as one fragment. Therefore, to obtain the entire 1695 base pair fragment, the two fragments would have to be isolated, ligated together, and then subcloned into the pGEM-2 plasmid. Due to the inherent difficulty in this method, a different strategy was devised and attempted first.

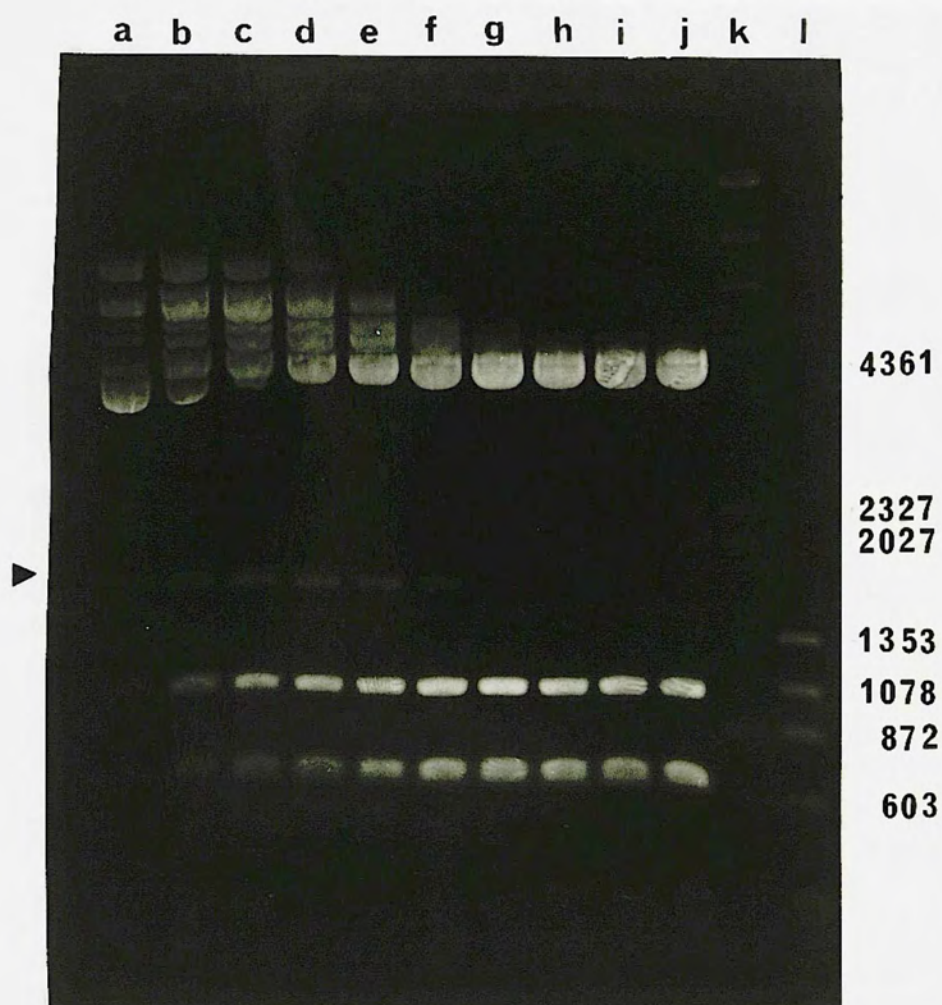
We argued that, if the S-86 plasmid was incubated with Pst I for

a short period of time, not all the Pst I sites would be digested. This would result in a mixture of partially cleaved fragments depending on how many of the three Pst I sites were cleaved. Our hope was that the 3' and 5' Pst I sites would be cleaved before the internal Pst I site was cleaved, allowing isolation of the intact 1695bp fragment. The result of such a partial restriction enzyme digest is shown in Figure 28. Several bands were produced, as predicted, including the desired 1695bp fragment (arrow) containing the HTV S segment cDNA. However, as seen in Figure 28, large amounts of plasmid DNA were required to obtain small amounts of the desired fragment. As yields from fragment purifications were often less than 50%, large quantities would be needed to produce sufficient amounts for subsequent ligations. To make matters worse, the S-86 plasmid did not yield large quantities of DNA in plasmid preparations, a problem sometimes encountered with particular plasmid constructs. Two additional strategies were designed, therefore, to subclone the S-86 Pst I cDNA insert into the pGEM-2 plasmid.

The first involved the isolation of the 1695bp fragment and the ligation of it directly into the pGEM-2 plasmid. In the event that difficulties were encountered with the first strategy, a second strategy was concurrently attempted. This involved the subcloning of the Pst I 1695bp fragment into the pUC9 plasmid (Figure 5) and was devised for two reasons. The pUC9 plasmid produces large quantities of DNA in plasmid preparations. Thus, it would be easier to generate the DNA necessary to obtain large quantities of the 1695bp fragment. Additionally, the pUC9 plasmid contains a multiple cloning site which could be utilized to provide a simpler means of obtaining the 1695bp fragment. Subcloning the 1695bp fragment into a plasmid with only a Pst I cloning site would still require a partial restriction endonuclease digest to remove the

Figure 28

Partial digestion with Pst I to obtain an intact HTV cDNA (1695bp) fragment. S-86 DNA was digested with Pst I and the enzyme inactivated at the indicated times. The fragments were separated by electrophoresis in a 1.0% (w/v) agarose gel at 40 volts for 18 hours. The gel was stained with ethidium bromide and photographed with ultraviolet light. The times of digestion before enzyme inactivation were: lane a, 1 minute; lane b, 3 minutes; lane c, 5 minutes; lane d, 7 minutes; lane e, 9 minutes; lane f, 11 minutes; lane g, 13 minutes; lane h, 15 minutes; lane i, 20 minutes; and lane j, 30 minutes. Lane k contains lambda DNA digested with Hind III and lane l contains ϕ X174 DNA digested with Hae III. The arrow indicates the position of the 1695bp fragment, and numbers to the right of the photograph are marker DNA fragment sizes in base pairs.



fragment. The pUC9 plasmid, however, offered the advantage of allowing cleavage of one end of the fragment with the Sma I enzyme, while the other end of the fragment could be cleaved in a partial digest with Hind III. The Hind III enzyme only cuts the plasmid twice, making it simpler than manipulating the three Pst I digests in S-86.

S-86 DNA was partially digested with Pst I and the fragments separated by agarose gel electrophoresis (Figure 28). The 1695bp fragment of S segment cDNA was then extracted from the agarose gel. The fragment was purified and ligated into the pGEM-2 plasmid or the pUC9 plasmid. Bacterial colonies transformed by the pGEM-2 plasmid were selected in the presence of ampicillin, while pUC9 plasmid transformants were selected in the presence of ampicillin plus Xgal and IPTG. All pGEM-2 transformants were transferred to Biodyne membrane for screening by colony hybridization. However, only the white bacterial colonies from the pUC9 plasmid transformation were transferred to Biodyne membrane for screening, as blue colonies represented the presence of religated plasmids without inserts. Colonies containing the S-86 cDNA were identified by probing the Biodyne membranes with the radiolabeled 1695bp fragment. An example of the autoradiogram from a colony hybridization is shown in Figure 29.

Both strategies were eventually successful. The HTV S segment cDNA was subcloned both into the pUC9 plasmid (labeled A-4) and into the pGEM-2 plasmid (labeled 403-2). To verify that the entire S-86 cDNA had been subcloned, the DNA from the pUC9 and pGEM-2 constructs were digested with Pst I and analyzed by agarose gel electrophoresis. As seen in Figure 30, the Pst I inserts of the A-4 plasmid (lane e) and the 403-2 plasmid (lane f) were indistinguishable from that in the original S-86 plasmid (lanes b and c).

FIGURE 29

Identification of bacterial colonies containing plasmids with HTV S segment cDNA sequences. Bacterial colonies transformed with pGEM-2 or pUC9 plasmids were selected on LB agar plates containing ampicillin and were transferred to Biodyne membranes. After overnight incubation at 37°C, membranes were treated as described in Materials and Methods. The membranes were hybridized with an HTV-S segment-specific labeled probe. A sample autoradiogram is depicted. Positive colonies appear as dark spots (arrows), while negative colonies are faint. Positive colonies were then selected for further analysis by restriction endonuclease digestion of the DNA.

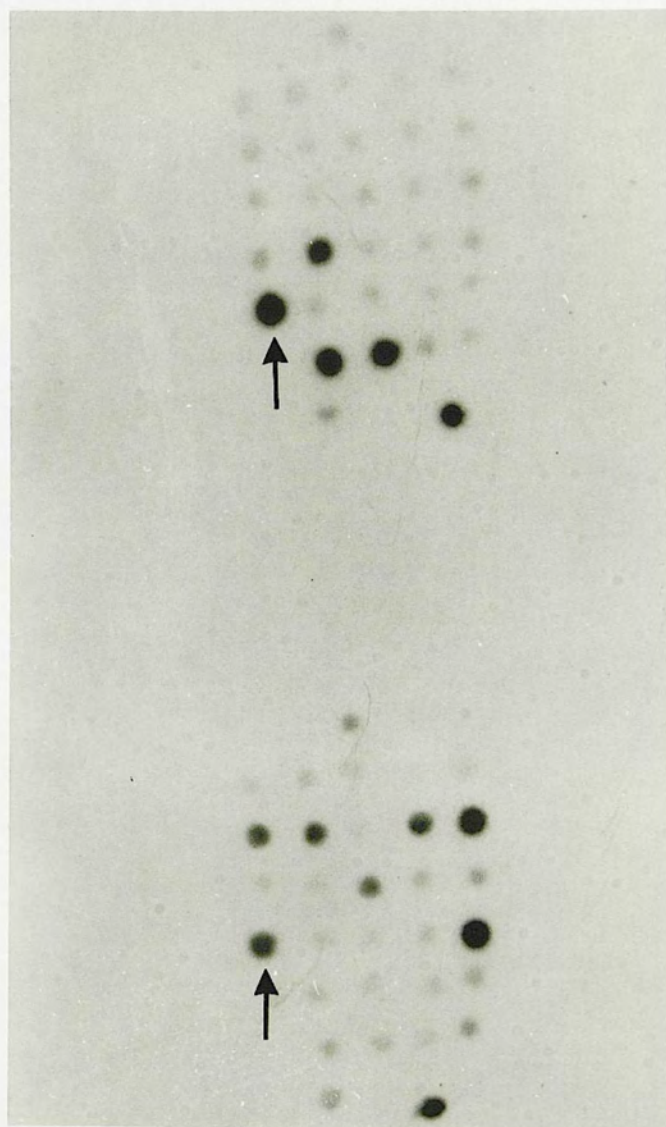


FIGURE 30

Identification of HTV S segment cDNA subclones in pUC9 and pGEM-2.

Plasmid DNAs were digested with Pst I and fragments separated by electrophoresis in a 1.0% (w/v) agarose gel at 40 volts for 18 hours. The gel was stained with ethidium bromide and photographed with ultra-violet light. Lane a contains pUC9 DNA; lanes b and c contain S-86 DNA; lane d contains S-8 DNA; lane e contains A-4 DNA; and lane f contains 403-2 DNA. The pUC9 plasmid without the Pst insert is a 2686 base pair fragment, while the pGEM-2 plasmid is a 2869 base pair fragment. No markers are shown as the size of fragments in lane b had been determined in Figure 19, lane a.



Prior to beginning transcription experiments, however, it was necessary to orient the HTV S segment cDNA within the pGEM-2 plasmid. This was essential for selecting the proper RNA polymerase to produce the viral complementary-sense RNA. DNA from the 403-2 plasmid was digested with Hind III, Pvu II, Sph I, or Bam HI and the fragments analyzed following separation by agarose gel electrophoresis (Figure 31). The orientation was determined in a manner similar to the orienting of the Bam HI fragments in the S-8 plasmid as discussed earlier (page 85). The calculations were based on the fact that the restriction endonuclease sites of pGEM-2 were known (Figure 5) and the restriction endonuclease map of the S segment cDNA had been determined (Figure 16). This analysis determined that the viral complementary-sense RNA would be produced by transcribing the cDNA with SP6 RNA polymerase.

For the transcription reaction, the plasmid is linearized for maximum production of RNA. Due to the numerous restriction endonuclease sites within the S segment cDNA, the only restriction endonuclease suitable for linearization was Xmn I, with a site located 1719bp downstream of the end of the cDNA. This particular restriction endonuclease was not very efficient at digesting the plasmid and resulted in both cut and uncut plasmid DNA. Nevertheless, we proceeded with the transcription reaction, and to insure that RNA was produced from the pGEM-2 construct, the radiolabeled product of the transcription reaction was analyzed by agarose gel electrophoresis (Figure 32, lane c). The other lanes represent the RNA products from other transcription reactions used to monitor this reaction and are described below.

Although the Figure shows that RNA was produced, size measurements could only be rough estimates since no marker was commercially available. Therefore, to assist in size determination, the plasmid was

FIGURE 31

Determination of the orientation of the HTV S segment cDNA in the pGEM-2 plasmid. DNA from the 403-2 plasmid was digested with restriction endonucleases and the fragments separated in a 1.0% (w/v) agarose gel by electrophoresis at 40 volts for 18 hours. The gel was stained with ethidium bromide and photographed with ultraviolet light. The 403-2 plasmid DNA was digested as follows: lane a, Hind III; lane b, Sph I; lane c, Pvu I; and lane d, Bam HI. Lane e contains lambda DNA digested with Hind III. Lane f contains λ X174 DNA digested with Hae III. To the right of the photograph is given the size of marker fragments in base pairs.

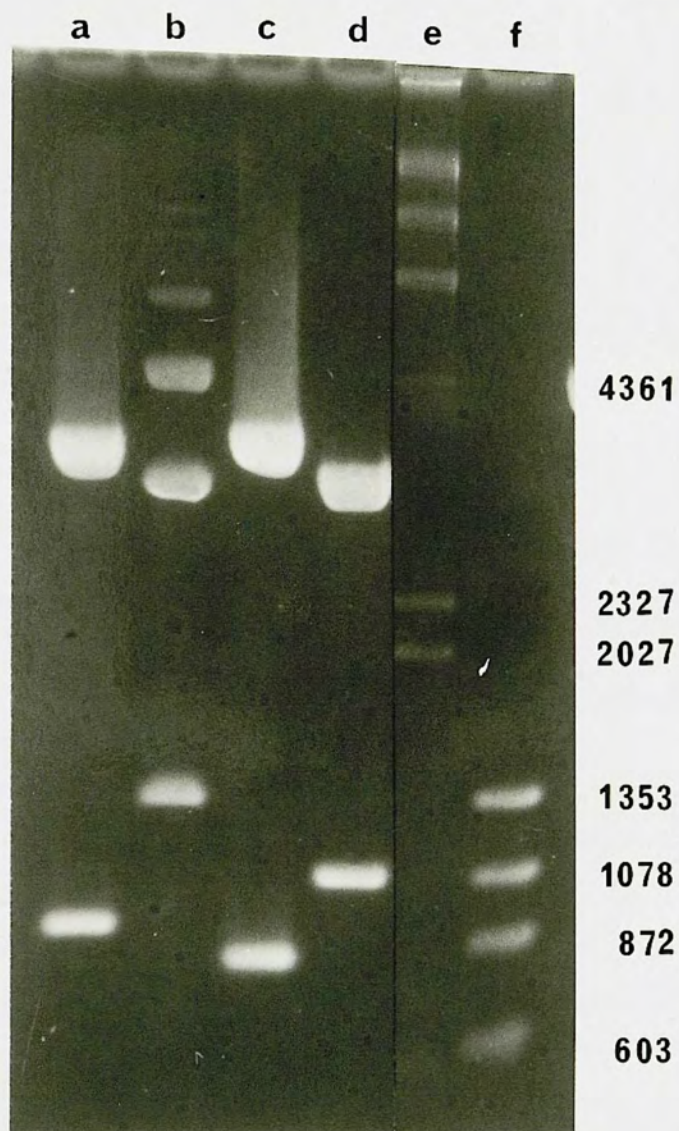
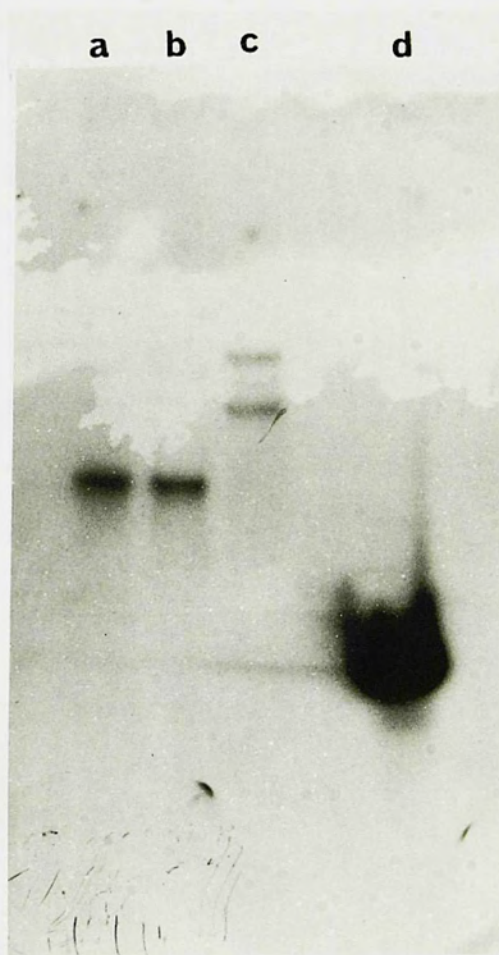


FIGURE 32

Characterization of RNA transcribed in vitro from pGEM-2 plasmids.

Radiolabeled RNA was transcribed in vitro and electrophoresed at 30 mAmps in a 1.5% (w/v) agarose gel containing formaldehyde until the dye front reached the bottom of the gel. The autoradiogram of the gel is depicted. Lanes a and b contain RNA transcribed from the Sal I-linearized 403-2 plasmid with T7 RNA polymerase (approximately 1700 nucleotides). Lane c contains RNA transcribed from the Xmn I-linearized 403-2 plasmid with SP6 RNA polymerase. Lane d contains RNA transcribed from the Hind III-linearized 5-6-43 plasmid with SP6 RNA polymerase (approximately 450 nucleotides). No markers of known size were available.



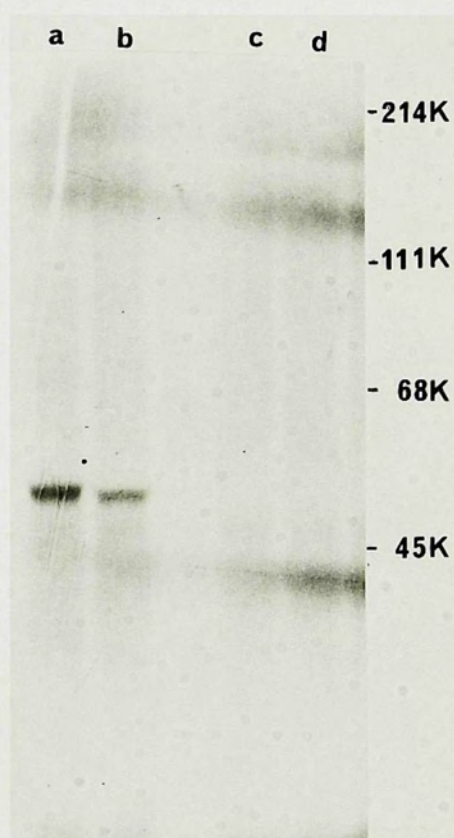
linearized 10bp downstream of the cDNA insert and transcribed with T7 RNA polymerase. This produced a viral-sense RNA (Figure 32, lane a and b) which would be approximately 1700 nucleotides in length. The two RNA bands produced by the SP6 RNA polymerase (Figure 32, lane c) were much larger than this and probably represented RNA synthesized from the Xmn I-digested template (approximately 3400 nucleotides) and the undigested template (approximately 4600 nucleotides). Based on these data, the transcription reaction appeared to produce the RNA necessary for testing in the translation system.

Unlabeled RNA was then transcribed from the 403-2 template with SP6 RNA polymerase and used in the in vitro translation system. The resulting labeled translation products were analyzed by PAGE (Figure 33). Translation of viral-complementary (message-sense) RNA resulted in the production of a single polypeptide of approximately 50,000 daltons (Figure 33, lane a). The size of the protein produced was in agreement with previous reports on the size of the HTV nucleocapsid protein (Elliot et al., 1984). No proteins were produced in the translation reaction in which no RNA or pGEM-2 RNA had been added (lane c and d, respectively). The protein appeared specifically encoded on the S segment viral complementary-sense RNA as the synthesis of the protein increased with increased amounts of added RNA (lane a versus lane b). We expected that the protein of the small ORF might also be translated in this system, but no other protein was seen, even when the translation products were electrophoresed on a 15% polyacrylamide gel.

The inability to demonstrate a protein from the small ORF, of the predicted 6000 daltons, could be due to several reasons. The protein may simply not be made or, if made, be produced at low levels. We felt that the latter was more probable. Most ribosomes initiating at

FIGURE 33

In vitro translation of RNA derived from HTV S segment cDNA. RNA transcribed in vitro from the 403-2 plasmid or the parent pGEM-2 plasmid were translated in a rabbit reticulocyte lysate and ^{35}S -methionine labeled proteins were electrophoresed on a 10% (w/v) polyacrylamide gel. The autoradiogram of the gel is shown. Lane a contains lysate which received RNA from the 403-2 plasmid. Lane b contains lysate which received 1/3 the amount of the same RNA as lane a. Lane c contains lysate which received no RNA. Lane d contains RNA transcribed from the pGEM-2 plasmid with no HTV insert. Apparent molecular weights were determined from prestained protein standards (BRL) electrophoresed in the same gel, and these are given in daltons to the right of the photograph.



nucleotide 36 (Figure 22) will probably fall off at the stop codon of the large ORF. This would leave few ribosomes to read past the stop codon and continue through or reinitiate at nucleotide 1329 (Figure 24). In order to increase the in vitro expression of this protein, the initiating codon for the large ORF was deleted and the ATG at nucleotide 1329 was moved closer to the 5' end of the message-sense RNA.

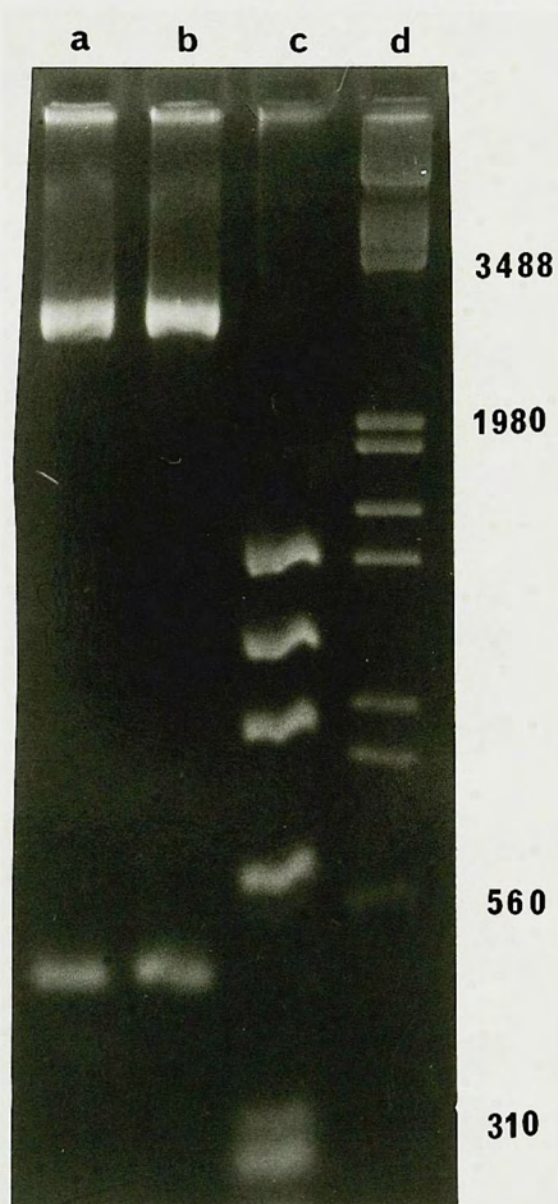
To accomplish this, the Bam HI-Pst I 450 base pair fragment of the S-86 cDNA (Figure 15A, lane i) was subcloned into the pGEM-2 plasmid. This fragment, corresponding to nucleotides 1241 to 1695 of the S-86 cDNA (Figures 23 and 24), contained the coding sequence of the small ORF but was missing most of the large ORF coding sequences. Therefore, the initiating codon for the small protein was only 90 nucleotides from the end of the insert versus 1330 bases from the end of the insert in the 403-2 clone. No other translation initiation codon was found in any of the reading frames between nucleotides 1241 and the start of the ORF at nucleotide 1329.

The fragment was ligated into the pGEM-2 plasmid and clones containing the insert were identified by colony hybridization as explained above (Figure 29). The DNA from the pGEM construct (5-6-43) was digested with Bam HI and Pst I and the fragments separated by gel electrophoresis (Figure 34, lanes a and b). This confirmed the correct size of the Bam HI-Pst I insert of 5-6-43. The orientation of the insert already was known, since the pGEM-2 vector had been digested with Bam HI and Pst I which would allow the fragment to be inserted in only one orientation.

The 5-6-43 plasmid was linearized adjacent to the Pst I site with Hind III enzyme. Radiolabeled RNA was synthesized with the SP6 RNA polymerase and the product examined by gel electrophoresis (Figure 32,

FIGURE 34

Identification of the pGEM-2 plasmid containing the Bam HI-Pst I fragment of the HTV S segment cDNA. DNA from a positive colony (5-6-43) was digested with Bam HI and Pst I and the fragments separated by electrophoresis in a 1.0% (w/v) agarose gel at 40 volts for 18 hours. The gel was stained with ethidium bromide and photographed with ultra-violet light. Lanes a and b contain 5-6-43 plasmid DNA digested with Bam HI and Pst I. Lane c contains ϕ X174 DNA digested with Hae III. Lane d contains lambda DNA digested with Hind III and EcoR I. Numbers to the right of the photograph are the size of marker fragments in base pairs.



lane d). The RNA was synthesized and, although the size of the RNA could only again be approximated, it appeared to be correct. We believe the RNA of 5-6-43 appears to be synthesized more efficiently than the 403-2 RNA because more copies could be synthesized due to its shorter length. Despite this effort, however, translation of the RNA from this pGEM construct still failed to produce evidence of a 6000 dalton protein by PAGE and autoradiography (data not shown).

We concluded that in this in vitro system only one protein was produced. The size of this protein was in agreement with not only the projected size of the large ORF, but also with the size of the HTV nucleocapsid protein. There was no evidence for production of a protein from the small ORF predicted by the HTV S segment cDNA sequence.

Expression of HTV S segment cDNA in a vaccinia virus vector system

We had established that the S segment cDNA could produce, in vitro, a protein with characteristics of the HTV nucleocapsid protein. We now had to confirm that this protein was indeed the HTV nucleocapsid protein. In addition, we wished to study the characteristics of the protein in a eukaryotic system in the absence of the other viral structural components, i.e. negative-sense RNA and glycoproteins, with the ultimate aim of developing a system for virion assembly to which they could be added back. To accomplish this, we choose the vaccinia virus expression system for several reasons (Mackett and Smith, 1986). The virus has a large genome and has been shown to accept and express **inserts** of foreign DNA. Transcription of the inserted DNA is controlled by **unique** vaccinia promoters and a virus-coded RNA polymerase, but translation is dependent upon the initiation site provided by the insert. Recombinant vaccinia viruses have a means of selection, and

expression can be studied in cell culture or in animals. Most importantly for our purpose, they have been shown to be useful as potential human and animal vaccines. In addition, a comparison could be made with a separate vaccinia virus construct which expresses the HTV glycoproteins.

Of the vaccinia vectors available, pSC11 was selected for use in this study for several reasons. The pSC11 plasmid (Figure 5) is constructed with the insertion site for the foreign DNA and the *E. coli* beta-galactosidase gene flanked by the vaccinia virus thymidine kinase (TK) gene. Following homologous recombination between wild type virus and the pSC11 plasmid at the TK gene, recombinant viruses will be TK⁻ and contain the foreign DNA and the beta-galactosidase gene. The replication of recombinant viruses (TK⁻) is selected over that of wild type virus (TK⁺) in the presence of BUdR. These recombinant viruses are therefore easy to select as they also appear as blue plaques on cell monolayers in the presence of Xgal, while wild type virus yields clear plaques. The expression of the beta-galactosidase gene and the foreign gene are controlled by the vaccinia virus promoters P11 and P7.5, respectively. There is no translation initiation codon in the plasmid sequences downstream of the P7.5. Thus, the first initiation codon encountered following the P7.5 promoter sequence is that supplied by the inserted foreign gene. This makes insertion of the foreign gene relatively straightforward, since the foreign gene does not have to be in-frame with a plasmid codon.

Two different approaches were used in subcloning the HTV S segment cDNA into the pSC11 plasmid. Both approaches utilized "shotgun" ligations. Rather than isolate a fragment, as had been carried out in previous ligations (for example the pGEM and pUC constructs on page

123), the "shotgun" ligation involves digestion of a plasmid with a restriction endonuclease, inactivation of the enzyme, and ligation of the mixture of fragments in the presence of the new plasmid into which the fragment is to be inserted. The advantage of this method is that it minimizes the manipulation of the DNA since isolation of individual DNA fragments is not necessary. The disadvantage of the method is that any of the many fragments which may be present can ligate into the vector, but this can be resolved by careful screening of bacterial transformants.

The strategy in the first approach was to subclone the HTV S segment cDNA from the A-4 plasmid (HTV cDNA in the pUC9 plasmid; Figure 30, lane e) into the pSC11 plasmid. To obtain the cDNA fragment, the A-4 plasmid was digested with Sma I enzyme followed by a partial restriction endonuclease digest with Hind III. The results of these digestions are shown in Figure 35. Fragments of various sizes were generated, ranging from the Sma I-linearized plasmid to the desired 1695bp HTV cDNA fragment (arrow). The unique Sma I site is the only cloning site in the pSC11 plasmid. Therefore, to make the fragment ends compatible with the vector system, it was necessary to convert the 5' overhanging Hind III end of the HTV fragment to a "blunt end" by incubation with DNA polymerase and the four deoxynucleoside triphosphates. Following the above digestions and the DNA polymerase reaction, this mixture of blunt-ended fragments (as seen in Figure 35) was incubated with the pSC11 plasmid in the ligation reaction.

The strategy of the second approach was to subclone the HTV S segment cDNA without the 3' viral-sense poly G tails. It is the unpublished belief of many that the poly G tails used for cDNA cloning at the ends of the insert interfere with the subsequent expression of that

FIGURE 35

Partial digestion of the A-4 plasmid to obtain an intact HTV cDNA (1695bp) fragment. A-4 plasmid DNA was digested with Sma I and then with Hind III for the indicated times. The fragments were separated by electrophoresis in a 1.0% (w/v) agarose gel at 40 volts for 18 hours. The gel was stained with ethidium bromide and photographed with ultra-violet light. Lane a contains DNA digested with Sma I only. Lanes b-g contain DNA digested with Sma I and then digested with Hind III as follows: lane b, 2 minutes; lane c, 3 minutes; lane d, 4 minutes; lane e, 5 minutes; lane f, 6 minutes; and lane g, 7 minutes. Lane h contains S-86 DNA digested with Pst I. The arrow indicates the position of the HTV S segment cDNA 1695bp fragment. Markers are not shown, as the size of the fragments in lane h had been determined in Figure 28, lane e.

insert, especially if they occur in the sequences corresponding to the 5' terminus of the message-sense RNA. As seen in Figure 15B (lanes b and c) and as discussed earlier, Acc I digested the HTV S segment cDNA of the S-8 plasmid in the 3' noncoding region (corresponding to the 5' message terminus) producing a fragment which did not contain the poly G tails. Although S-8 is not a full length clone, it does contain the entire protein coding region. The Acc I digest of the S-8 plasmid produces three fragments, two of which contain only pBR322 sequences (although one of these would also contain the 3' poly G tails). The fragment of interest, approximately 3000bp, contained approximately 1650bp of the S segment cDNA (but missing the 3' viral sense poly G tails) plus, at the 5' viral-sense end, approximately 1400bp of the pBR322 plasmid. The S-8 plasmid was digested with Acc I and the ends of these fragments converted to "blunt ends" as described above. This mixture of blunt-ended fragments was then ligated to the Sma I-digested pSC11 plasmid.

Following ligation of the fragments into the pSC11 plasmid, by either method, bacterial transformants were selected on LB agar plates containing ampicillin. All bacterial colonies were transferred to Biodyne membrane and screened for the presence of S segment cDNA by colony hybridization as discussed earlier (Figure 29). This was critical as, due to the "shotgun" ligation, many different fragments could insert into the plasmid. DNA was prepared from positive clones and analyzed by restriction endonuclease digestion to confirm the presence of the entire cDNA fragment and determine the orientation of the insert within the plasmid. The orientation of the insert was determined with a Bam HI digestion of three positive clones (203-28, 203-9, and 103-40) analyzing the fragments by agarose gel electro-

phoresis (Figure 36). Large amounts of DNA from the clones were used for analysis, so that visualization of very small fragments was possible. However, it also created problems of smearing and partial digestion of larger fragments.

Knowledge of the orientation of the insert was crucial as the 3' viral-sense end of the cDNA had to be adjacent to the P7.5 promoter to obtain expression of the proteins encoded by the S segment cDNA. The sizes of fragments were calculated by comparison with marker fragments of known sizes (Figure 36, lanes e and f) and the Pst I-Bam HI fragments of A-4 DNA (lane a: 2700bp, 900bp, 450 bp, 200bp, and 150bp). As the positions of the Bam HI sites were known for both pSC11 and the HTV S segment cDNA (Figure 16), a map could be constructed representing the fragments generated if the cDNA had inserted in the correct or incorrect orientation (Figure 37). The detailed analysis of each of the three constructs is given below.

The 203-28 construct originated from the "shotgun" ligation of the partial digest fragments of the A-4 plasmid (Figure 35). The sizes of the fragments in the Bam HI digestion of 203-28 DNA (Figure 36, lane b) indicated that the clone contained the S segment cDNA with residual pUC9 plasmid sequences in the correct orientation (Figure 37A). This approximately 4400bp insert was generated by partial digestion of the A-4 in which the plasmid was simply linearized with Sma I enzyme (Figure 35). Although the exact size of the 7450bp fragment (Figure 37A; 3150bp from pUC9 and HTV cDNA sequences + 4300bp from pSC11 sequences) was difficult to discern due to the excess amount of DNA (Figure 36, lane b), there was no 4300bp fragment (Figure 37A; incorrect orientation) indicative of the incorrect orientation.

The 203-9 construct also originated from the "shotgun" ligation

FIGURE 36

Characterization of the pSC11 plasmids containing the HTV S segment cDNA. Plasmid DNA from HTV-positive pSC11 clones 203-28, 203-9, and 103-40 were digested with Bam HI and the fragments separated by electrophoresis in a 1.0% (w/v) agarose gel at 40 volts for 18 hours. The gel was stained with ethidium bromide and photographed with ultraviolet light. Lane a contains A-4 plasmid DNA digested with Bam HI and Pst I. Lanes b, c, and d contain plasmid DNA from 203-28, 203-9, and 103-40, respectively, digested with Bam HI. Lane e contains the 123bp ladder (BRL). Lane f contains the 1KB ladder (BRL). Numbers to the right of the photograph are the sizes of the marker fragments in base pairs,

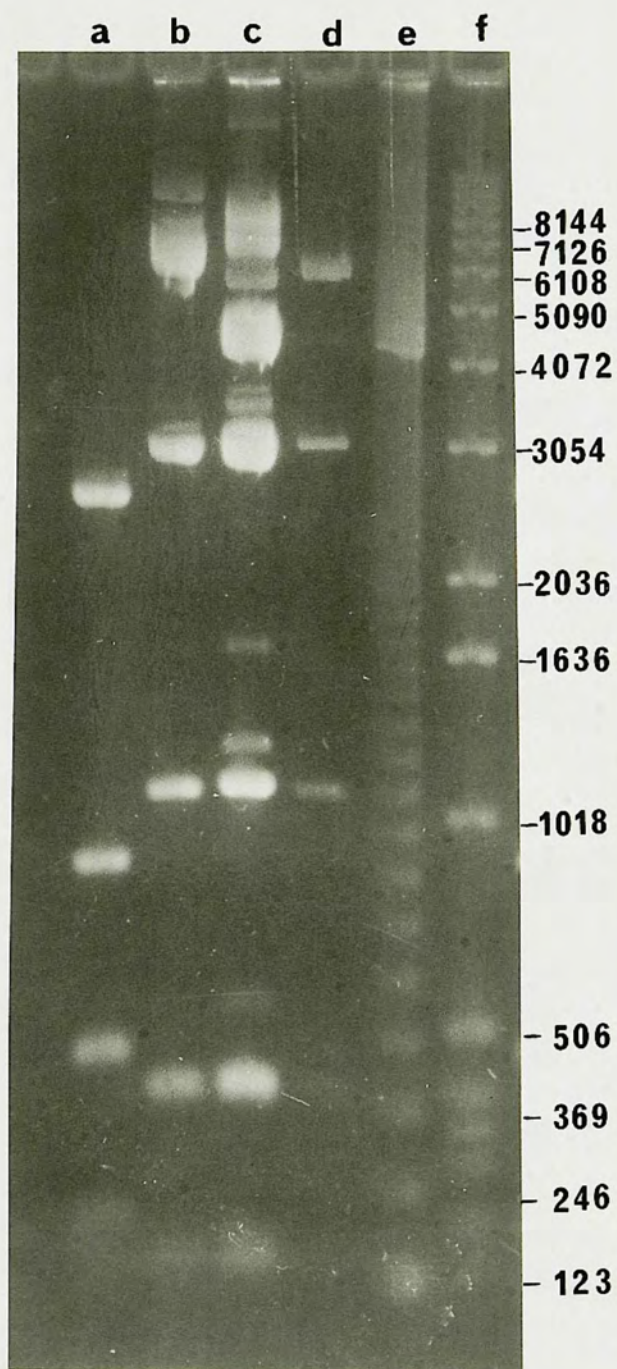


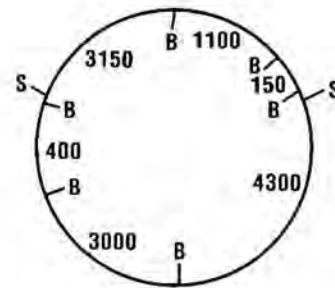
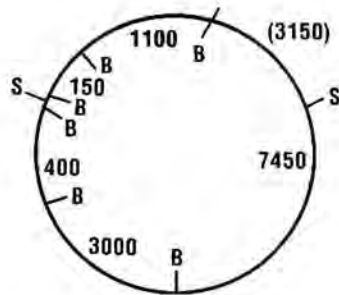
FIGURE 37

Schematic diagram of the possible orientations of the HTV S segment cDNA in the pSC11 plasmid. Plasmids depicted are 203-28 (A), 203-9 (B), and 103-40 (C) with the inserted HTV DNA in the correct or incorrect orientation. The inserted DNA is shown between the Sma I (S) cloning sites of the pSC11 plasmids. Plasmids are not drawn to scale, but fragment sizes are given in base pairs. The size of each fragment generated by the Bam HI digest (B) is given inside the circle. The number in parentheses outside the circle corresponds to the size of the Bam HI-Sma I fragment.

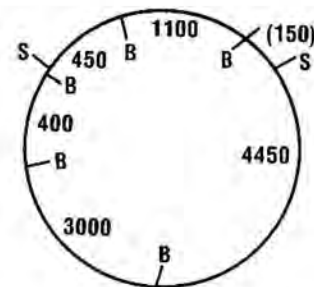
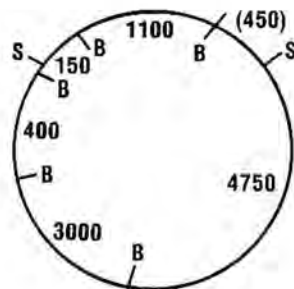
CORRECT

INCORRECT

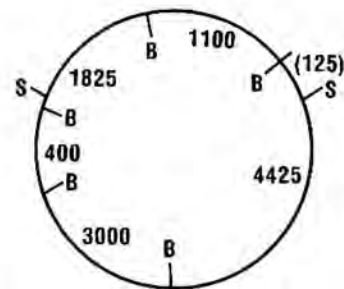
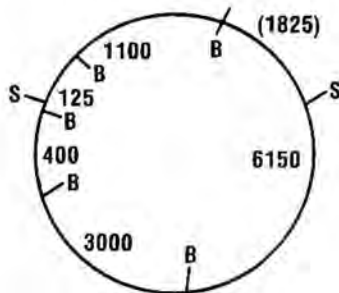
A.



B.



C.



of the partial digest fragments of the A-4 plasmid (Figure 35). The size of the fragments in the Bam HI digestion of the 203-9 DNA (Figure 36, lane c) indicated that this clone contained the S segment cDNA in the correct orientation (Figure 37B). This approximately 1700bp insert contained only the HTV cDNA sequences as it was excised from the A-4 plasmid with Sma I and Hind III (Figure 35). The extra bands in Figure 36, lane c were due to a partial digestion of the excess DNA, but the presence of the 150bp fragment (Figure 37B, correct orientation) and the lack of a 450bp fragment (Figure 37B, incorrect orientation) confirmed the presence of the insert in the correct orientation.

The 103-40 construct originated from the "shotgun" ligation of the S-8 Acc I digest fragments (Figure 15B, lane b). The size of the fragments in the Bam HI digestion of the 103-40 DNA (Figure 36, lane d) indicated the clone contained the approximately 3000bp fragment from the Acc I digest of S-8 DNA (Figure 15B, lane b), once again in the correct orientation (Figure 37C). Although the 400bp and 125bp fragments (Figure 37C, correct orientation) could not be discerned in this gel due to the small amount of DNA, the lack of the 4425bp and 1825bp fragments (Figure 37, incorrect orientation) confirmed the presence of the insert in the correct orientation. We had originally used several different strategies to clone HTV S segment cDNA into pSC11. All three approaches were simultaneously successful and, by chance, all positive clones selected contained inserted HTV cDNA in the correct orientation.

Formation of the recombinant virus from these pSC11 constructs now required the homologous recombination between these plasmids and wild type vaccinia virus. To accomplish this, CV-1 cells were infected with wild type vaccinia virus and each plasmid transfected separately by the calcium phosphate method into these infected cells. These cells

were harvested and prepared for assay of the presence of recombinant viruses. Blue vaccinia virus plaques, the result of the beta-galactosidase gene expression, indicated the presence of a recombinant virus. Recombinant viruses were isolated and subjected to three rounds of plaque purification. The recombinant viruses, v1003A, v1009A, and v1001C, originated from transfections with the plasmids 203-28, 203-9, and 103-40, respectively.

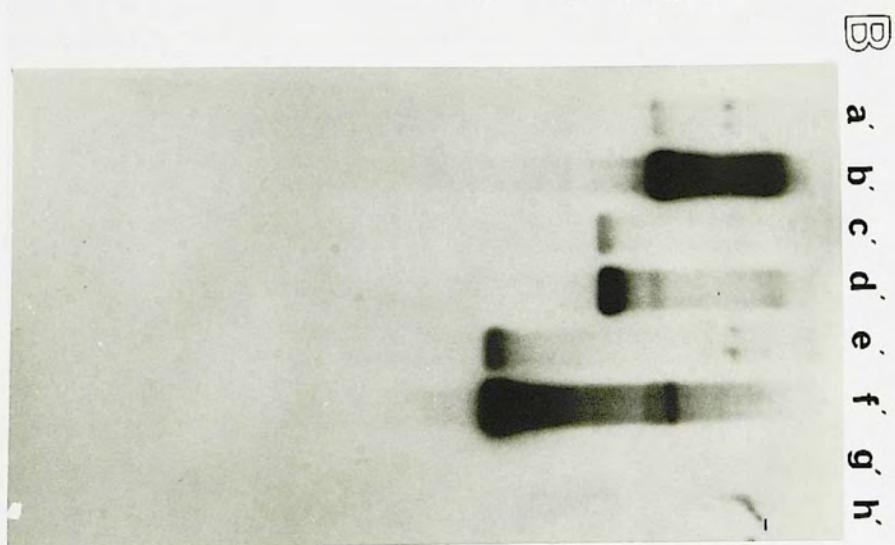
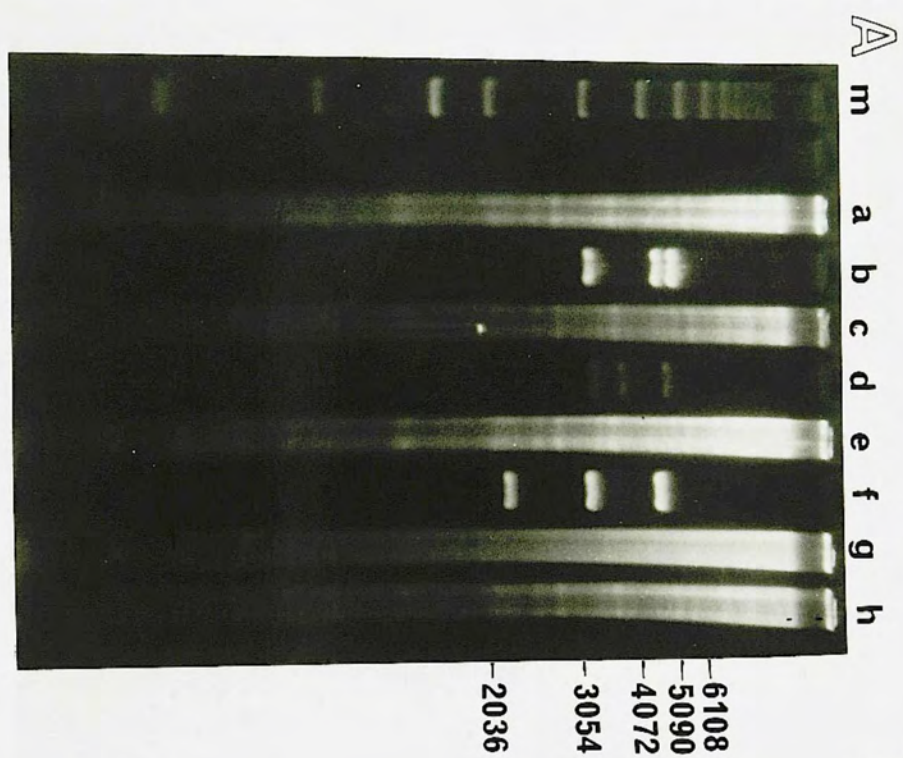
It was necessary, of course, to confirm that the recombinant viruses contained the subcloned HTV fragments which we had previously inserted in the constructed pSC11 plasmids. An EcoR I digest of the parent pSC11 plasmid produces three fragments (Figure 5), although the exact location of one of the EcoR I sites is not known. The other two EcoR I sites, however, generate a fragment which contains the inserted foreign gene plus approximately 500 nucleotides of the pSC11 plasmid. These provide an excellent means of determining the presence of the foreign gene in the recombinant virus since these two EcoR I sites are contained within the recombination site of the TK gene (Figure 5).

Whole-cell DNA was prepared from cells infected with each of the recombinant viruses. This DNA and DNA from vSC8-(a recombinant vaccinia virus with the parent pSC11 plasmid DNA inserted) and mock-infected cells were digested with EcoR I and the fragments separated by agarose gel electrophoresis (Figure 38A). The DNA was transferred to a Biodyne membrane and analyzed by Southern blotting, using the 1695bp S segment cDNA fragment as the probe (Figure 38B). The specificity of the probe was evident since there was no binding of the probe to DNA from the vSC8-or mock-infected cells (Figure 38B, lane g' and h').

The blot demonstrated that the recombinant virus v1003A and the 203-28 clone contained the same fragment - the S segment cDNA plus

FIGURE 38

Identification of recombinant vaccinia viruses containing HTV S segment cDNA. Plasmid DNA or DNA isolated from recombinant vaccinia virus infected cells was digested with EcoR I. The fragments were separated by electrophoresis in a 1.0% (w/v) agarose gel at 40 volts for 18 hours. The gel was stained with ethidium bromide and photographed with ultra-violet light. Lane m contains a 1KB ladder (BRL); lane a contains DNA from vl003A-infected cells; lane b contains 203-28 DNA; lane c contains DNA from vl001C-infected cells; lane d contains 103-40 DNA; lane e contains DNA from vl009A-infected cells; lane f contains 203-9 DNA; lane g contains DNA from mock-infected cells; and lane h contains DNA from vSC8-infected cells. The DNA in the gel (A) was transferred by Southern blot to a Biodyne membrane and hybridized with ^{32}P -labeled, S-86 Pst I (1695bp) fragment. The autoradiogram is shown in panel B. The lanes in panel B correspond to the lanes in panel A. The numbers to the right of the gel represent sizes of marker fragments in base pairs.



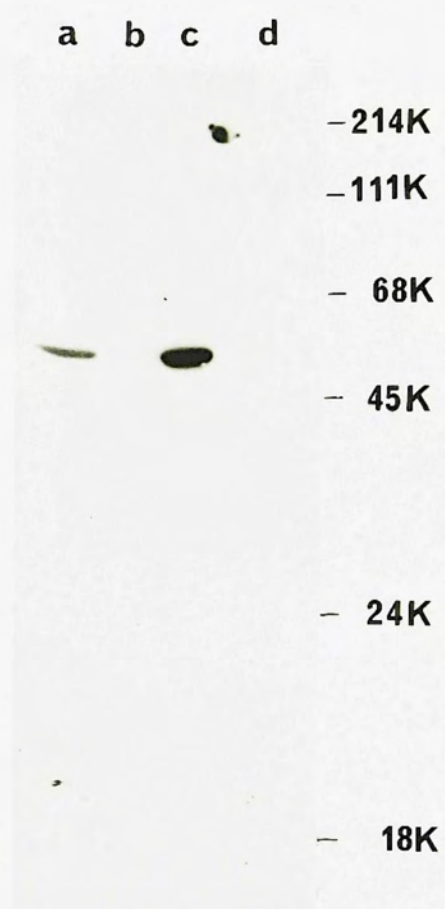
approximately 2700 bases from the pUC9 plasmid (lane a' and b', respectively). The recombinant virus vl001C and the 103-40 plasmid contained the same fragment (approximately 3000bp) - the S segment cDNA plus 1400 base pairs from the pBR322 plasmid, but minus the 3' cDNA poly G tails (lane c' and d', respectively). The recombinant virus vl009A and the 203-9 plasmid also contained the same fragment - the 1695bp of the HTV S segment cDNA (lane e' and f', respectively). The Southern blot analysis, therefore, confirms the precise transfer of the HTV S segment cDNA to each of these recombinant vaccinia viruses.

Expression of the protein(s) encoded by the HTV S segment cDNA in cells infected with the recombinant viruses could now be tested. Lysates were made from cells infected with one of the recombinant viruses (vl009A) and from authentic HTV-infected cells. The HTV infections were carried out under P3 containment at USAMRIID. The proteins in the lysates were separated by PAGE and transferred to nitrocellulose for analysis by Western blotting (Figure 39).

The antibody used in the Western blot was antiserum from a rabbit injected with a synthetic oligopeptide. The sequence of the oligopeptide was deduced from the region of our S segment nucleotide sequence which encoded the carboxy terminal eleven amino acids of the predicted HTV nucleocapsid protein (Figure 23). This amino acid sequence was selected to meet the criteria of Palfreyman et al. (1984) for producing positive antisera from oligopeptides. These are: carboxy or amino terminal sequences, at least 10 amino acids in length, and a relatively hydrophilic region. Using an ELISA, with this peptide as the antigen, serum from the rabbit, following injection, reacted with the peptide, while pre-immune serum was negative. The Western blot, therefore, would serve two purposes. It would be proof that the HTV S

FIGURE 39

Identification by rabbit anti-peptide serum of HTV nucleocapsid protein in HTV- and recombinant vaccinia virus-infected cells. The proteins of lysates prepared from infected- or mock-infected cells were electrophoresed in a 10% (w/v) polyacrylamide gel, transferred to nitrocellulose, and analysed by Western blot using ^{125}I -labeled Staphylococcus protein A. Rabbit antiserum to the synthetic peptide, deduced from our sequence, was used to identify proteins. The autoradiogram of the gel is depicted. Lane a contains lysate from vl009A-infected CV-1 cells; lane b contains lysate from vSC8-infected CV-1 cells; lane c contains lysate from HTV-infected Vero E6 cells; and lane d contains lysate from mock-infected Vero E6 cells. Apparent molecular weights were determined from prestained protein standards (BRL) electrophoresed in the same gel and these are given in daltons to the right of the photograph.



segment coded for the viral nucleocapsid protein, and additionally, it would test for the production of the same HTV nucleocapsid protein in the recombinant virus-infected cells.

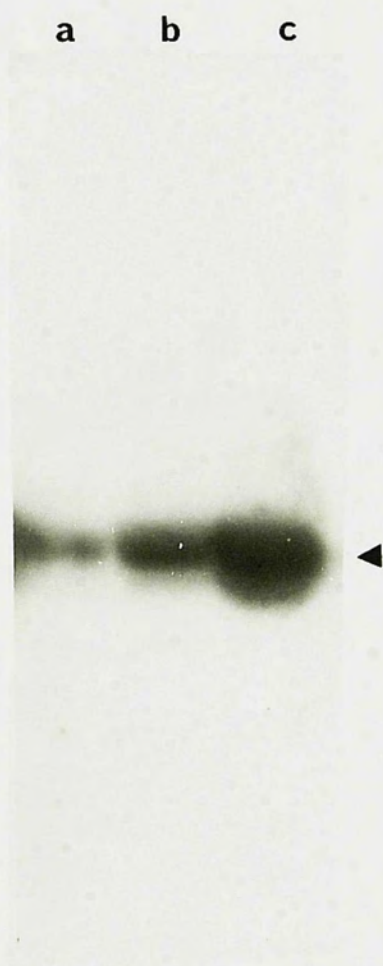
The Western blot in Figure 39 demonstrated the ability of the rabbit anti-peptide serum to bind to the nucleocapsid protein in HTV-infected cells (lane c) (Elliot *et al.*, 1984). The specificity of the antibody was demonstrated by the lack of binding to any proteins in the vSC8- or mock-infected cells (lane b and d). In addition, cells infected with the recombinant vaccinia virus produced a protein bound by the antiserum and having the same apparent molecular weight as the authentic HTV nucleocapsid protein. We conclude, therefore, that the HTV S genomic RNA codes for the HTV nucleocapsid protein and that at least one of the recombinant vaccinia viruses produced this protein.

Since we possessed vaccinia recombinant viruses with differently constructed HTV inserts, a comparison was possible between the three recombinant viruses in levels of expression of the HTV nucleocapsid protein. As mentioned earlier, there are those who believe that poly G tails on inserts in vaccinia virus vectors interfere with maximum expression of encoded proteins.

Lysates were prepared from cells infected with each of the three recombinant vaccinia viruses. The proteins in equal amounts of the lysates were separated by PAGE and transferred to nitrocellulose for analysis by Western blotting. The Western blot of the proteins produced by each of the recombinant viruses is shown in Figure 40. Clearly, all three viruses were able to express the HTV nucleocapsid protein. However, although it was not an absolutely quantitative determination, the Western blot also clearly showed a greater amount of nucleocapsid protein being produced in vl009A-infected cells (lane c) compared to the

FIGURE 40

Comparison of HTV nucleocapsid protein synthesis in the three recombinant vaccinia viruses. Equal amounts of lysates from recombinant vaccinia virus-infected CV-1 cells were electrophoresed in a 10% (w/v) polyacrylamide gel, transferred to nitrocellulose, and analysed by Western blot using ^{125}I -labeled Staphylococcus protein A. The rabbit anti-peptide serum was used to identify the HTV nucleocapsid protein. The autoradiogram of the gel is depicted. Lane a contains lysate from vl001C-infected cells; lane b contains lysate from vl003A-infected cells; and lane c contains lysate from vl009A-infected cells. The arrow indicates the position of the HTV nucleocapsid protein. The sizes of the protein standards are not shown as the size of the vl009A protein (lane c) had been determined in Figure 39, lane a.



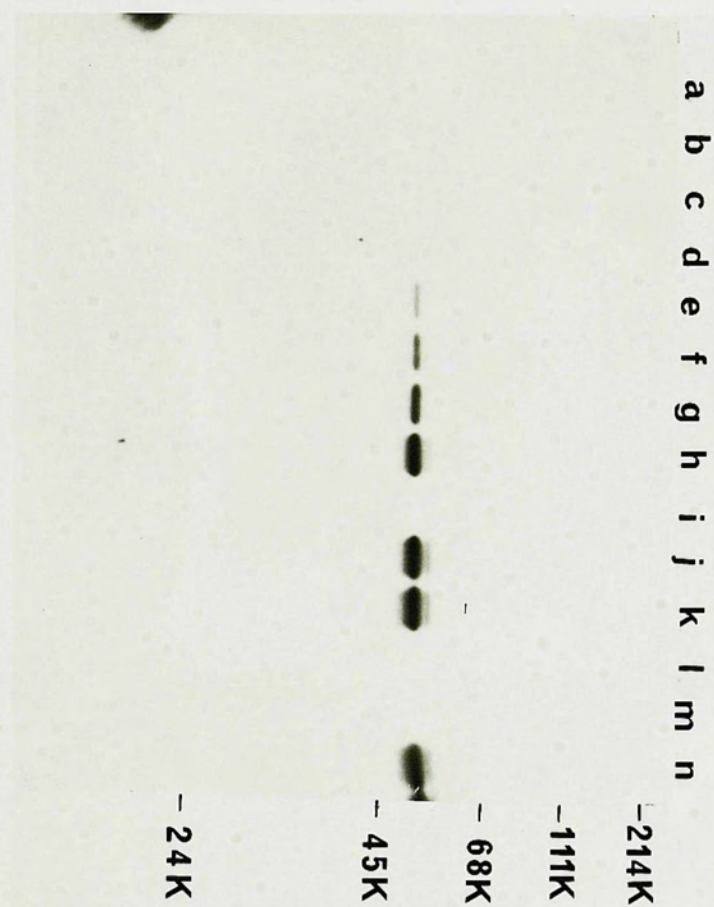
other infected cells (lane a and b). The recombinant virus vl009A was therefore selected for further studies in the expression on the HTV nucleocapsid protein.

A study was now undertaken to determine the time for maximum production of HTV nucleocapsid protein in vl009A-infected cells, since large amounts of the protein were required for future experiments. Lysates were made from vl009A-, vSC8-, and mock-infected cells at various times post infection. The proteins in the lysates were separated by PAGE and transferred to nitrocellulose for analysis by Western blotting. The Western blot of the lysates from the time course study is depicted in Figure 41. As seen in the Figure, levels of HTV nucleocapsid protein expression became detectable beginning 8 hours after infection (lane e), and maximum synthesis of the protein was reached at 48 hour post infection (lane k). This pattern is reflective of expression from the vaccinia P7.5 promoter (Mackett *et al.*, 1984). No proteins were detected in the vSC8- or mock-infected cells (lane i, l, or m).

Interestingly, a faint band was detected above the HTV nucleocapsid protein band, appearing first at 24 hours post infection (lane h). This band was not seen in the *in vitro* translation system (Figure 33) or in HTV-infected cells (Figure 39). The apparent molecular weight of this protein is approximately 6000 daltons larger than the HTV nucleocapsid protein. The ratio of the amount of this protein to the amount of nucleocapsid protein appeared to remain constant while production of this protein appeared to increase at the same rate as the nucleocapsid protein. Additionally, an even fainter band was detected just below the HTV nucleocapsid protein band and may represent a breakdown product or an unprocessed early form of that protein.

FIGURE 41

Time course of HTV nucleocapsid protein synthesis in v1009A-infected cells. Equal amounts of lysates from v1009A- or vSC8- or mock-infected CV-1 cells were electrophoresed in a 10% (w/v) polyacrylamide gel, transferred to nitrocellulose, and analysed by Western blot using 125 I-labeled Staphylococcus protein A. The rabbit anti-peptide serum was again used to identify the nucleocapsid protein. The autoradiogram of the gel is depicted. Lanes a-h, j, k, and n contain lysate from v1009A-infected CV-1 cells harvested at 0 hours (lane a), 2 hours (lane b), 4 hours (lane c), 6 hours (lane d), 8 hours (lane e), 10 hours (lane f), 12 hours (lane g), 24 hours (lane h), 36 hours (lane j), 48 hours (lane k), and 60 hours (lane n) after infection. Lane i contains lysate from vSC8-infected CV-1 cells 24 hours after infection. Lane l contains lysate from vSC8-infected CV-1 cells 48 hours after infection. Lane m contains lysate from mock-infected CV-1 cells 48 hours after infection. Numbers to the right of the photograph represent the apparent molecular weights of protein standards.



As we had shown that the recombinant vaccinia virus-expressed HTV nucleocapsid protein behaved in PAGE like the authentic HTV protein, it was important to examine its location in the infected cell. Therefore, concurrent with the preparation of lysates for the Western blot analysis, infected cells were prepared for examination by immunofluorescence. CV-1 cells were infected with v1009A or vSC8, or mock-infected and prepared for the immunofluorescence study as described in Materials and Methods. The anti-peptide antiserum, used in the Western blot experiments described above, produced a high degree of background fluorescence in the cells and was unable to be utilized. Therefore, a rabbit polyclonal anti-HTV serum (made against whole HTV virus) was used in this study; it produces a diffuse cytoplasmic staining with bright, perinuclear fluorescence in HTV-infected cells (Figure 42a). The perinuclear staining is caused by the presence of the HTV glycoproteins in the Golgi, while the cytoplasmic staining is attributed to the HTV nucleocapsid protein. The specificity of the antibody binding was demonstrated by the lack of fluorescence in vSC8-infected cells (Figure 42b) or in v1009A-infected cells at time zero or 4 hours after infection (Figure 42c and 42d, respectively).

The kinetics of synthesis of HTV nucleocapsid protein seen in this immunofluorescence study corroborated the kinetics seen earlier in the Western blot analysis. However, the pattern of fluorescence in the v1009A-infected cells contrasted markedly with the pattern in HTV-infected cells. The first detectable fluorescence in the 1009A-infected cells is seen 8 hours post infection as a diffuse cytoplasmic staining (Figure 43e) which is what we expected to see, based on the studies with HTV-infected cells. However, two hours later, the pattern has developed into a granular fluorescence, diffusely scattered throughout the

FIGURE 42

Immunofluorescent studies of HTV nucleocapsid protein synthesis in v1009A-infected cells. CV-1 cells infected with 1009A, vSC8, or HTV were prepared for immunofluorescent studies at the indicated times. The antibody used in the study was polyclonal antiserum from HTV-infected rabbits. Panel a shows HTV-infected cells prepared 8 days after infection. Panel b shows vSC8-infected cells prepared 24 hours after infection. Panel c and d show v1009A-infected cells prepared 0 hours and 4 hours after infection, respectively.

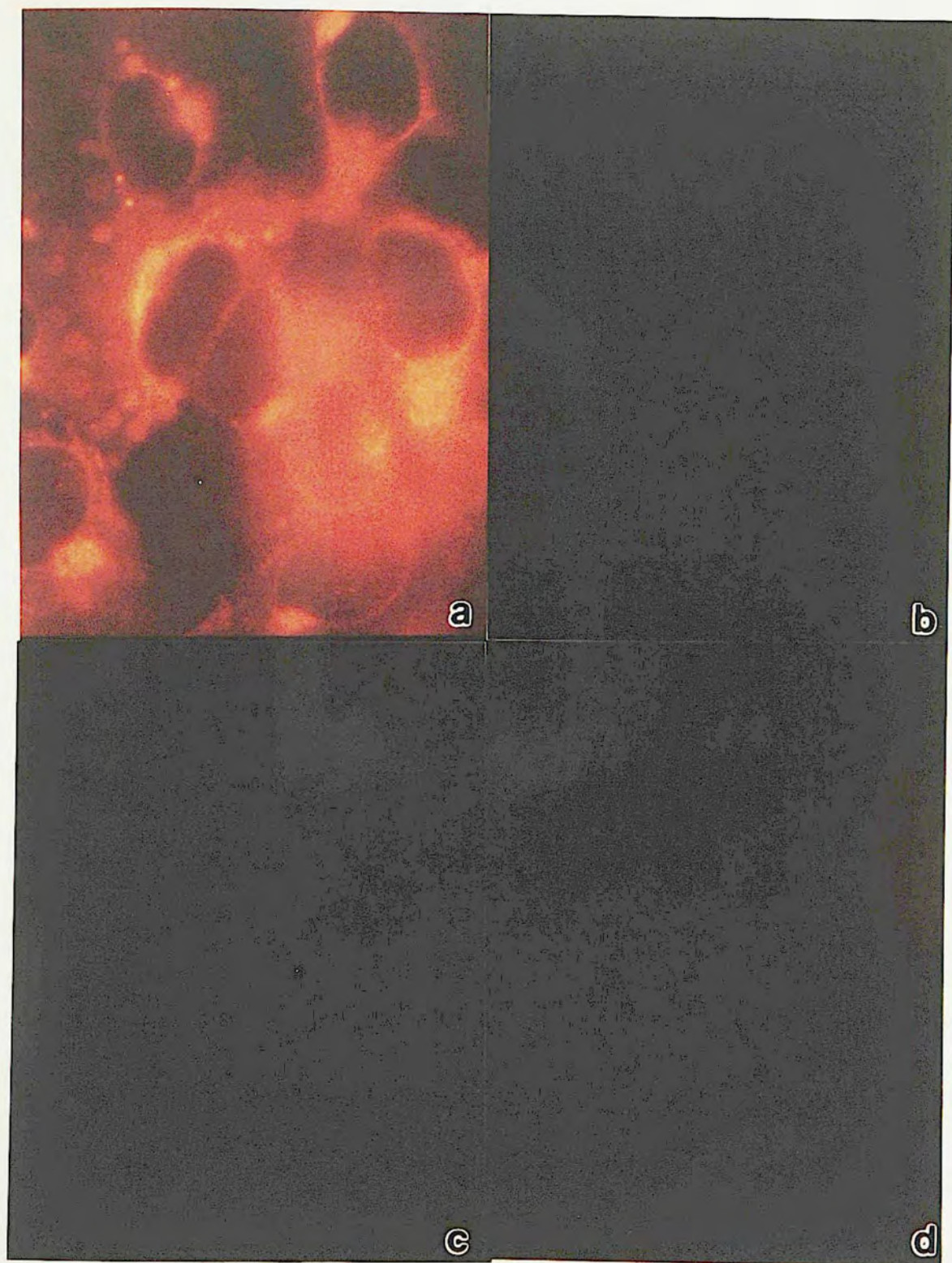
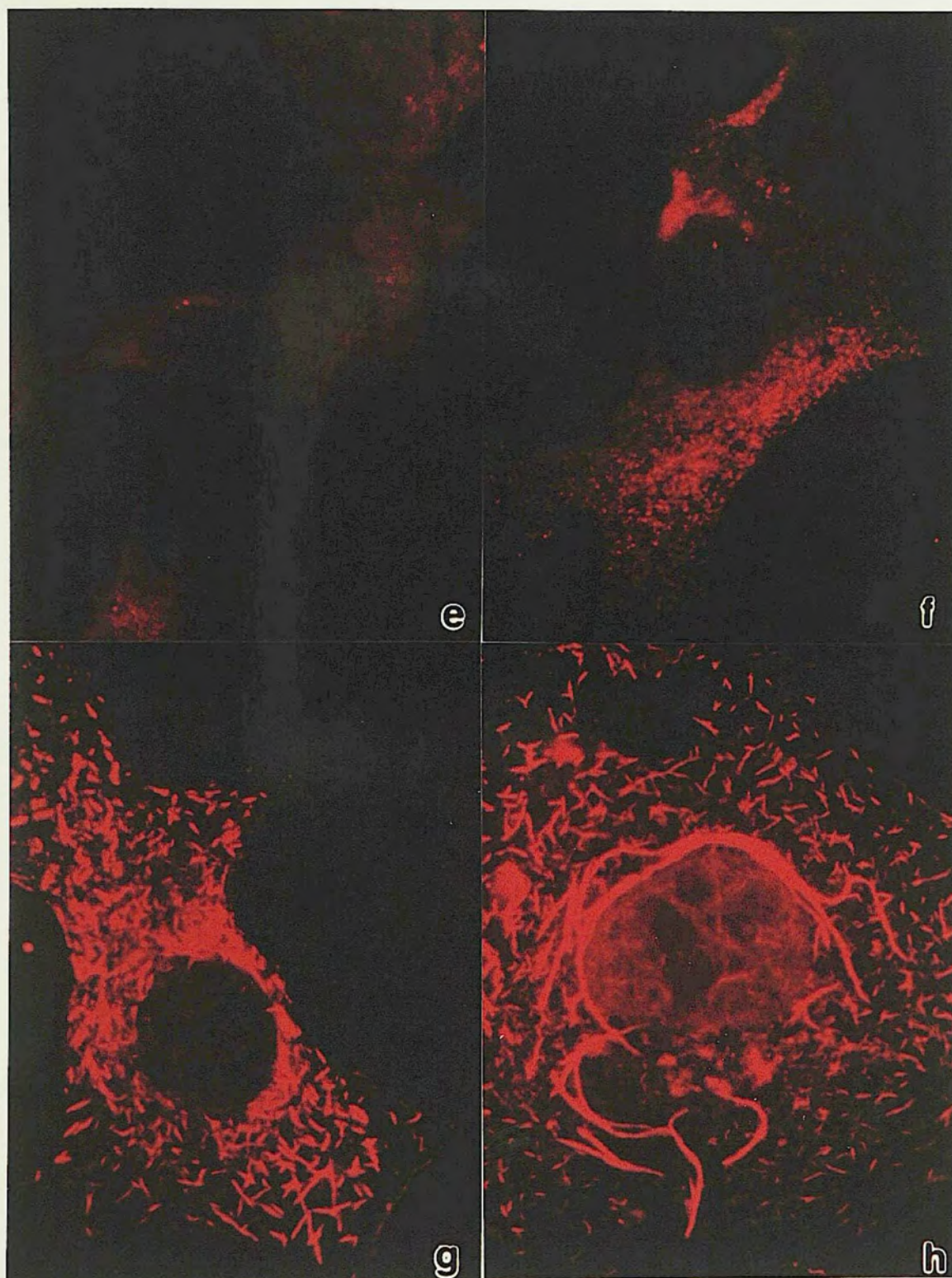


FIGURE 43

Immunofluorescent studies of HTV nucleocapsid protein synthesis in v1009A-infected cells. Cells, virus, and antibody used were as described in Figure 42. Panels e, f, g, and h show v1009A-infected cells prepared at 8 hours, 10 hours, 24 hours, and 48 hours after infection, respectively. This represents a continuation of the data in Figure 42.



cytoplasm, with some of the granules appearing as small, rod-shaped fluorescent structures (Figure 43f). These structures then developed into large rods by 24 hours after infection (Figure 43g) and eventually formed long strands of fluorescent material, located close to the nucleus, at 48 hours post infection (Figure 32h). This pattern of fluorescence was not seen in HTV-infected cells. There was no evidence of fluorescence on the cell membrane or in the nucleus. The pattern of fluorescence did not indicate association with the Golgi, such as develops with the glycoproteins in HTV-infected cells or in cells infected with a recombinant vaccinia virus (vMP2) expressing the glycoproteins (Pensiero *et al.*, 1987). The long strands of fluorescence around the nucleus in Figure 32h may indicate, however, an association with the endoplasmic reticulum or a self-aggregation of the nucleocapsid protein in an end-to-end fashion.

We concluded that the HTV S segment cDNA produced the HTV nucleocapsid protein as predicted by the sequence data. When the cDNA was expressed in eukaryotic cells in the absence of the other viral components an additional protein (56,000 daltons) was synthesized. Furthermore, the fluorescence pattern of the nucleocapsid protein within recombinant virus-infected cells was unlike that seen in HTV-infected cells, and suggested a self-aggregation of the protein.

Immunogenicity of HTV recombinant vaccinia viruses

One advantage of the recombinant vaccinia virus expression system is that a single inserted gene product can be examined in animals, as well as in tissue culture. We have described above the ability of the recombinant vaccinia virus to express the HTV nucleocapsid protein in cell culture. Our laboratory has also constructed a

recombinant vaccinia virus (vMP2), containing the HTV M segment cDNA, which has been demonstrated to produce the HTV glycoproteins (G₁ and G₂) in infected cell culture (Pensiero *et al.*, 1987).

The ultimate goal for expression of these gene products in such a vector system is to engineer a vaccine to prevent disease caused by HTV. Our specific recombinant vaccinia viruses are not themselves possible human vaccine candidates, due to their selection in BUdR and to the presence of the "foreign" gene sequences (poly G tails and the beta-galactosidase gene). Indeed, a recombinant vaccinia virus has yet to be constructed which takes these points into consideration and would be acceptable to government regulators. However, we can use our recombinant viruses to lay the groundwork for determining which viral components should be included in any genetically-engineered vaccine. It would also now be relatively straightforward to re-engineer our cDNA constructs into any newly developed vaccinia vector.

A necessary first step in vaccine investigation would be to determine if animals infected with the two HTV recombinant viruses can elicit antibodies to the HTV glycoproteins and nucleocapsid protein. Positive results would indicate both expression of the HTV gene products in the animal and the ability of the animal to generate an immune response to them. This is a critical investigation before considering any other animal experiments examining the immunological importance of HTV components during an HTV infection.

Mice were selected for these experiments because of their low cost and ease of handling, while the specific strain of mice, BALB/cByJ, was chosen due to its uniform resistance to the lethal effect of vaccinia virus (Buller *et al.*, 1985). Mice were infected by tail scarification since it is identical to the method used to vaccinate

humans and has been shown to produce consistent infection in mice. The control virus for the experiment, vSC 8, is identical to wild type vaccinia virus except for the insertion of the beta-galactosidase gene into the thymidine kinase gene. This virus was chosen as a control since it more closely resembles the recombinant viruses than does the wild type vaccinia virus.

Mice were vaccinated with v1009A, vMP2, vSC8, or saline on day zero, with a booster vaccination of the same virus four weeks later. Mice developed the typical vaccinia lesion at the site of inoculation, but otherwise remained healthy, and serum was obtained at two, four, and six weeks following initial vaccination. These sera were tested for the presence of antibodies capable of neutralizing HTV in an *in vitro* virus plaque assay. All mice infected with vMP2, expressing the HTV glycoproteins, developed neutralizing antibodies to HTV, while all control mice were negative (Table 1). A strong, systemic antibody response against the HTV glycoproteins resulted from the primary vaccination, and re-vaccination raised antibody levels only slightly.

On the other hand, recombinant virus 1009A (expressing the nucleocapsid protein) had either failed to elicit any antibodies to HTV proteins in infected mice, or the antibodies which were produced did not neutralize the virus. We decided to attempt immunoprecipitation of HTV proteins with sera from the mice to determine which of these situations had occurred. Sera from the two cages (five mice per cage) of v1009A-infected mice were pooled separately into two samples. Sera from one cage of vSC8-infected mice and one cage of mock-infected mice were also pooled separately. HTV-infected and mock-infected cell lysates were prepared and the sera used to immunoprecipitate the radiolabeled proteins. The immunoprecipitated proteins were separated by PAGE and

Table 1. Serum neutralization titers^a to HTV of mice vaccinated with vMP2, v1009A, vSC8, or mock-vaccinated.

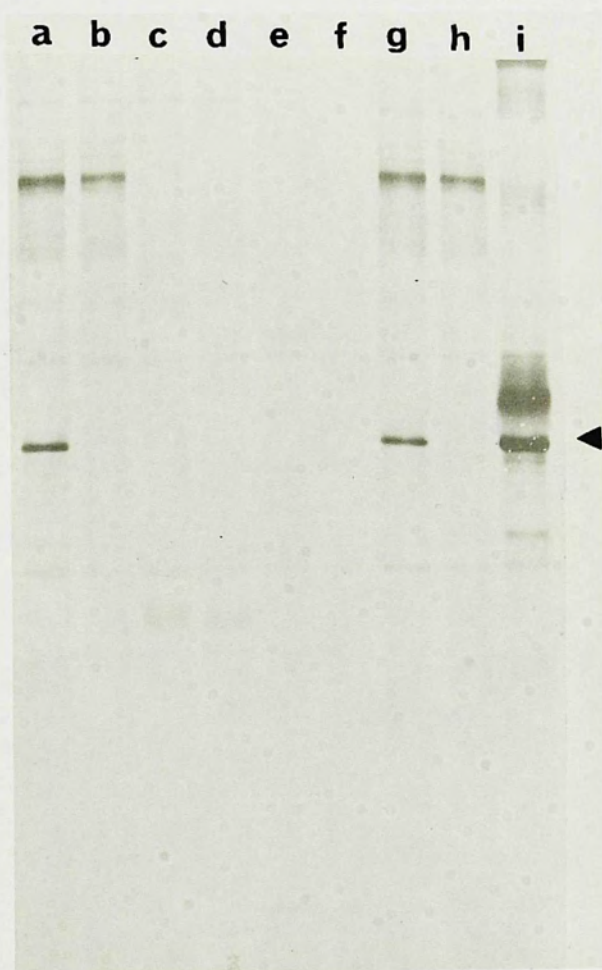
Virus Received	Animal Number	Day 14	Day 28	Day 42
vMP2	1-1	160	160	320
	1-2	--- ^b	320	320
	1-3	320	160	160
	1-4	160	160	160
	1-5	320	640	640
	2-1	320	320	320
	2-2	640	640	640
	2-3	160	320	640
	2-4	--- ^b	640	640
	2-5	320	160	320
v1009A	ALL	<20	<20	<20
vSC8	ALL	<20	<20	<20
Medium	ALL	<20	<20	<20

^aTiters are expressed as the reciprocal of the highest dilution of serum giving a reduction of HTV plaques that was greater than 80%.

^bSerum not obtained from that mouse on indicated day.

FIGURE 44

Immunoprecipitation of HTV nucleocapsid protein with serum from vl009-infected mice. Lysates from uninfected or HTV-infected cells were prepared and immunoprecipitated with sera pooled from the vl009A-, vSC8-, or mock-infected mice. Immunoprecipitates were electrophoresed in a 10% (w/v) polyacrylamide gel and the gel dried. The autoradiogram of the gel is shown. Lanes a, c, e, and g were HTV-infected lysates. Lanes b, d, f, and h were uninfected lysates. Lanes a and b (from cage 1) and lanes g and h (from cage 2) were precipitated with sera from vl009A infected-mice. Lanes c and d were precipitated with sera from vSC8-infected mice. Lanes e and f were precipitated with sera from mock-infected mice. Lane i was HTV-infected lysate precipitated with polyclonal sera from HTV-infected rabbits. The arrow indicates the position of the HTV nucleocapsid protein in lane i.



the gel analyzed following autoradiography (Figure 44). As expected, no proteins were precipitated with the sera from vSC8- or mock-infected mice (lanes c through h). However, sera from mice infected with v1009A precipitated a protein from the HTV-infected cells which was not precipitated from the mock-infected cells (lane a and g versus b and h). This protein was the same apparent molecular weight as the HTV nucleocapsid protein (lane i). We concluded that mice inoculated with v1009A had developed antibodies to the HTV nucleocapsid protein. These antibodies, however, were unable to neutralize the virus in vitro.

The next step would be to determine if the HTV recombinant viruses, individually or combined, afforded mice protection from challenge with HTV. This experiment, however, is currently impossible. Challenge of these recombinant virus-infected mice would not have been worthwhile since adult mice do not develop disease from HTV infection. The only animal model for HTV infection is the suckling mouse, but as we have discussed earlier, it must be infected with HTV by 96 hours of age to be susceptible. Therefore, the mouse would be unable to respond to a vaccination before natural resistance to infection develops. One possible alternative was to immunize mice passively with serum from the animals infected with the recombinant viruses. In discussion with USAMRIID personnel, who are experts in this area, it was decided that this indirect approach was inadequate for the proper evaluation of the immune response necessary to determine the importance of HTV components in preventing HTV infection. It seems likely that the first direct test of the efficacy of an HTV vaccine candidate may have to take place in human populations. The risk in some parts of the world for HTV infection is sufficiently high to justify the probable slight risk associated with such vaccination.

DISCUSSION

When this work began virtually nothing was known about HTV at the genetic or molecular level. It had been tentatively proposed as a member of the Bunyaviridae family, but that remained to be established. Many general conclusions had been drawn about the virus because of its similarity to other bunyaviruses, but few specific details were known for certain. Preliminary information of the molecular make-up of the virus had been reported, but there was little knowledge of the specific coding strategies of the individual RNA segments, and the roles of the individual HTV proteins in the course of infection were uncertain.

The present work set out to explain the molecular genetics of the two HTV genome segments (S and M) suspected to code for viral structural proteins: the glycoproteins and the nucleocapsid protein. The work can be divided into three main sections. The initial section provided sequence data for the complete M and S segments, to allow comparisons with each other and with other bunyavirus genomes. In addition, we were able to determine the coding capacity of each segment. As the work evolved, a greater emphasis was placed on the encoded protein(s) of the S segment. Thus, in the second section, we examined the expression of the S segment encoded protein(s) both in vitro, with the Gemini system, and in vivo, with the vaccinia virus expression system.

Expression of the individual encoded protein(s) permitted the third section of our work to center on the function of the HTV nucleocapsid protein. The immunological function of the protein was studied in comparison with the HTV glycoproteins. Attempts were also made to

study the functions of the protein in virus assembly, specifically the binding of the nucleocapsid protein to the RNA, and the association of the nucleocapsid protein with the glycoproteins. This discussion will be divided into these three sections. This seems the most logical approach, but occasionally the significance of some of the data will be eluded to early in the discussion, but will not be completely discussed until later sections.

Comparison of the 3' terminal sequences of the HTV M and S genome segments

We started analysis of our sequences by examining the 3' noncoding regions (viral-sense RNA) from the HTV M and S segments to determine the extent of conserved sequences, since the 3' genomic termini are conserved amongst the bunyaviruses. Schmaljohn *et al.* (1985) had shown, by direct terminal RNA sequencing of the HTV S, M, and L segments, that seventeen of the first twenty-five nucleotides were conserved. We extended this sequencing data to show that in the entire 3' noncoding region of the M and S RNA segments twenty nucleotides were conserved (Figure 45). However, the greatest concentration of conserved sequence was in the terminal 18 nucleotides.

One interesting early finding was that there was some variation in the 3' (and sometimes 5') terminal sequences of different HTV cDNA clones. Thus, there were differences between our sequence data for the 3' noncoding regions and the sequence reported by Schmaljohn *et al.* (1985, 1987a). These differences were probably due to two problems with cDNA synthesis. First, the difference between the primers used for cDNA synthesis of the M and S segments (see page 39) was in only two nucleotides, positions 15 and 16 (S: CU; M: GC). If the annealing conditions

FIGURE 45

Comparison of the 3' sequences of the HTV M and S RNA segments. Shown is the 3' noncoding region of each of the genomic(negative)-sense RNA of the M and S segments. Horizontal lines indicate spaces in the sequence that allow best alignment of the sequences. Vertical lines indicate those nucleotides that are identical in the two sequences.

M SEGMENT

3' — A — C A U C A U C U G A G G G A U U U C U U U C G U C A G U U A G U C G U U G

| | | | | | | | | | | | | | | |

3' — A U C A U C A — C U G A G G G A U U U C U C G A U G A U C U U G U U G C

S SEGMENT

for the cDNA synthesis reaction were not sufficiently stringent, the S segment primer could have annealed with the M segment, resulting in a cDNA clone of the M segment with 3' sequences of the S segment primer. This apparently happened, for when the S segment primer is compared with the M-17 clone (Figure 11), the sequence is identical for the length of the primer and then diverges.

Secondly, nucleotide 2 in the M segment and nucleotide 8 in the S segment were absent from the cDNA sequence when compared to the direct RNA sequencing results. We believe, based on the direct RNA sequence results, that these mistakes (base mismatches) were made at the terminus during second strand synthesis of the cDNA. This would also explain the difference in Acc I digestion of the S-86 and S-8 clones (Figure 20). If the copying is exact, an Acc I site begins at nucleotide 6; if nucleotide 8 is missing, the Acc I site is lost. When these changes are made, adding a U at position 2 and 8 and changing nucleotides 15 and 16 to GC, the 3' noncoding region of the two segments remains conserved in 20 of the nucleotides. Equally, however, these differences may simply reflect the microheterogeneity in the population of genomic RNAs, particularly since they lie in the noncoding terminal regions.

This pattern of conserved terminal genomic sequences is similar to that found in other bunyaviruses. Snowshoe hare virus (Bunyavirus genus) is conserved for 25 of the 60 nucleotides in the 3' noncoding region of the M and S RNA segments, especially the 13 terminal nucleotides. Punta Toro virus (Phlebovirus genus) is conserved for 15 of the 34 nucleotides in the 3' noncoding region of the M and S RNA segments, especially the 8 terminal nucleotides. The purpose of a 3' terminal conserved sequence is unknown, but may act as a signal for encapsidation of the RNA by the nucleocapsid protein (Bishop and Shope, 1979), as

discussed below.

Sequences flanking the AUG initiation codon of the HTV M and S genome segments

Although the 3' noncoding regions of the HTV M and S segments show few conserved sequences beyond the 18th nucleotide, the number of nucleotides preceding the first AUG in the two segments is nearly identical (Figures 11 and 22). It may be that the length of the 3' noncoding region is important in determining which of the two possible AUG initiation codons is used, since this region corresponds to the 5' end of the mRNA. The first AUG encountered in the M segment is at nucleotide 40, while in the S segment it is at nucleotide 36. Both segments have a second in-frame initiation codon; at nucleotide 64 of the M segment and nucleotide 45 of the S segment. Thus, there is no obvious conclusion to be drawn on AUG usage based simply on distance from the 5' end of the mRNA. Therefore, the sequences surrounding these four initiation codons were examined for a possible consensus sequence which might give a clue to potential AUG usage.

A comparison of sequences surrounding the AUG of some bunyavirus segments (snowshoe hare and Aino viruses; Eshita and Bishop, 1984) has indicated a preference for purine residues at positions -3, -1, and +4 (with -3 being 3 nucleotides upstream from the AUG codon). With the exception of the -1 position, this was in agreement with the identified optimal sequence for initiation by eukaryotic ribosomes, 5'-ACCATG, with the -3 position being the most critical (Kozak, 1986).

The four HTV initiation codons are all conserved at these critical positions with the exception of the -1 position. The second AUG of the M segment also has a guanosine at the critical -3 position.

In a case such as this, with two in-frame AUGs, both having near optimal sequences for initiation, ribosomes initiate primarily at the first AUG encountered (Kozak, 1986). Therefore, it appears likely that the first AUG in the HTV M and S genome segments initiates translation of the encoded proteins. Such a pattern would make the 5' noncoding region essentially identical in length for each segment: 40 nucleotides for the M segment and 35 nucleotides for the S segment (Figures 11 and 22). This, therefore, may be a factor in the translation of the encoded proteins or in the "cap stealing" mechanism of the virus. Amino-terminal sequencing of the nucleocapsid protein should allow a determination of the exact AUG utilized in the S segment. However, the sequence of the amino terminus of the first M segment glycoprotein has shown an apparent cleavage of the amino acids preceding the threonine at nucleotide position 91 (Schmaljohn *et al.*, 1987a), making determination of initiation codon usage difficult.

Possible transcription termination signals in the HTV M and S genome segments

In the 5' noncoding region (viral-sense RNA), the sequence homology between M and S segments is primarily at the terminal eight nucleotides. The length of the M RNA segment 5' noncoding region is 168 nucleotides (Schmaljohn *et al.*, 1987a), while this region in the S RNA segment is 220 nucleotides beyond the end of the small ORF. The message-sense RNA from other bunyavirus segments has been shown to lack nucleotides corresponding to the 5' noncoding region (Rift Valley fever virus, Collett, 1986; and snowshoe hare virus, Eshita *et al.*, 1985). The mechanism by which bunyavirus mRNAs become truncated is unknown, but may involve a transcription termination signal (Collett 1986). The

exact sizes of the HTV M and S mRNA molecules were not discernable in earlier experiments (Schmaljohn *et al.*, 1987b) and require further examination. Therefore, we analyzed the noncoding region of the 5' viral-sense RNA for a common sequence which might act as a transcription termination signal in HTV RNA segments.

In neither HTV segment was there found the transcription termination-polyadenylation signal common to other negative-strand RNA viruses (Sendai virus: 5'-TAAGAAAA and vesicular stomatitis virus: TATGAAAA; Gupta and Kingsbury, 1982). A similar sequence has been found in some members of the *Bunyavirus* genus (S segment of La Crosse and snowshoe hare viruses: 5'-CCCACAAAAAT; Eshita and Bishop, 1984) and in a member of the *Phlebovirus* genus (Punta Toro virus; Ihara *et al.*, 1985). Nor was there a purine-rich sequence analogous to that in the 5' noncoding region of the segments of some bunyaviruses and proposed as a possible termination signal (M segment of Rift Valley fever and snowshoe hare viruses; Collett 1986).

Examination of the HTV segments revealed three sets of nearly identical sequences in the 5' noncoding region of the M and S genome segments which may have a role in termination. The sequence, 5'-CACAAAACT, is found in the cDNA sequence of both the M and S segment (Figure 24, nucleotides 1625-1633). The location of this sequence in both genomic segments is nearly identical in relation to the 5' viral-sense end of the sequence: 63 nucleotides from the end of the S segment and 49 nucleotides from the end of the M segment. Another common sequence is found in the M and S segment, 5'-TATATA; however, unlike the above sequence, the locations are more closely analogous to the end of the ORF than to the 5' end of the RNA segment. This sequence is 50 nucleotides from the end of the small ORF of the S segment (Figure 24,

nucleotides 1526-1532) and 42 nucleotides from the end of the M segment ORF. The third common sequence is 5'-TTCTTCTTCTCG in the M segment and 5'-TTTCCCTTTCTTTCTG in the S segment. This pyrimidine-rich sequence does not have such a similar location, as the other sequences in the M and S segments, since it is located 123 nucleotides from the end of the M segment ORF and 97 nucleotides from the end of the small ORF in the S segment (Figure 24, nucleotides 1573-1588)

Whether any or all of these sequences are involved in transcription termination requires further investigation. The first sequence (5'-CACAAAAC) seems the probable signal since it is found on both segments, in nearly identical positions, and is reminiscent of the termination-polyadenylation signal (5'-CAAAAA) of other negative-strand RNA viruses. The S1 nuclease enzyme, which digests single-stranded but not double-stranded nucleic acid, could be utilized to determine the exact 3' terminus of the mRNA. The S segment Bam HI-Pst I (450bp) cDNA fragment could be annealed to RNA from HTV-infected cells and subsequently treated with the S1 nuclease. Size determination of this fragment by gel electrophoresis would determine the 3' end of the S segment mRNA.

One possible explanation for not finding the 6000 dalton protein in HTV-infected cells was that the mRNA had been truncated and did not contain the sequences to encode the protein. Therefore, the comparison of the M and S segments was extended into the coding region of the small ORF of the S segment. However, no stretches of common sequence were evident. It appears, therefore, that the mRNA of the S segment should include the small ORF encoding the 6000 dalton protein, but definitive studies, as discussed above, are still required.

Complementarity at the 5' and 3' termini of the HTV M and S genome segments

The extent of the complementarity found at the termini (5' and 3') of the M and S segments was similar for each of the segments. The S segment sequences were complementary for 19 out of 23 nucleotides (Figure 21). The M segment RNA is complementary for 18 out of 22 nucleotides if one corrects for nucleotide positions 2, 15, and 16 (as discussed above) and if one assumes the terminal 5' (viral-sense) UAG is missing due to a cDNA synthesis mistake (Figure 12). This is comparable to the complementary sequences at the termini of other bunyavirus segments, discussed in the Introduction. An interesting feature is the mismatch at nucleotides 9 and 11 of the S segment and nucleotide 12 of the M segment. Such a mismatch has been found at nucleotide 9 or 10 of all bunyavirus segments sequenced to date (Obijeski *et al.*, 1980; Bishop *et al.*, 1982; Ihara *et al.*, 1984; Akashi *et al.*, 1984; Eshita *et al.*, 1984; Ihara *et al.*, 1985; Collett *et al.*, 1985; Lees *et al.*, 1986). The purpose of this mismatch is not known, but may have a function in the proposed role of these conserved sequences in viral RNA transcription, replication, and/or encapsidation.

Coding strategy of the HTV S genome segment

The sequences of the S segment (Figures 22-24) were then examined for coding strategy and coding capacity. The S segment of viruses in the Bunyavirus genus (for example Aino virus) have been shown to encode the nucleocapsid protein and a nonstructural protein in overlapping reading frames. On the other hand, Punta Toro virus, a Phlebovirus, encodes its nucleocapsid protein on the message-sense RNA

of the S segment, while a nonstructural protein is encoded on the viral-sense RNA; hence the name "ambisense RNA".

Of the three reading frames of the HTV S segment RNA (viral complementary-sense), only one appeared to encode the expected proteins (Figure 25). There was no evidence for a coding strategy employing an overlapping reading frame, since any ORF in the other reading frames either lacked an initiating AUG, or encoded proteins of less than 50 amino acids. There were two ORFs in the viral-sense RNA of the HTV S segment which did contain an AUG and encoded proteins of more than 50 amino acids. However, they were in different reading frames and in the middle of the nucleotide sequence. This is unlike the ambisense coding strategy of Punta Toro virus which utilizes the sequences at the ends of each RNA molecule to encode the two proteins in a non-overlapping organization. Thus, it seemed unlikely that the HTV S segment RNA employs an ambisense coding strategy.

Since there is no evidence for an encoded protein in any other reading frame, the HTV S segment appeared to have a unique coding strategy amongst bunyaviruses. The encoding of the nucleocapsid protein by the large ORF of the S segment is analogous to all other bunyaviruses analyzed. However, unlike other bunyaviruses, the only ORF encoding a possible nonstructural protein of any significant size is found immediately after the large ORF. Thus the coding strategy of the HTV S segment RNA utilizes the same reading frame to encode two proteins. Of course, HTV might be even more unusual than other bunyaviruses since the protein of the small ORF has not been detected in HTV-infected cells, and we have not been able to detect it in our expression experiments. Thus, HTV may fail to express a nonstructural protein from its S segment.

Characteristics of the large ORF protein in the HTV S genome segment

The large ORF in the S segment encodes a protein (Figures 22 and 23) with a predicted molecular weight consistent with the reported value for the HTV nucleocapsid protein (Elliot *et al.*, 1984). The 429 amino acid sequence of the predicted protein was compared to other nucleocapsid proteins for any similarities. Within the Bunyaviridae family, the molecular weight of the HTV nucleocapsid protein most closely resembles the reported size of the nucleocapsid protein in the Nairovirus genus (Clerx *et al.*, 1981). Unfortunately, there is no sequence information available from any member of that genus to permit amino acid comparisons. None of the areas of conserved amino acids found in the nucleocapsid proteins of some Bunyavirus genus members (Akashi *et al.*, 1984) were found in the amino acid sequence of the HTV nucleocapsid protein.

The greatest degree of similarity between the nucleocapsid protein of HTV and that of other viruses does not lie in a specific amino acid sequence, but in a clustering of positively charged amino acids. This clustering has been found in bunyaviruses (Aino, La Crosse, and snowshoe hare viruses; Akashi *et al.*, 1984) as well as other RNA viruses (Semliki Forest virus, Garoff *et al.*, 1980; influenza virus, van Rompuy *et al.*, 1981). One of the functions of the nucleocapsid protein is to bind to the viral genomic RNA, and it is believed that these clusters are involved in this function. These positively charged amino acids are in hydrophilic areas of the protein and are thus likely to be exposed on the outside of the tertiary structure of the protein. The basic side chains of these amino acids could, therefore, offer charged groups for interaction with the phosphate groups of RNA (Garoff *et al.*,

1980).

Characteristics of the small ORF protein in the HTV S genome segment

The sequence data also predicted that an ORF encoding a small (nonstructural) protein in the HTV S segment initiates at an AUG three nucleotides downstream of and in-frame with the termination codon of the large ORF (Figure 24). There is no evidence amongst bunyaviruses for the production of different mRNA species representing the two gene products of the S segment (Eshita *et al.*, 1985). Therefore, the synthesis of the small ORF protein from a large S segment mRNA would require either the ribosome to attach and initiate translation at the internal AUG (Figure 24, nucleotide position 1329), or the ribosome to remain on the mRNA beyond the termination codon of the large ORF, resume scanning, and continue translation at the AUG of the small ORF. The latter model is the most attractive in terms of the currently held theory (Kozak, 1986), however, the sequences surrounding this AUG stray from the theory in lacking the optimal sequences for ribosome initiation, especially with regards to the purine at position -3 (Figure 24, nucleotide position 1326).

The 6,000 dalton protein encoded by this ORF is much smaller than the S segment nonstructural proteins of the Bunyavirus genus (10,000 daltons) or the Punta Toro virus (Phlebovirus genus, 29,000 daltons). A protein of this size (6000 daltons) might be encoded on the S segment of the nairoviruses since the molecular weights of the S RNA and the nucleocapsid protein of these viruses are nearly identical with HTV, thus leaving no coding capacity for a nonstructural protein the size of other bunyaviruses. However, no sequence data is available from the nairoviruses to address this point. Conversely, as the size of the

HTV nucleocapsid protein is much larger than in the other Bunyaviridae genera, it alone may serve the dual functions of the nucleocapsid protein and the nonstructural protein. Again, however, this can only be speculated upon, since the function of any bunyavirus nonstructural protein has not yet been determined.

Although there is considerable size difference between the proteins, the hydropathic plot of the HTV 6000 dalton protein is quite similar to that of other bunyavirus S segment nonstructural proteins. These nonstructural proteins all have hydrophilic amino acids in the middle of the protein and hydrophobic sequences at the amino and carboxy termini. This suggests that these proteins have a similar function, which may be related to membrane-association.

Analogous small proteins with characteristics for membrane association are produced by other viruses. For example, a 6000 dalton has been described in cells infected with Semliki Forest virus, an alphavirus, but it is not found in the mature virion (Welch and Sefton, 1980). This hydrophobic protein is not freely soluble in the cytoplasm and it is found predominantly associated with rough microsomal membranes. The protein is believed to facilitate the movement of one or both of the viral glycoproteins across the membrane of the endoplasmic reticulum; whether there are any additional functions is unknown. A 7000 dalton protein has been identified as one of two proteins responsible for the transformation of cells infected with bovine papilloma-virus (Schlegel et al., 1986). This protein is hydrophobic and is present primarily in cellular membranes. Additionally, a 5000 dalton hydrophobic protein has been identified in cells infected with Simian virus 5, the prototype virus of the Paramyxoviridae (Hiebert et al., 1985). The function of the protein is unknown, but it is classified as

nonstructural since it is found in infected cells and not in purified virions. Whether the HTV 6000 dalton protein could function in a fashion similar to any of the above proteins is not known, but the similarities in overall structure are certainly suggestive of an analogous role.

The predicted structure of the protein (Figure 27) indicates a beta sheet structure with turns in hydrophilic areas around amino acid positions 14, 28, and 42. It is generally assumed that membrane-spanning domains are alpha-helices and require at least 20 amino acids to span the membrane (Sabatini *et al.*, 1982). However, it was recently shown that as few as 14 amino acids could span the membrane, with these shorter transmembrane domains likely to have a more extended structure (Adams and Rose, 1985). The predicted beta sheet structure of the 6000 dalton protein would provide such an extended structure. The turns could involve amino acids positioned at the hydrophilic ends of the phospholipid bilayer where the protein folds to again bury itself in the membrane. Whatever the exact configuration of the protein in the membrane, the 6000 dalton protein could be expected to be membrane-bound due to its hydrophobic nature.

In vitro and in vivo expression of the HTV nucleocapsid protein from the HTV S segment cDNA

The sequencing data provided the information necessary to predict the protein(s) which could result from in vitro or in vivo expression of the S segment. Both forms of expression (Gemini and vaccinia virus systems) produced a protein of the same apparent molecular weight (50,000 daltons) as reported for the HTV nucleocapsid protein (Figures 33 and 39). The size of the protein was also in

agreement with our sequence-predicted molecular weight for the large ORF encoded protein. The synthetic peptide deduced from our sequencing data elicited antibodies which reacted both with the authentic HTV nucleocapsid protein and with the protein produced from the S segment cDNA in the vaccinia virus expression system (Figure 39). This confirmed that the large ORF produces the HTV nucleocapsid protein and that the cDNA of the S segment can produce the same protein.

There were differences in the levels of nucleocapsid protein expression from the three recombinant vaccinia virus constructs (Figure 40). In the v1009A construct, the 3' terminal poly G tails of the cDNA insert did not appear to adversely affect synthesis of the nucleocapsid protein. The level of expression from the other two constructs may have been decreased due to the effect of the extra 5' terminal sequences of the insert and/or the effect of the S segment nucleotides lost in the Acc I digestion. Further detailed studies are required before the effect of the poly G tails on expression can be determined. However, our results do indicate the need for these studies since the removal of the poly G tails may be an unnecessary task for recombinant vaccinia virus expression.

In vivo expression of the small ORF from the HTV S segment cDNA

As mentioned above, the 6000 dalton protein of the small ORF could not be detected in the in vitro expression experiments, despite extensive efforts. In the in vivo expression system, no antiserum was available to the 6000 dalton protein and without such the protein would be difficult to detect. The inability to detect the protein in vitro may have been due to the dependence on radiolabeling with methionine for the detection of the protein. The 6000 dalton protein has only a single

initiating methionine, and this may be insufficient to permit detection. Conversely, of course, the protein may simply not be expressed as a 6000 dalton protein.

Based on the analysis of the 5' noncoding region discussed earlier, we believe the coding sequences of the small ORF should be contained in the mRNA of the S segment. Therefore, the protein should be synthesized, yet it remains undetected. One explanation for the data presented might be that, rather than making an individual 6000 dalton protein, HTV may express the small ORF sequence as part of a larger polyprotein contiguous with the nucleocapsid protein, resulting in a 56,000 dalton protein. In fact, a protein of this apparent molecular weight correlates with the protein detected in recombinant vaccinia virus-infected cells by the antipeptide antibody to the nucleocapsid protein (Figure 41).

Synthesis of this larger protein would require read-through of the termination codon of the large ORF, and several examples of such read-through have been described in plant and animal virus systems. The single-stranded RNA of tobacco mosaic virus yields a 110,000 dalton protein and a 160,000 dalton protein. Pelham (1978) showed the 160,000 dalton protein was a result of the read-through of an amber termination codon (UAG). Read-through of an opal termination codon (UGA) results in the synthesis of a nonstructural protein in the two alphaviruses, Sindbis virus and Middelburg virus (Strauss *et al.*, 1983). It is believed the slow accumulation of this protein may act as a controlling or modifying factor for the viral RNA polymerase.

Translational read-through of an amber termination codon also occurs in the two retroviruses, murine leukemia virus and feline leukemia virus, to produce a precursor polyprotein larger than normal

(Yoshinaka et al., 1985a and b). This larger precursor is synthesized in amounts 4-10% of those of the normal precursor. Amino acid sequencing has shown glutamine to be inserted at the termination codon (UAG) during translation. Whether this suppression results from a misreading of the UAG codon by normal tRNA^{Gln} or by a specific nonsense suppressor tRNA is not known. In the HTV situation we are discussing, the suppression of the large ORF termination codon by a specific, nonsense suppressor tRNA would seem unlikely, as the termination codon of the small ORF, and the next three in-frame termination codons, are all ochre codons. However, other possible mechanisms exist for the suppression of this HTV termination codon.

The sequence of the large ORF termination codon and the codon preceding the initiating methionine of the small ORF is 5'-TAATTA (Figure 24, nucleotides 1323-1328). One mechanism for read-through might involve the occasional formation of a stable stem-loop structure at this site in the mRNA, thereby preventing normal termination of translation. If this occurred, the ribosome could translate the final codon of the large ORF and then the first codon of the small ORF, bypassing the looped-out codons. Another possibility is that the read-through results from a low frequency, chance misreading of the termination codon. This is the favored explanation in the leukemia virus example given above, with the UAG codon being misread and a glutamine inserted into the protein. Thus, a precedent for read-through from the large to the small HTV ORF does exist. The determination of which mechanism might be utilized to allow read-through would involve experiments, discussed below, which manipulate the sequences of the termination codon and surrounding sequences.

Expression of the 56,000 dalton protein

Although the 56,000 dalton, "read-through" protein is found in recombinant vaccinia-infected cells, it was not demonstrated in the in vitro translation of the HTV S segment cDNA, nor has it been found in HTV-infected cells. We believe that the reason the protein was not detected in the in vitro expression experiments was because of the low level of expression. Supporting this notion, is the observation that the detection of the 56,000 dalton protein in recombinant vaccinia-infected cells correlated with the increased synthesis of the nucleocapsid protein (Figure 41).

The inability to detect the 56,000 dalton protein in HTV-infected cells might be related to a rapid turnover of the protein in vivo. It is possible that the larger protein is cleaved to produce the 50,000 dalton nucleocapsid protein and the 6000 dalton protein (or fragments thereof). This mechanism would be analogous to the synthesis of the two bunyavirus glycoproteins (G₁ and G₂) of the M segment RNA. Cleavage of a precursor polyprotein to produce the two glycoproteins is characteristic of bunyaviruses (Ulmanen et al., 1981). The glycoprotein precursor cannot be detected in infected cells and this has been interpreted to indicate an immediate cleavage, presumably by a cellular protease, as no known protease is encoded by the bunyaviruses. Cleavage of the glycoprotein precursor by a cellular, rather than virally encoded, protease is suspected by the proper cleavage of the precursor in the recombinant vaccinia virus containing only the HTV M segment cDNA (Pensiero et al., 1987).

We do not believe the in vivo synthesis of the 56,000 dalton protein to be an anomaly of the vaccinia expression system. There are, as yet, no documented examples of read-through of translation termin-

ation codons in the vaccinia expression system, but there are examples of incorrect post-translational modification of expressed foreign proteins (Mackett and Smith, 1986). The fusion proteins of respiratory syncytial virus and the human T cell leukemia virus type III envelope protein are not appropriately proteolytically cleaved in their respective recombinant vaccinia virus constructs. There is no certain explanation for this, but it could be due to the lack of a cellular protease if the recombinant vaccinia virus is tested in a cell line different from the cell line normally used for producing the viral protein, the deficiency of a virally-encoded protease, or the absence of a necessary signal which causes a conformational change in the protein which allows cleavage to occur.

HTV polyprotein processing does not appear to require a specific cell protease or viral-encoded protease (unless the polyprotein cleaves itself) since the HTV glycoprotein are properly processed in the recombinant vaccinia virus-infected cells. Therefore, the appearance of the 56,000 dalton protein in recombinant vaccinia virus infected-cells, absent in HTV-infected cells, may indicate the need for other viral components to trigger the cleavage. A possible reason for the existence of the 56,000 dalton protein and its cleavage is outlined below.

Possible function for the "read-through" protein

The hydrophobic amino acids of the small ORF added to the carboxy-terminus of the nucleocapsid protein, may function to target and anchor the read-through protein to the membrane of the endoplasmic reticulum. This hydrophobic tail would be similar to the signal sequence or the "halt" signal of membrane-bound proteins (Sabatini *et al.*, 1982). Once inserted in the membrane, the conformation of the

protein changes as it associates with the HTV glycoproteins or the genomic RNA (or both) and the protein can then be cleaved. This cleavage releases the nucleocapsid protein and its associated RNA from its close association with the membrane.

A mechanism such as this may be necessary for virus assembly and may also explain some characteristics of the virus. HTV (and the other bunyaviruses) requires a means of associating the nucleocapsid structures with the membrane-bound glycoproteins. Other RNA viruses contain an M (matrix) protein to accomplish this function, but the bunyaviruses lack this protein and the association mechanism has remained obscure. With the occasional read-through of a termination codon, HTV can produce a protein which associates a portion of the synthesized nucleocapsid proteins with the membrane. This protein, in association with the membrane-bound glycoproteins, can then act as a nidus for further virus assembly. It may function, therefore, as a nucleocapsid protein and an M protein.

The 50,000 dalton portion of the membrane-bound protein might bind genomic RNA, triggering subsequent binding of other nucleocapsid proteins to complete encapsidation of the RNA. Conversely, the 50,000 dalton portion of the membrane-bound protein might bind other nucleocapsid proteins already associated with the genomic RNA. Thus, by either method, the completed nucleocapsid structure is associated with the membrane-bound glycoproteins and the structure is ready for final packaging.

The persistent infection, with low virus yields, seen in HTV-infected cells may be partly the result of this mechanism, as the requirement for the read-through protein might produce mature virions slowly. The majority of the 50,000 dalton nucleocapsid protein would be

free in the cytoplasm to associate with the genomic RNA or perform other nucleocapsid protein functions. The nucleocapsid protein might then accumulate as it awaits read-through events, resulting in the formation of the inclusion bodies recently seen in HTV-infected cells (Hung et al., 1987).

The fluorescent antibody studies of recombinant vaccinia virus-infected cells expressing the HTV nucleocapsid protein (Figure 43) also support the idea of a membrane-bound portion associated with the nucleocapsid protein. The rod-shaped structures seen early in the course of infection most probably indicate self-aggregation of the nucleocapsid protein. However, the location of the long strands of fluorescence, seen around the nucleus late in infection, are analogous to the location of the endoplasmic reticulum. This could indicate the accumulation of the 56,000 dalton protein in the membrane of the endoplasmic reticulum and subsequent self-aggregation of molecules of the nucleocapsid protein.

Experiments to identify the HTV 56,000 dalton protein

Further experiments will be needed to confirm this hypothesis. For example, a thorough examination of HTV-infected cells for the 56,000 dalton protein is necessary. This protein may be as difficult to detect as the glycoprotein precursor, particularly if it is cleaved as quickly. However, the 6000 dalton protein which should remain membrane-bound after the cleavage may be detectable. The protein may not have been described previously due to its small size, its association with cellular membranes, the presence of only one methionine residue (Elliot et al., 1984), or the lack of a specific antiserum to the protein.

There are several new approaches, based on our model, which

might allow us to identify the protein. Radiolabeling HTV proteins in infected cells with one or two of the more abundantly found amino acids (leucine or tyrosine; Figure 24) in the 6000 dalton protein should aid in its identification. An antiserum to a peptide, deduced from the sequence of the 6000 dalton protein, may also be required to identify the protein since HTV does not shut-off host protein synthesis, and the background will be high. In addition, rough microsomal membranes can be prepared from HTV-infected cells, as described by Welch and Sefton (1980) in characterizing the 6000 dalton protein of Semliki Forest virus. This may aid, not only in the identification of the membrane-bound protein, but also in defining its location in the cell. If the protein can be identified and purified, proof of its identity would involve the amino acid sequencing of its amino-terminus, plus a determination of the carboxy-terminal amino acid sequence of the nucleocapsid protein.

However, one can also determine the likelihood of read-through of the termination codon by manipulating the coding sequences in the recombinant vaccinia virus expression system. For example, the termination codon for the large ORF (Figure 23, nucleotide position 1323) can be removed by site-directed mutagenesis, and the modified S segment cDNA be recloned into vaccinia virus. In addition, the termination codon may have to be replaced (rather than removed) with a codon for a neutral amino acid (such as alanine) since an amino acid may be inserted in the "read-through" protein (analogous to the leukemia virus example above). This would determine if a viable 56,000 dalton protein can actually be synthesized. More importantly, fluorescent antibody studies could then be carried out with this new recombinant virus to observe if the nucleocapsid protein remains free in the cytoplasm or if all (or some)

of it now becomes membrane-bound.

Site-directed mutagenesis can also be used to change the sequence, 5'-TAATTA (Figure 24, nucleotide positions 1323-1328), to determine the importance of the possible stem-loop structure in the read-through of the termination codon. Several changes are possible which would affect the ability of this sequence to base pair. For example, if the last nucleotide is changed, the nucleotide triplet would still encode a leucine residue; and the third nucleotide can be changed to form an amber termination codon. Some of the mutagenesis experiments are already in progress.

Encapsidation of RNA by the HTV nucleocapsid protein

One important use for the expression vectors we had constructed with the HTV S segment cDNA would be to begin an analysis of the functions of the nucleocapsid protein. Using our constructs, functions could be examined with or without the presence of other HTV viral components. We first wished to examine the functions of the nucleocapsid protein in virus assembly including the role of the protein in self-association, association with the genomic RNA, and association with cellular membranes. Our proposed model for this latter association in HTV assembly was discussed earlier. We hoped to be able to demonstrate the association of the HTV nucleocapsid protein with its RNA genome, and specifically the initiating step for the formation of the nucleocapsid structure. This step would involve the recognition of a specific, genomic RNA sequence by a nucleocapsid protein.

A specific sequence has been postulated as an initiation signal for encapsidation of vesicular stomatitis virus (VSV) RNA and tobacco mosaic virus (TMV) RNA. VSV RNA has been studied by the in vitro

encapsidation of the 46 nucleotide leader RNA which is complementary to the 3' end of the genomic RNA. Blumberg *et al* (1983) has demonstrated the signal for encapsidation of this leader RNA to lie within the first 14 nucleotides of the 5' terminus. This sequence contained an A residue at every third nucleotide, and the authors proposed that this feature is at least part of the specific signal for encapsidation. Similarly, a sequence in TMV containing a G at every third residue, about 1000 nucleotides from the 3' genome terminus, is thought to be its encapsidation signal (Zimmern, 1977).

If there is a signal for initiating encapsidation of the bunyavirus RNA, it must be common to all three RNA segments, since each is encapsidated. It is speculated that one purpose of the conserved sequences at the 3' terminus is for this initiation (Bishop and Shope, 1979). However, the complement of the conserved sequence is also conserved at the 5' terminus of each segment. These sequences are believed to be important in the circularization of the RNA, but it is not known if the RNA circularizes before or after encapsidation (Bishop and Shope, 1979). If it circularizes first, then both the 3' and the 5' terminal sequences might be important signals for the initiation of encapsidation.

Based on these ideas, we attempted to develop an *in vitro* assay to study the encapsidation of HTV RNA. The viral-sense RNA could be generated in quantity using our Gemini construct and T7 RNA polymerase (Figure 32). In addition, we could study the importance of specific sequences by examining the encapsidation of synthetic oligonucleotides. For this purpose, we synthesized oligonucleotides corresponding to the conserved sequences at the 3' terminus of the S segment RNA as well as a 72-mer corresponding to the 36 nucleotides from each end (3' and 5') of

the S segment RNA. This latter oligonucleotide should be able to form a stem-loop structure similar to that in viral genomic RNA.

The oligonucleotides or the viral-sense RNA were radiolabeled, incubated with the preparation of the nucleocapsid protein, and the mixture filtered through nitrocellulose. The presence of RNA-protein complexes was detected by the amount of radioactivity which remained on the nitrocellulose paper since these will bind to the nitrocellulose, while single-stranded RNA alone does not (Kingsbury *et al.*, 1987).

As a source of HTV nucleocapsid protein, we attempted to purify the HTV protein from recombinant vaccinia virus-infected cells which contained large amounts of this protein (Figure 41). Affinity chromatography was used, employing the nucleocapsid protein antipeptide rabbit serum (Figure 39). Unfortunately the protein did not bind to the column-bound antibody, because, most probably, the antibody recognizes an epitope exposed only on the denatured protein. This would also explain our failure to detect specific fluorescence in recombinant virus-infected cells when the antipeptide serum was used (see page 160).

Since we had no other useful antibody, ion exchange chromatography was utilized in further attempts to purify the nucleocapsid protein. We did not expect to purify the protein to homogeneity using this approach, but hoped to remove other RNA binding proteins. With this preparation, we were able to detect binding of protein to the synthesized HTV RNA in the filter binding assay. Unfortunately, preparations from vSC8(control recombinant vaccinia virus)-infected cells bound RNA just as well as preparations from the HTV recombinant vaccinia virus infection.

In retrospect, we are confident that the experiment would succeed if the protein could be purified. What is required, however, is

a good polyclonal or monoclonal antibody with appropriate nucleocapsid protein binding ability. This is currently in preparation.

Specific regions of the nucleocapsid protein are involved in the recognition of the signal in the RNA to initiate encapsidation and in the recognition of other nucleocapsid proteins to complete the encapsidation of the RNA. The positively charged regions of the HTV nucleocapsid protein (see page 114), might be involved in the interaction of the protein-RNA complex. Although it might be more difficult to predict specific amino acid sequences which are important for protein-protein interactions, Blumberg *et al* (1984) have demonstrated *in vitro* the self-association of purified vesicular stomatitis virus nucleocapsid protein in the absence of RNA. Antipeptide antibodies might be useful in determining the importance of these specific regions in encapsidation experiments.

Evaluation of the immune response to HTV recombinant vaccinia viruses

The animal studies were successful in demonstrating the ability of the HTV recombinant vaccinia viruses to elicit antibodies to their respective proteins (Table 1 and Figure 44). The neutralizing antibody response, detected as early as 14 days following vaccination with vMP2, is comparable to the response of animals vaccinated with recombinant vaccinia viruses expressing other viral glycoproteins (vesicular stomatitis virus, Mackett *et al.*, 1985b; influenza virus, Smith *et al.*, 1983). However, the lack of a significant increase in antibody titer following re-vaccination is unlike the response demonstrated in previous vaccination trials.

Generally, re-vaccination with recombinant vaccinia virus results in boosting of antibody levels despite the existing immunity to

vaccinia virus (Macket and Smith, 1986). This pre-existing immunity may, however, have an effect on the level of response, since animals immunized first with wild type vaccinia virus and subsequently with a recombinant vaccinia virus mounted an immune response, but with levels lower than those induced by a primary vaccination (Smith *et al.*, 1986). In addition, these previous studies did not use a recombinant vaccinia virus which expresses beta-galactosidase. A diminished immune response against the expressed foreign gene product may result if the vaccinated animal has pre-existing antibodies to beta-galactosidase from natural bacterial infection (Macket and Smith, 1986). The combination of these two limiting effects might explain the lack of a large response to the booster vaccination.

Nevertheless, the antibody response was sufficient to neutralize the virus *in vitro*. Unfortunately, due to the deficiencies in the single HTV animal model, the protective immunity of these antibodies could not be tested. Nevertheless, the recombinant vaccinia virus appears to be a very promising means for vaccinating humans against disease from HTV.

Immunogenic properties of the HTV nucleocapsid protein

Another function of the nucleocapsid protein we wished to examine was its role in the host in generating an immune response which could combat HTV infection. With our molecular constructs, we felt we had the ideal tools to examine its importance without the presence of other viral components. The results of the animal vaccination studies had indicated the importance of the HTV viral glycoproteins in generating antibodies which neutralized the virus. Conversely, it also demonstrated the inability of the nucleocapsid protein to elicit neutra-

lizing antibodies.

The humoral component of the immune system has been shown to recognize the proteins of the viral surface hence, in our experiment, it seemed logical that the glycoproteins would generate neutralizing antibodies. The cellular component of the immune response, specifically the cytotoxic T cell (CTL), has been believed to recognize those same viral proteins in the membrane of infected cells. The internal proteins of the virus, such as the nucleocapsid protein, were thus thought to be of little importance in the immune response of the host.

Recently, however, an examination of the CTLs from influenza virus-infected mice revealed a major population which recognized the viral nucleocapsid protein (Townsend *et al.*, 1984). The nucleocapsid protein does not contain sequences characteristic of an integral membrane protein, but the protein is believed to be degraded within the infected cell and transported to the cell surface by an unknown mechanism (Townsend *et al.*, 1986). The nucleocapsid proteins of other viruses (vesicular stomatitis virus, Yewdell *et al.*, 1986; and respiratory syncytial virus, King *et al.*, 1987) have also been shown to be major target antigens for the CTLs of the infected host. These studies have been carried out using recombinant vaccinia viruses which express foreign antigens on the surface of the infected cell in conjunction with the antigens of the major histocompatibility complex (Yewdell *et al.*, 1985).

This finding, of a major CTL population recognizing the nucleocapsid protein in other viral infections, has an added significance in HTV studies since a particular importance has been shown for the role of T cells in HTV infection. A role for T cells in resistance to fatal HTV infection in suckling mice has been recently proposed (Nakamura *et al.*,

1985). Administration of T cells from HTV immune mice to susceptible suckling mice protected mice from fatal infection. It is believed this (and age-dependent resistance) occurs by arresting infection at the peripheral level thereby preventing central nervous system involvement (McKee *et al.*, 1985). Very recently, Asada *et al.* (1987) have shown CTLs to be important not only in HTV clearance, but also in protection against HTV infection.

As mentioned above, the nucleocapsid protein of vesicular stomatitis virus (VSV) has been studied using a recombinant vaccinia virus which expresses the protein (Yewdell *et al.*, 1986). CTLs from mice infected with VSV were capable of lysing histocompatible target cells infected with recombinant vaccinia virus containing the gene for the nucleocapsid protein or the viral glycoprotein. The CTL recognition of the glycoproteins was highly serotype specific, while the nucleocapsid protein was recognized by CTLs for different strains of VSV.

We attempted to examine the HTV nucleocapsid protein in a similar manner. Splenocytes were harvested from mice infected with HTV or Puumala virus (the causative agent of nephropathia epidemica). These effector cells were secondarily stimulated *in vitro* by splenocytes infected with HTV or Puumala virus. Target cells were generated by infecting the histocompatible P815 cell line with the HTV recombinant vaccinia viruses-v1009A (nucleocapsid protein) or vMP2 (HTV glycoproteins). P815 cells were infected with HTV or Puumala virus as positive controls, while vSC8- or mock-infected cells were the negative controls. The target cells were radiolabeled with $\text{Na}^{51}\text{CrO}_4$ and then incubated with the effector cells. The target cells appeared to radiolabel well, based on the results from the spontaneous release and the detergent treated cell controls. Unfortunately, there was no

specific lysis of the target cells by CTLs beyond the highest dilution of effector to target cells.

There are several possible reasons for the the lack of success of this experiment. Most obviously, of course, the HTV nucleocapsid protein may not be a target for specific CTLs. Before we can be certain of this, however, additional experiments will have to be carried out. For example, more rigorous screening of the P815 cells (i.e. for surface fluorescence) would be helpful and the route and dose of virus inoculum and the time to harvest should be varied, since they were based on previous studies of others (Nakamura *et al.*, 1985 and Yewdell *et al.*, 1986) and may not have been appropriate. Finally, the extent to which HTV and Puumala can infect splenocytes and effectively present the antigens necessary for the critical secondary *in vitro* stimulation remains to be properly established.

It will be important, especially from a vaccine development standpoint, to pursue these experiments, particularly examining the ability of the HTV recombinant viruses to prime mice for an HTV-specific CTL response. Recombinant vaccinia viruses have been shown to prime and stimulate CTLs in vaccinated animals (Bennick *et al.*, 1984), and the authors (and we) believe this to be important in designing a vaccine, since humoral as well as cellular immunity should be stimulated for maximal vaccine effectiveness.

It was stated in 1951 that the U.S. Army had begun development of a specific vaccine for epidemic hemorrhagic fever using infected mites (Mayer, 1952). This, of course, was not successful, and the need for a vaccine still exists, although the approach to vaccine development has been radically changed. A vaccine inducing only neutralizing antibodies may not provide complete protection, since cellular immunity is

likely to be an important part of the host response in preventing HTV infection (Asada et al., 1987). A primed CTL population may be particularly important in HTV infection, due to the persistent infection of cells by the virus. This, therefore, warrants a close examination of the inclusion of the nucleocapsid antigen in a possible HTV vaccine preparation.

We thus have been largely successful in accomplishing our initial aims. The complete nucleotide sequence of the HTV S genome segment has been determined and, from it, the unique coding strategy of the S segment was revealed. Comparisons between the sequences of the HTV M genome segment and the S segment have found features common to other bunyaviruses such as conserved 3' termini, complementarity of the 5' and 3' termini, and possible transcription termination signals. The encoded proteins of the S segment cDNA were expressed in vitro and in vivo, and a previously undescribed HTV protein identified. Lastly, the immunogenic properties of the HTV glycoproteins and the nucleocapsid protein were examined, and both are candidates for important components of any future HTV vaccine.

REFERENCES

- Adams, G.A. and J.K. Rose. 1985. Structural requirements of a membrane-spanning domain for protein anchoring and cell surface transport. *Cell* 41: 1007-1015.
- Akashi, H., M. Gay, T. Ihara, and D.H.L. Bishop. 1984. Localized conserved regions of the S RNA gene products of bunyaviruses are revealed by sequence analyses of the Simbu serogroup Aino virus. *Vir. Res.* 1: 51-63.
- Antoniadis, A., M. Pyrpasopoulos, M. Sion, S. Daniel, and C.J. Peters. 1984. Two cases of hemorrhagic fever with renal syndrome in northern Greece. *J. Infect. Dis.* 149: 1011-1013.
- Asada, H., M. Tamura, K. Kondo, Y. Okuno, Y. Takahashi, Y. Dohi, T. Nagai, T. Kurata, and K. Yamanishi. 1987. Role of T lymphocyte subsets in protection and recovery from Hantaan virus infection in mice. *J. Gen. Virol.* 68: 1961-1969.
- Beaty, B.J., M. Holterman, W. Tabachnick, R.E. Shope, E.J. Rozhon, and D.H.L. Bishop. 1981. Molecular basis of Bunyavirus transmission by mosquitoes: Role of the middle-sized RNA segment. *Science* 211: 1433-1434.
- Bennick, J.R., J.W. Yewdell, G.L. Smith, C. Moller, and B. Moss. 1984. Recombinant vaccinia virus primes and stimulates influenza haemagglutinin-specific cytotoxic T cells. *Nature* 311: 578-579.
- Bishop, D.H.L. and R.E. Shope. 1979. Bunyaviridae. In Comprehensive Virology, 1-156. Edited by H. Fraenkel-Conrat and R.R. Wagner. New York: Plenum Press.
- Bishop, D.H.L., C.H. Calisher, J. Casals, M.P. Chumakov, S.Y.

- Gaidamovich, C. Hannoun, D.K. Lvov, I.D. Marshall, N. Oker-Blom, R.F. Pettersson, J.S. Porterfield, P.K. Russell, R.E. Shope, and E.G. Westaway. 1980. *Bunyaviridae*. *Intervirology* 14: 125-143.
- Bishop, D.H.L., K.G. Gould, H. Akashi, and C.M. Clerx-van Haaster. 1982. The complete nucleotide sequence and coding content of snowshow hare bunyavirus small (S) viral RNA species. *Nucl. Acids Res.* 10: 3703-3713.
- Bishop, D.H.L. 1985. Replication of arenaviruses and bunyaviruses. In *Virology*, 1083-1110. Edited by B.N. Fields, D.M. Knipe, R.M. Chanock, J.L. Melnick, B. Roizman, and R.E. Shope. New York: Raven Press.
- Blumberg, B.M., C. Giorgi, and D. Kolakofsky. 1983. N protein of vesicular stomatitis virus selectively encapsidates leader RNA in vitro. *Cell* 32: 559-567.
- Bolivar, F., R.L. Raymond, P.J. Greene, M.C. Betlach, H.L. Heyneker, and H.W. Boyer. 1977. Construction and characterization of new cloning vehicles. *Gene* 2: 95-113.
- Boyer, H.W. and D. Roulland-Dussoix. 1969. A complementation analysis of the restriction and modification of DNA in *Escherichia coli*. *J. Mol. Biol.* 41: 459-472.
- Brummer-Korvenkontio, M., A. Vaheri, T. Hovi, C.-H. von Bonsdorff, J. Vuorimies, T. Manni, K. Penttinen, N. Oker-Blom, and J. Lahdevirta. 1980. Nephropathia epidemica: Detection of antigen in bank voles and serologic diagnosis of human infection. *J. Infect. Dis.* 141: 131-134.
- Buller, R.M.L., G.L. Smith, K. Cremer, A.L. Notkins, and B. Moss. 1985. Decreased virulence of recombinant vaccinia virus expression vectors is associated with a thymidine kinase-negative phenotype. *Nature*

- 317: 813-815.
- Chakrabarti, S., K. Brechling, and B. Moss. 1985. Vaccinia virus expression vector: Coexpression of beta-galactosidase provides visual screening of recombinant virus plaques. *Mol. Cell. Biol.* 5: 3403-4309.
- Childs, J.E., G.W. Korch, G.A. Smith, A.D. Terry, and J.W. LeDuc. 1985. Geographical distribution and age related prevalence of antibody to Hantaan-like virus in rat populations of Baltimore, Maryland, USA. *Am. J. Trop. Med. Hyg.* 34: 385-387.
- Clerx, J.P.M., J. Casals, and D.H.L. Bishop. 1981. Structural characteristics of Nairoviruses (Genus Nairovirus, Bunyaviridae). *J. Gen. Virol.* 55: 165-178.
- Clerx-van Haaster, C.M., J.P.M. Clerx, H. Ushijima, H. Akashi, F. Fuller, and D.H.L. Bishop. 1982. The 3' terminal RNA sequences of Bunyaviruses and Nairoviruses (Bunyaviridae): Evidence of end sequence generic differences within the virus family. *J. Gen. Virol.* 61: 289-292.
- Collett, M.S., A.F. Purchio, K. Keegan, S. Frazier, W. Hays, D.K. Anderson, M.D. Parker, C.S. Schmaljohn, J. Schmidt, and J.M. Dalrymple. 1985. Complete nucleotide sequence of the M RNA segment of Rift Valley fever virus. *Virol.* 144: 228-245.
- Collett, M.S. 1986. Messenger RNA of the M segment RNA of Rift Valley fever virus. *Virol.* 151: 151-156.
- Denhardt, D.T. 1966. A membrane-filter technique for the detection of complementary DNA. *Biochem. Biophys. Res. Com.* 23: 641-646.
- Desmyter, J., J.W. LeDuc, K.M. Johnson, F. Brasseur, C. Deckers, and C. van Ypersele de Strihou. 1983. Laboratory rat associated outbreak of haemorrhagic fever with renal syndrome due to Hantaan-like virus

- in Belgium. *Lancet* 2: 1445-1448.
- Dournon, D., N. Brion, J.P. Gonzalez, and J.B. McCormick. 1983. Further cases of haemorrhagic fever with renal syndrome in France. *Lancet* 2: 1419.
- Dournon, E., B. Moriniere, S. Matheron, P.M. Girard, J.-P. Gonzalez, F. Hirsch, and J.B. McCormick. 1984. HFRS after a wild rodent bite in the Haute-Savoie and risk of exposure to Hantaan-like virus in a Paris laboratory. *Lancet* 1: 676-677.
- Earle, D.P. 1954. Symposium on epidemic hemorrhagic fever (Forward). *Am. J. Med.* 16: 617-618.
- Editorial. 1982. Muroid Virus Nephropathies. *Lancet* 2: 1375-1377.
- Elliot, L.H., M.P. Kiley, and J.B. McCormick. 1984. Hantaan virus: Identification of virion proteins. *J. Gen. Virol.* 65: 1285-1293.
- Eshita, Y. and D.H.L. Bishop. 1984. The complete sequence of the M RNA of snowshoe hare bunyavirus reveals the presence of internal hydrophobic domains in the viral glycoprotein. *Virol.* 137: 227-240.
- Eshita, Y. B. Ericson, V. Romanowski, and D.H.L. Bishop. 1985. Analyses of the mRNA transcription processes of snowshoe hare Bunyavirus S and M RNA species. *J. Virol.* 55: 681-689.
- Feinberg, A.P. and B. Vogelstein. 1983. A technique for radiolabeling DNA restriction endonuclease fragments to high specific activity. *Anal. Biochem.* 132: 6-13.
- French, G.R., R.S. Foulke, O.A. Brand, G.A. Eddy, H.W. Lee, and P.W. Lee. 1981. Korean hemorrhagic fever: Propagation of the etiologic agent in a cell line of human origin. *Science* 211: 1046-1048.
- Gajdusek, D.C. 1962. Virus hemorrhagic fevers. Special reference to hemorrhagic fever with renal syndrome (epidemic hemorrhagic fever).

- J. Pediatr. 60: 841-857.
- Gajdusek, D.C. 1982. Muroid virus nephropathies and muroid viruses of the Hantaan virus group. Scand. J. Infect. Dis., Suppl. 36: 96-108.
- Gan, S., H. Chang-shou, Q. Zue-zhao, N. Da-shi, L. Hua-xin, G. Guang-zhong, D. Yong-lin, X. Jian-kun, W. Yang-shen, Z. Jun-neng, K. Bi-xia, W. Zheng-shun, Z. Zhi-qiang, S. Hong-kai, and Z. Ning. 1983. Etiologic studies of epidemic hemorrhagic fever (hemorrhagic fever with renal syndrome). J. Infect. Dis. 147: 654-659.
- Ganong, W.F., E. Zucker, C.K. Clawson, E.C. Voss, M.L. Klotzbach, and K. A. Platt. 1953. The early field diagnosis of epidemic hemorrhagic fever. Ann. Int. Med. 38: 61-72.
- Garoff, H., A.-M. Frischauf, K. Simons, H. Lehrach, and H. Delius. 1980. The capsid protein of Semliki Forest virus has clusters of basic amino acids and prolines in its amino-terminal region. Proc. Natl. Acad. Sci. USA 77: 6376-6380.
- Gavrilovskaya, I.N., N.S. Apekina, Y.A. Myasnikov, A.D. Bernshtein, E.V. Ryltseva, E.A. Gorbachkova, and M.P. Chumakov. 1983. Features of circulation of hemorrhagic fever with renal syndrome (HFRS) virus among small mammals in the European U.S.S.R. Arch. Virol. 75: 313-316.
- Gentsch, J.R. and D.H.L. Bishop. 1978. Small viral RNA segment of Bunyaviruses codes for viral nucleocapsid protein. J. Virol. 28: 417-419.
- Gentsch, J.R. and D.H.L. Bishop. 1979. M viral RNA segment of Bunyaviruses codes for two glycoproteins, G1 and G2. J. Virol. 30: 767-770.
- Gentsch, J.R., E.J. Rozhon, R.A. Klimas, L.H. El Said, R.E. Shope, and

- D.H.L. Bishop. 1980. Evidence from recombinant bunyavirus studies that the M RNA gene products elicit neutralizing antibodies. *Viol.* 102: 190-204.
- Gibbs, C.J., A. Takenaka, M. Franko, D.C. Gajdusek, M.D. Griffin, J. Chiels, G.W. Korch, and D. Wartzok. 1982. Seroepidemiology of Hantaan virus. *Lancet* 2: 1406-1407.
- Giles, R.B., J.A. Sheedy, C.N. Ekman, H.F. Froeb, C.C. Conley, J.L. Stockard, D.W. Cugell, J.W. Vester, R.K. Kiyasu, G. Entwisle, and R.H. Yoe. 1954. The sequelae of epidemic hemorrhagic fever. *Am. J. Med.* 16: 629-638.
- Goldgaber, D., C.J. Gibbs, D.C. Gajdusek, and A. Svedmyr. 1985. Definition of three serotypes of Hantaviruses by a double sandwich ELISA with biotin-avidin amplification system. *J. Gen. Virol.* 66: 1733-1740.
- Gonzalez-Scarano, F., R.E. Shope, C.E. Calisher, and N. Nathanson. 1982. Characterization of monoclonal antibodies against the G1 and N proteins of La Crosse and Tahyna, two California serogroup Bunyaviruses. *Viol.* 120: 42-53.
- Graham, F.L. and A.J. van der Eb. 1973. A new technique for the assay of infectivity of human adenovirus 5 DNA. *Viol.* 52: 456-467.
- Grunstein, M. and D.S. Hogness. 1975. Colony hybridization: A method for the isolation of cloned DNAs that contain a specific gene. *Proc. Natl. Acad. Sci. USA* 72: 3961-3965.
- Gupta, K.C. and D.W. Kingsbury. 1982. Conserved polyadenylation signals in two negative strand RNA virus families. *Viol.* 120: 518-523.
- Hanahan, D. 1983. Studies on transformation of Escherichia coli with plasmids. *J. Mol. Biol.* 166: 557-580.

- Hewlett, M.J., R.F. Pettersson, and D. Baltimore. 1977. Circular forms of Uukuniemi virion RNA: An electron microscopic study. *J. Virol.* 21: 1085-1093.
- Hiebert, S.W., R.G. Paterson, and R.A. Lamb. 1985. Identification and predicted sequence of a previously unrecognized small hydrophobic protein, SH, of the Paramyxovirus Simian virus 5. *J. Virol.* 55: 744-751.
- Hsiang, C. 1986. What should we call haemorrhagic fever with renal syndrome?. *Lancet* 1: 274.
- Huggins, J.W., G.R. Kim, O.M. Brand, and K.T. McKee. 1986. Ribavirin therapy for Hantaan virus infection in suckling mice. *J. Infect. Dis.* 153: 489-497.
- Hullinghorst, R.L. and A. Steer. 1953. Pathology of epidemic hemorrhagic fever. *Ann. Int. Med.* 38: 77-101.
- Hung, T., S.-M. Xia, T.X. Zhao, J.Y. Zhou, G. Song, G.X.H. Liao, W.W. Ye, Y.L. Chu, and C.S. Hang. 1983a. Morphological evidence for identifying the viruses of hemorrhagic fever with renal syndrome as candidate members of the Bunyaviridae family. *Arch. Virol.* 78: 137-144.
- Hung, T., S.-M. Xia, T.X. Zhao, J.Y. Zhou, G. Song, G.X.H. Liao, and C.S. Hang. 1983b. Viruses of classical and mild forms of hemorrhagic fever with renal syndrome isolated in China have similar Bunyavirus-like morphology. *Lancet* 1: 589-591.
- Hung, T., S.-M. Xia, T.X. Zhao, Z. Chou, and C.S. Hang. 1985. Morphology and morphogenesis of viruses of hemorrhagic fever with renal syndrome (HFRS). *Intervirology* 23: 97-108.
- Hung, T., S.-M. Xia, Z. Chou, G. Song, and R. Yanagihara. 1987. Morphology and morphogenesis of viruses of hemorrhagic fever with

- renal syndrome (HFRS). *Intervirology*. 27: 45-52.
- Hurault De Ligny, B., J.P. Prieur, J.L. Schmitt, M. Kessler, P. Canton, J.B. Dureux, P.E. Rollin, P. Sureau, J.B. McCormick, and E. Dournon. 1984. Ten new cases of HFRS in north-eastern France. *Lancet* 2: 864-865.
- Ihara, T., H. Akashi, and D.H.L. Bishop. 1984. Novel coding strategy (ambisense genomic RNA) revealed by sequence analyses of Punta Toro Phlebovirus S RNA. *Virology*. 136: 293-306.
- Ihara, T., J. Smith, J.M. Dalrymple, and D.H.L. Bishop. 1985. Complete sequences of the glycoproteins and M RNA of Punta Toro Phlebovirus compared to those of Rift Valley fever virus. *Virology*. 144: 246-259.
- Janssen, R.S., N. Nathanson, M.J. Enders, and F. Gonzalez-Scarano. 1986. Virulence of La Crosse virus is under polygenic control. *J. Virology*. 59: 1-7.
- Karanthanas, S. 1982. M13 DNA sequencing using reverse transcriptase. *Focus* 4(3): 6-7.
- Kim, G.R. and K.T. McKee. 1985. Pathogenesis of Hantaan virus infection in suckling mice: Clinical, virological, and serological observations. *Am. J. Trop. Med. Hyg.* 34: 388-395.
- King, A.M.Q., E.J. Stott, S.J. Langer, K.K.-Y. Young, L.A. Ball, and G.W. Wertz. 1987. Recombinant vaccinia viruses carrying the N gene of human respiratory syncytial virus: Studies of gene expression in cell culture and immune response in mice. *J. Virology*. 61: 2885-2890.
- Kingsbury, D.W., I.M. Jones, and K.G. Murti. 1987. Assembly of influenza ribonucleoprotein in vitro using recombinant nucleoprotein. *Virology*. 156: 396-403.
- Kitaumra, T., C. Morita, T. Komatsu, K. Sugiyama, J. Arikawa, S. Shiga, H. Takeda, Y. Akao, K. Imaizumi, A. Oya, N. Hashimoto, and S.

- Urasawa. 1983. Isolation of virus causing hemorrhagic fever with renal syndrome (HFRS) through a cell culture system. *Japan. J. Med. Sci. Biol.* 36: 17-25.
- Kozak, M. 1986. Point mutations define a sequence flanking the AUG initiator codon that modulates translation by eukaryotic ribosomes. *Cell* 44: 283-292.
- Kuismanen, E., L. Hedman, J. Saraste, and R.F. Pettersson. 1982. Uukuniemi virus maturation: Accumulation of virus particles and viral antigens in the Golgi complex. *Mol. Cell. Biol.* 2: 1444-1458.
- Kuismanen, E., B. Bang, M. Hurme, and R.F. Pettersson. 1984. Uukuniemi virus maturation: Immunofluorescence microscopy with monoclonal glycoprotein-specific antibodies. *J. Virol.* 51: 137-146.
- Kurata, T., T.F. Tsai, S.P. Bauer, and J.B. McCormick. 1983. Immunofluorescence studies of disseminated Hantaan virus infection of suckling mice. *Infect. Immun.* 41: 391-398.
- Laemmli, U.K. 1970. Cleavage of structural proteins during the assembly of the head of bacteriophage T4. *Nature* 227: 680-685.
- LeDuc, J.W., G.A. Smith, L.R. Bagley, S.E. Hasty, and K.M. Johnson. 1982. Preliminary evidence that Hantaan or a closely related virus is enzootic in domestic rodents. *N. Engl. J. Med.* 307: 624.
- LeDuc, J.W., G.A. Smith, and K.M. Johnson. 1984. Hantaan-like viruses from domestic rats captured in the United States. *Am. J. Trop. Med. Hyg.* 33: 992-998.
- LeDuc, J.W., G.A. Smith, M. Macy, and R.J. Hay. 1985. Certified cell lines of rat origin appear free of infection with Hantavirus. *J. Infect. Dis.* 152: 1082-1083.
- LeDuc, J.W., A. Antoniadis, and K. Siamopoulos. 1986a. Epidemiological

- investigations following an outbreak of hemorrhagic fever with renal syndrome in Greece. *Am. J. Trop. Med. Hyg.* 35: 654-659.
- LeDuc, J.W., G.A. Smith, J.E. Childs, F.P. Pinheiro, J.I. Maiztegui, B. Niklasson, A. Antoniadis, D.M. Robinson, M. Khin, K.F. Shortridge, M.T. Wooster, M.R. Elwell, P.L.T. Ibery, D. Koech, E.S.T. Rosa, and L. Rosen. 1986b. Global survey of antibody to Hantaan-related viruses among peridomestic rodents. *Bull. WHO Organ.* 64: 139-144.
- Lee, H.W., P.W. Lee, and K.M. Johnson. 1978. Isolation of the etiologic agent of Korean hemorrhagic fever. *J. Infect. Dis.* 137: 298-308.
- Lee, H.W., P.W. Lee, J. Lahdevirta, and M. Brummer-Korvenkontio. 1979a. Aetiological relation between Korean haemorrhagic fever and nephropathia epidemica. *Lancet* 1: 186-187.
- Lee, H.W., P.W. Lee, M. Tamura, T. Tamura, and Y. Okuno. 1979b. Etiological relation between Korean hemorrhagic fever and epidemic hemorrhagic fever in Japan. *Biken J.* 22: 41-45.
- Lee, H.W., M.C. Lee, and K.S. Cho. 1980. Management of Korean haemorrhagic fever. *Med. Prog. Technol.*: 15-21.
- Lee, H.W., G.R. French, P.W. Lee, L.J. Baek, K. Tsuchiya, and R.S. Foulke. 1981a. Observations on natural and laboratory infection of rodents with the etiologic agent of Korean hemorrhagic fever. *Am J. Trop. Med. Hyg.* 30: 477-482.
- Lee, H.W., P.W. Lee, L.J. Baek, C.K. Song, and I.W. Seong. 1981b. Intraspecific transmission of Hantaan virus etiologic agent of Korean hemorrhagic fever, in the rodent Apodemus agrarius. *Am. J. Trop. Med. Hyg.* 30: 1106-1112.
- Lee, H.W. and K.M. Johnson. 1982. Laboratory-acquired infections with Hantaan virus, the etiologic agent of Korean hemorrhagic fever. *J.*

- Infect. Dis. 146: 645-651.
- Lee, H.W., L.J. Baek, and K.M. Johnson. 1982. Isolation of Hantaan virus, the etiologic agent of Korean hemorrhagic fever, from wild urban rats. J. Infect. Dis. 146: 638-644.
- Lee, H.W., I.W. Seong, L.J. Baek, D.A. McLeod, J.S. Seo, and C.Y. Kang. 1984. Positive serological evidence that Hantaan virus, the etiologic agent of hemorrhagic fever with renal syndrome, is endemic in Canada. Can. J. Microbiol. 30: 1137-1139.
- Lee, P.W., D.C. Gajdusek, C.J. Gibbs, and Z. Xu. 1980. Aetiological relation between Korean haemorrhagic fever with renal syndrome in People's Republic of China. Lancet 1: 819-820.
- Lee, P.W., H.L. Amyx, D.C. Gajdusek, R.T. Yanagihara, D. Goldgaber, and C.J. Gibbs. 1982. New haemorrhagic fever with renal syndrome-related virus in indigenous wild rodents in United States. Lancet 2: 1405.
- Lee, P.W., C.J. Gibbs, D.C. Gajdusek, and R. Yanagihara. 1985. Serotypic classification of Hantaviruses by indirect immunofluorescent antibody and plaque reduction neutralization tests. J. Clin. Micro. 22: 940-944.
- Lee, P.W., R. Yanagihara, C.J. Gibbs, and D.C. Gajdusek. 1986. Pathogenesis of experimental Hantaan virus infection in laboratory rats. Arch Virol. 88: 57-66.
- Lees, J.F., C.R. Pringle, and R.M. Elliott. 1986. Nucleotide sequence of the Bunyamwera virus M segment: Conservation of structural features in the Bunyavirus glycoprotein gene product. Virol. 148: 1-14.
- Lloyd, G., E.T.W. Bowen, N. Jones, and A. Pendry. 1984. HFRS outbreak associated with laboratory rats in UK. Lancet 1: 1175-1176.

- Lukes, R.J. 1954. The pathology of thirty-nine fatal cases of epidemic hemorrhagic fever. *Am. J. Med.* 16: 639-650.
- Mackett, M., G.L. Smith, and B. Moss. 1984. General method for production and selection of infectious vaccinia virus recombinants expressing foreign genes. *J. Virol.* 49: 857-864.
- Mackett, M., G.L. Smith, and B. Moss. 1985a. The construction and characterisation of vaccinia virus recombinants expressing foreign genes. In DNA Cloning Volume II, 191-211. Edited by D.M. Glover. Oxford: IRL Press.
- Mackett, M., T. Yilma, J.K. Rose, and B. Moss. 1985b. Vaccinia virus recombinants: Expression of VSV genes and protective immunization of mice and cattle. *Science* 227: 433-435.
- Mackett, M. and G.L. Smith. 1986. Vaccinia virus expression vectors. *J. Gen. Virol.* 67: 2067-2082.
- Maniatis, T., E.F. Fritsch, and J. Sambrook. 1982. Molecular cloning, a laboratory manual. Cold Spring Harbor Laboratory, Cold Spring Harbor, New York.
- Maxam, A.M. and W. Gilbert. 1977. A new method for sequencing DNA. *Proc. Natl. Acad. Sci. USA* 74: 560-564.
- Mayer, C.F. 1952. Epidemic hemorrhagic fever of the Far East, or endemic hemorrhagic nephroso-nephritis. *Mil. Surgeon* 110: 276-284.
- McCormick, J.B., D.R. Sasso, E.L. Palmer, and M.P. Kiley. 1982. Morphological identification of the agent of Korean haemorrhagic fever (Hantaan virus) as a member of the Bunyaviridae. *Lancet* 1: 765-768.
- McKee, K.T., G.R. Kim, D.E. Green, and C.J. Peters. 1985. Hantaan virus infection in suckling mice: Virologic and pathologic correlates. *J. Med. Virol.* 17: 107-117.

- McNinch, J.H. 1953. Far East Command conference on epidemic hemorrhagic fever: Introduction. *Ann. Int. Med.* 38: 53-60.
- Messing, J., R. Crea, and P.H. Seeburg. 1981. A system for shotgun DNA sequencing. *Nuc. Ac. Res.* 9: 309-321.
- Nakamura, T., R. Yanagihara, C.J. Gibbs, and D.C. Gajdusek. 1985. Immune spleen cell-mediated protection against fatal Hantaan virus infection in infant mice. *J. Infect. Dis.* 151: 691-697.
- Obijeski, J.F., D.H.L. Bishop, E.L. Palmer, and F.A. Murphy. 1976. Segmented genome and nucleocapsid of La Crosse virus. *J. Virol.* 20: 664-675.
- Obijeski, J.F. and F.A. Murphy. 1977. Bunyaviridae: Recent biochemical developments. *J. Gen. Virol.* 37: 1-14.
- Obijeski, J.F., J. McCauley, and J.J. Skehel. 1980. Nucleotide sequences at the termini of La Crosse virus RNAs. *Nucl. Acids Res.* 8: 2431-2438.
- Ostrove, J.M., W. Reinhold, C.-M. Fan, S. Zorn, J. Hay, and S.E. Straus. 1985. Transcription mapping of the Varicella-Zoster virus genome. *J. Virol.* 600-606.
- Overton, H.A., T. Ihara, and D.H.L. Bishop. 1987. Identification of the N and NS_s proteins coded by the ambisense S RNA of Punta Toro Phlebovirus using monospecific antisera raised to Baculovirus expressed N and NS_s proteins. *Virol.* 157: 338-350.
- Palfreyman, J.W., T.C. Aitcheson, and P. Taylor. 1984. Guidelines for the production of polypeptide specific antisera using small synthetic oligopeptides as immunogens. *J. Immunol. Meth.* 75: 383-393.
- Pelham, H.R.B. 1978. Leaky UAG termination codon in tobacco mosaic virus RNA. *Nature* 272: 469-471.
- Pensiero, M.N. and J.M. Lucas-Lenard. 1985. Evidence for the presence

- of an inhibitor on ribosomes in mouse L cells infected with Mengo-virus. *J. Virol.* 56: 161-171.
- Pensiero, M.N., G.B. Jennings, C.S. Schmaljohn, and J. Hay. 1987. Studies on the expression of the Hantaan virus M genome segment using a vaccinia recombinant virus. *J. Virol.* in press.
- Penttinen, K., J. Lahdevirta, R. Kekomaki, B. Ziola, A. Salmi, A. Hautanen, P. Lindstrom, A. Vaheri, M. Brummer-Korvenkontio, and O. Wager. 1981. Circulating immune complexes, immunoconglutinins, and rheumatoid factors in nephropathia epidemica. *J. Infect. Dis.* 143: 15-21.
- Pettersson, R.F., M.J. Hewlett, D. Baltimore, and J.M. Coffin. 1977. The genome of Uukuniemi virus consists of three unique RNA segments. *Cell* 11: 51-63.
- PHLS Report. 1985. Haemorrhagic fever with renal syndrome: Hantaan virus infection. *Brit. Med. J.* 290: 1410.
- Poncz, M., D. Solowiejczyk, M. Ballantine, E. Schwartz, and S. Surrey. 1982. "Nonrandom" DNA sequence analysis in bacteriophage M13 by the dideoxy chain-termination method. *Proc. Natl. Acad. Sci. USA* 79: 4298-4302.
- Rhim, J.S., H.Y. Cho, and F.G. Duh. 1973. Nonproducer clones of murine sarcoma virus transformed guinea pig embryo cells. *Virol.* 54: 547-551.
- Richardson, C.D., A. Berkovich, S. Rozenblatt, and W.J. Bellini. 1985. Use of antibodies directed against synthetic peptides for identifying cDNA clones, establishing reading frames, and deducing the gene order of measles virus. *J. Virol.* 54: 186-193.
- Rigby, P.W.J., M. Dieckmann, C. Rhodes, and P. Berg. 1977. Labeling deoxyribonucleic acid to high specific activity in vitro by nick

- translation with DNA polymerase I. *J. Mol. Biol.* 113: 237-251.
- Sabatini, D.K., G. Kreibich, T. Morimoto, and M. Adesnik. 1982. Mechanisms for the incorporation of proteins in membranes and organelles. *J. Cell. Biol.* 92: 1-22.
- Sanger, F. and A.R. Coulson. 1978. The use of thin acrylamide gels for DNA sequencing. *FEBS Letters* 87: 107-110.
- Sanger, F., A.R. Coulson, B.G. Barrell, A.J.H. Smith, and B.A. Roe. 1980. Cloning in single-stranded bacteriophage as an aid to rapid DNA sequencing. *J. Mol. Biol.* 143: 161-178.
- Schlegel, R., M. Wade-Glass, M.S. Rabson, and Y.-C. Yang. 1986. The transforming gene of bovine papillomavirus encodes a small, hydrophobic polypeptide. *Science* 233: 464-467.
- Schmaljohn, C.S., S.E. Hasty, S. A. Harrison, and J.M. Dalrymple. 1983a. Characterization of Hantaan virions, the prototype virus of hemorrhagic fever with renal syndrome. *J. Infect. Dis.* 148: 1005-1012.
- Schmaljohn, C.S. and J.M. Dalrymple. 1983b. Analysis of Hantaan virus RNA: Evidence for a new genus of Bunyaviridae. *Virology* 131: 482-491.
- Schmaljohn, C.S., S.E. Hasty, J.M. Dalrymple, J.W. LeDuc, H.W. Lee, C.-H. von Bonsdorff, M. Brummer-Korvenkontio, A. Vaheri, T.F. Tsai, H.L. Regnery, D. Goldgaber, and P.W. Lee. 1985. Antigenic and genetic properties of viruses linked to hemorrhagic fever with renal syndrome. *Science* 227: 1041-1044.
- Schmaljohn, C.S., S.E. Hasty, L. Rasmussen, and J.M. Dalrymple. 1986a. Hantaan virus replication: Effects of monensin, tunicamycin and endoglycosidases on the structural glycoproteins. *J. Gen. Virol.* 67: 707-717.

- Schmaljohn, C.S., G.B. Jennings, J. Hay, and J.M. Dalrymple. 1986b. Coding strategy of the S genome segment of Hantaan virus. *Virology* 155: 633-643.
- Schmaljohn, C.S., A.L. Schmaljohn, and J.M. Dalrymple. 1987a. Hantaan virus M RNA: Coding strategy, nucleotide sequence, and gene order. *Virology* 157: 31-39.
- Schmaljohn, C.S., G.B. Jennings, and J.M. Dalrymple. 1987b. Identification of Hantaan virus messenger RNA species. In The Biology of Negative Strand Viruses, 116-121. Edited by B. Mahy and D. Kolakofsky. Amsterdam: Elsevier Science Publishers.
- Sheedy, J.A., H.F. Froeb, H.A. Batson, C.C. Conley, J.P. Murphy, R.B. Hunter, D.W. Cugell, R.B. Giles, S.C. Bershadsky, J.W. Vester, and R.H. Yoe. 1954. The clinical course of epidemic hemorrhagic fever. *Am. J. Med.* 16: 619-628.
- Shope, R.E., E.J. Rozhon, and D.H.L. Bishop. 1981. Role of the middle-sized Bunyavirus RNA segment in mouse virulence. *Virology* 114: 273-276.
- Smith, G.L., B.R. Murphy, and B. Moss. 1983. Construction and characterization of an infectious vaccinia virus recombinant that expresses the influenza hemagglutinin gene and induces resistance to influenza virus infection in hamsters. *Proc. Natl. Acad. Sci. USA* 80: 7155-7159.
- Smith, G.L., J.R. Bennink, J.W. Yewdell, P.A. Small, B.R. Murphy, and B. Moss. 1986. Vaccinia virus recombinants expressing influenza virus genes. In Options for the Control of Influenza, 375-389. Edited by A.P. Kendal. New York: Alan R. Liss.
- Smith, J.F. and D.Y. Pifat. 1982. Morphogenesis of sandfly fever viruses (Bunyaviridae family). *Virology* 121: 61-81.

- Song, G., C. Hang, H. Liao, J. Fu, G. Gao, H. Qiu, and Q. Zhang. 1984. Antigenic difference between viral strains causing classical and mild types of epidemic hemorrhagic fever with renal syndrome in China. *J. Infect. Dis.* 150: 889-894.
- Southern, E.M. 1975. Detection of specific sequences among DNA fragments separated by gel electrophoresis. *J. Mol. Biol.* 98: 503-517.
- Strauss, E.G., C.M. Rice, and J.H. Strauss. 1983. Sequence coding for the alphavirus nonstructural proteins is interrupted by an opal termination codon. *Proc. Natl. Acad. Sci. USA* 80: 5271-5275.
- Sugiyama, K., C. Morita, Y. Matsuura, S. Shiga, T. Komatsu, S. Morikawa, and T. Kitamura. 1984a. Isolation of a virus related to hemorrhagic fever with renal syndrome from urban rats in a nonendemic area. *J. Infect. Dis.* 149: 473.
- Sugiyama, K., Y. Matsuura, C. Morita, S. Shiga, Y. Akao, T. Komatsu, and T. Kitamura. 1984b. An immune adherence assay for discrimination between etiologic agents of hemorrhagic fever with renal syndrome. *J. Infect. Dis.* 149: 67-73.
- Sugiyama, K., S. Morikawa, Y. Matsuura, E.A. Tkachenko, C. Morita, T. Komatsu, Y. Akao, and T. Kitamura. 1987. Four serotypes of haemorrhagic fever with renal syndrome viruses identified by polyclonal and monoclonal antibodies. *J. Gen. Virol.* 68: 979-987.
- Svedmyr, A., H.W. Lee, A. Berglund, B. Hoorn, K. Nystrom, and D.C. Gajdusek. 1979. Epidemic nephropathy in Scandinavia is related to Korean haemorrhagic fever. *Lancet* 1: 100.
- Svedmyr, A., P.W. Lee, D.C. Gajdusek, C.J. Gibbs, and K. Nystrom. 1980. Antigenic differentiation of the viruses causing Korean haemorrhagic fever and epidemic (endemic) nephropathy of Scandinavia. *Lancet* 2:

315-316.

- Tamura, M. 1964. Occurrence of epidemic hemorrhagic fever in Osaka City: First cases found in Japan with characteristic feature of marked proteinuria. *Biken J.* 7: 79-94.
- Tang, Y.W., Z.Y. Xu, Z.Y. Zhu, and T.F. Tsai. 1985. Isolation of haemorrhagic fever with renal syndrome virus from Suncus murinus, an insectivore. *Lancet* 1: 513-514.
- Towbin, H., T. Staehelin, and J. Gordon. 1979. Electrophoretic transfer of proteins from polyacrylamide gels to nitrocellulose sheets: Procedure and some applications. *Proc. Natl. Acad. Sci. USA* 76: 4350-4354.
- Townsend, A.R.M., A.J. McMichael, N.P. Carter, J.A. Huddleston, and G.G. Brownlee. 1984. Cytotoxic T cell recognition of the influenza nucleoprotein and hemagglutinin expressed in transfected mouse L cells. *Cell* 39: 13-25.
- Townsend, A.R.M., J. Rothbard, F.M. Gotch, G. Bahadur, D. Wraith, and A.J. McMichael. 1986. The epitopes of influenza nucleoprotein recognized by cytotoxic T lymphocytes can be defined with short synthetic peptides. *Cell* 44: 959-968.
- Tsai, T.F., S.P. Bauer, D.R. Sasso, J.B. McCormick, H. Bradford, T.C. Caraway, L.M. McFarland, O. Medrano, and G. Soulie. 1982. Preliminary evidence that Hantaan or a closely related virus is enzootic in domestic rodents. *N. Engl. J. Med.* 307: 623-624.
- Tsai, T.F., S.P. Baurer, D.R. Sasso, S.G. Whitfield, J.B. McCormick, T.C. Caraway, L. McFarland, H. Bradford, and T. Kurata. 1985. Serological and virological evidence of a Hantaan Virus-related enzootic in the United States. *J. Infect. Dis.* 152: 126-136.
- Ulmmanen, I., P. Seppala, and R.F. Pettersson. 1981. In vitro trans-

- lation of Uukuniemi virus-specific RNAs: Identification of a nonstructural protein and a precursor to the membrane glycoproteins. *J. Virol.* 37: 72-79.
- Umenai, T., H.W. Lee, P.W. Lee, T. Saito, T. Toyoda, M. Hongo, K. Yoshinaga, T. Nobunaga, T. Horiuchi, and N. Ishida. 1979. Korean haemorrhagic fever in staff in an animal laboratory. *Lancet* 1: 1314-1316.
- van der Groen, G., P. Piot, J. Desmyter, J. Colaert, L. Muylle, E.A. Tkachenko, A.P. Ivanov, R. Verhagen, and C. van Ypersele de Strihou. 1983. Seroepidemiology of Hantaan-related virus infections in Belgian populations. *Lancet* 2: 1493-1494.
- van Rempuy, L., W.M. Jou, D. Huylebroeck, R. Devos, and W. Fiers. 1981. Complete nucleotide sequence of the nucleoprotein gene from the human influenza strain A/PR/8/34(HON1). *Eur. J. Biochem.* 116: 347-353.
- Vieira, J. and J. Messing. 1982. The pUC plasmids, an M13mp7-derived system for insertion mutagenesis and sequencing with synthetic universal primers. *Gene* 19: 259-268.
- Walker, E., I.W. Pinkerton, and G. Lloyd. 1984. Scottish case of haemorrhagic fever with renal syndrome. *Lancet* 2: 982.
- Weir, J.P., G. Bajszar, and B. Moss. 1982. Mapping of the vaccinia virus thymidine kinase gene by marker rescue and by cell-free translation of selected mRNA. *Proc. Natl. Acad. Sci. USA* 79: 1210-1214.
- Welch, W.J. and B.M. Sefton. 1980. Characterization of a small, nonstructural viral polypeptide present late during infection of BHK cells by Semliki Forest virus. *J. Virol.* 33: 230-237.
- White, J.D., F.G. Shirley, G.R. French, J.W. Huggins, O.M. Brand, and

- H.W. Lee. 1982. Hantaan virus, aetiological agent of Korean haemorrhagic fever, has Bunyaviridae-like morphology. *Lancet* 1: 768-771.
- Yan, D., X. Gu, D. Wang, and S. Yang. 1981. Studies on immunopathogenesis in epidemic hemorrhagic fever: Sequential observations on activation of the first complement component in sera from patients with epidemic hemorrhagic fever. *J. Immunol.* 127: 1064-1067.
- Yanagihara, R., D.C. Gajdusek, C.J. Gibbs, and R. Traub. 1984. Prospect Hill virus: Serological evidence for infection in mammalogists. *N. Engl. J. Med.* 310: 1325-1326.
- Yanagihara, R., C.-T. Chin, M.B. Weiss, D.C. Gajdusek, A.R. Diwan, J.B. Poland, K.T. Kleeman, C.M. Wilfert, G. Meiklejohn, and W.P. Glezen. 1985. Serological evidence of Hantaan virus infection in the United States. *Am. J. Trop. Med. Hyg.* 34: 396-399.
- Yanisch-Perron, C., J. Vieira, and J. Messing. 1985. Improved M13 phage cloning vectors and host strains: nucleotide sequences of the M13mp18 and pUC19 vectors. *Gene* 33: 103-119.
- Yewdell, J.W., J.R. Bennink, G.L. Smith, and B. Moss. 1985. Influenza A virus nucleoprotein is a major target antigen for cross-reactive anti-influenza A virus cytotoxic T lymphocytes. *Proc. Natl. Acad. Sci. USA* 82: 1785-1789.
- Yewdell, J.W., J.R. Bennick, M. Mackett, L. Lefrançois, D.S. Lyles, and B. Moss. 1986. Recognition of cloned vesicular stomatitis virus internal and external gene products by cytotoxic T lymphocytes. *J. Exp. Med.* 163: 1529-1538.
- Yoshinaka, Y., I. Katoh, T.D. Copeland, and S. Oroszlan. 1985a. Murine leukemia virus protease is encoded by the gag-pol gene and is synthesized through suppression of an amber termination codon.

Proc. Natl. Acad. Sci. USA 82: 1618-1622.

Yoshinaka, Y. I. Katoh, T.D. Copeland, and S. Oroszlan. 1985b.

Translation readthrough of an amber termination codon during
synthesis of feline leukemia virus protease. J. Virol. 55: 870-
873.

Zeier, M., K. Andrassy, R. Waldherr, and E. Ritz. 1986. Akutes
nierenversagen durch Hantavirus. Dtsch. Med. Wschr. 111: 207-210.

Zimmern, D. 1977. The nucleotide sequence at the origin for assembly
on tobacco mosaic virus RNA. Cell 11: 463-482.